

Supporting Information

**Tandem Manganese Catalysis for the Chemo-, Regio-, and
Stereoselective Hydroboration of Terminal Alkynes: In Situ
Precatalyst Activation as a Key to Enhanced Chemoselectivity**

*Victor Duran Arroyo and Rebeca Arevalo**

*Department of Chemistry and Biochemistry
University of California, Merced, 95343, USA*

rebecaarevalo@ucmerced.edu

Table of Contents

1. General Considerations	S2
2. Preparation and Characterization of [(Mn(^t BuPNP)Cl ₂)] (Mn3)	S3
3. General Catalytic Procedures	S4
4. Efficiency of Mn2 for the functionalization of terminal alkynes with HBPi	S6
5. Optimization of the Conditions for the Hydroboration of Terminal Alkynes Employing Mn2 as Precatalyst	S6
6. Control Experiments	S12
7. Characterization of alkenylboronate esters	S14
8. NMR Monitoring of Catalytic and Stoichiometric Reactions	S18
9. NMR spectra of alkenylboronate esters	S46
10. References	S75

1. General Considerations

All air- and moisture-sensitive manipulations were carried out using vacuum line, Schlenk and cannula techniques or in an MBraun inert atmosphere (argon) glovebox unless otherwise noted. All glassware was stored in a pre-heated at 200 °C oven prior to use. All glassware was cleaned using base (KOH, *i*PrOH) and acid (HCl (aq)) baths. All reported reaction temperatures correspond to external silicone oil bath temperatures. Room temperature (RT) was approximately 23 °C.

The solvents used for air- and moisture-sensitive manipulations were dried and deoxygenated using literature procedures.¹ MnCl₂ was purchased from Fisher Scientific (99.99%, ultra dry) and dried under high vacuum for 8 h prior to use. Mesitylene was dried over CaH₂ degassed by three freeze-pump-thaw cycles, and distilled under vacuum prior to use. The terminal alkynes employed in the substrate scope were purchased from commercial sources (Thermo Fisher Scientific, AmBeed and Sigma Aldrich), dried over lithium aluminum hydride and distilled prior to use. NaHBEt₃ (1.0 M toluene or 1.0 M in THF), MeLi (1.6 M solution in Et₂O), SiMe₃CH₂MgCl (1 M solution in Et₂O), HBPi_n, B₂Pi_n₂ and HBCat were purchased from Sigma-Aldrich as used as received. All other reagents were used as received. [Mn(SiNSi)Cl₂] (**Mn1**),² [Mn(^{*i*}PrPNP)Cl₂]³ (**Mn2**), [Mn(^{*Et*}PDI)Cl₂] (**Mn4**),⁴ ^{*t*}BuPNP (**Mn3**),⁵ and HBDan⁶ were prepared according to literature procedures.

CDCl₃ (Thermo Fisher Scientific) was distilled from CaH₂ under an atmosphere of argon prior to its use and stored over 4 Å molecular sieves. THF-d₈ (Thermo Fisher Scientific) was distilled from sodium metal and benzophenone under an atmosphere of argon and stored under argon. Toluene-d₈ (Thermo Fisher Scientific) was distilled from sodium metal under an atmosphere of argon and stored under argon. Benzene-d₆ was purchased from commercial sources and used as is.

¹H NMR spectra were recorded on an Agilent 400 spectrophotometer operating at 400 MHz. ¹³C NMR spectra was recorded on Agilent 400 spectrophotometer operating at 100 MHz, ¹⁹F at 376 MHz, ¹¹B 128 MHz, and ³¹P at 163 MHz. All ¹H and ¹³C NMR chemical shifts are reported in ppm relative to SiMe₄ using the ¹H (chloroform-*d*: 7.26 ppm; THF-d₈ 1.67 ppm; benzene-d₆ 7.16 ppm; toluene-d₈ 6.90 ppm) and ¹³C (chloroform-*d*: 77.16 ppm; THF-d₈ 67.21 ppm; Benzene-d₆ 128.06ppm; toluene-d₈ 137.48ppm) chemical shifts of the

solvent as a standard. ^1H NMR data for diamagnetic compounds are reported as follows: chemical shift, multiplicity (s = singlet, d = doublet, t = triplet, q = quartet, p = pentet, br = broad, m = multiplet, app = apparent, obsc = obscured), coupling constants (Hz), integration, assignment. ^{13}C NMR data for diamagnetic compounds are reported as follows: chemical shift, number of protons attached to carbon (e.g. CH_2), assignment. QC stands for quaternary carbon.

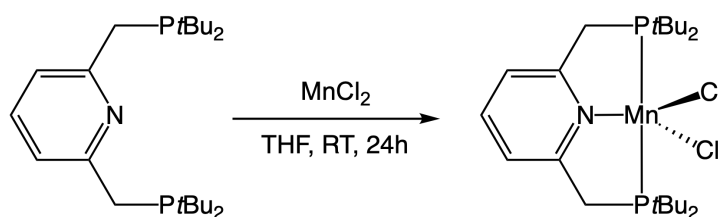
GC analyses were performed using a Shimadzu GC-2014 gas chromatograph equipped with a Shimadzu AOC-20s autosampler and a Shimadzu SHRXI-5MS capillary column (15 m x 250 μm) with an inlet and detector temperature of 250 $^\circ\text{C}$. UHP-grade (99.999%) helium was used as carrier gas with a flow rate of [1.82] mL/min. The temperature program used for GC analyses was as follows: 60 $^\circ\text{C}$, isothermal 1 min; 15 $^\circ\text{C}/\text{min}$ to 250 $^\circ\text{C}$, isothermal 2 min.

Solid-state magnetic moments were determined using a Johnson Matthey Magnetic Susceptibility balance that was calibrated with a pre-made MnCl_2 standard.

Elemental analyses were performed at the microanalytical facility at the University of California, Berkeley.

Infrared spectroscopy was conducted on a Bruker Alpha II FT-IR (ATR) spectrometer.

2. Preparation and Characterization of $[(\text{Mn}(\text{t}^\text{Bu}\text{PNP})\text{Cl}_2)]$ (Mn3)



In an argon-filled glovebox a scintillation vial was charged with a magnetic stir bar, MnCl_2 (40 mg, 0.378 mmol), 2,6-bis((di-tert-butylphosphino)methyl)pyridine ($\text{t}^\text{Bu}\text{PNP}$, 149 mg, 0.378 mmol) and THF (15 mL). The resulting mixture was stirred at room temperature (23 $^\circ\text{C}$) for 24 hours. Volatiles were removed under vacuum yielding a off-white solid that was

washed with Et₂O (15 mL x 3) followed by hexane (15 mL x 3) and dried under vacuum. **Mn3** was isolated as an off-white solid in 97% yield (158 mg). Anal Calcd for [C₂₃H₄₃Cl₂MnNP₂]: C, 52.98; H, 8.31; N, 2.69. Found: C, 52.61; H, 8.15; N, 2.86. Magnetic Susceptibility (Gouy balance, 19 °C): $\mu_{\text{eff}} = 5.4 \mu_{\text{B}}$. IR (ATR, cm⁻¹): 419 (w), 433 (w), 477 (w), 530 (w), 578 (w), 689 (w), 708 (w), 747 (w), 770 (w), 792 (m), 823 (m), 845 (s), 912 (w), 937 (w), 1004 (w), 1026 (w), 1067 (w), 1099 (w), 1182 (m), 1284 (w), 1371 (m), 1395 (w), 1454 (s), 1476 (m), 1571 (w), 1598 (w), 2871 (w), 2902 (w), 2948 (w), 2978 (w), 3057 (w).

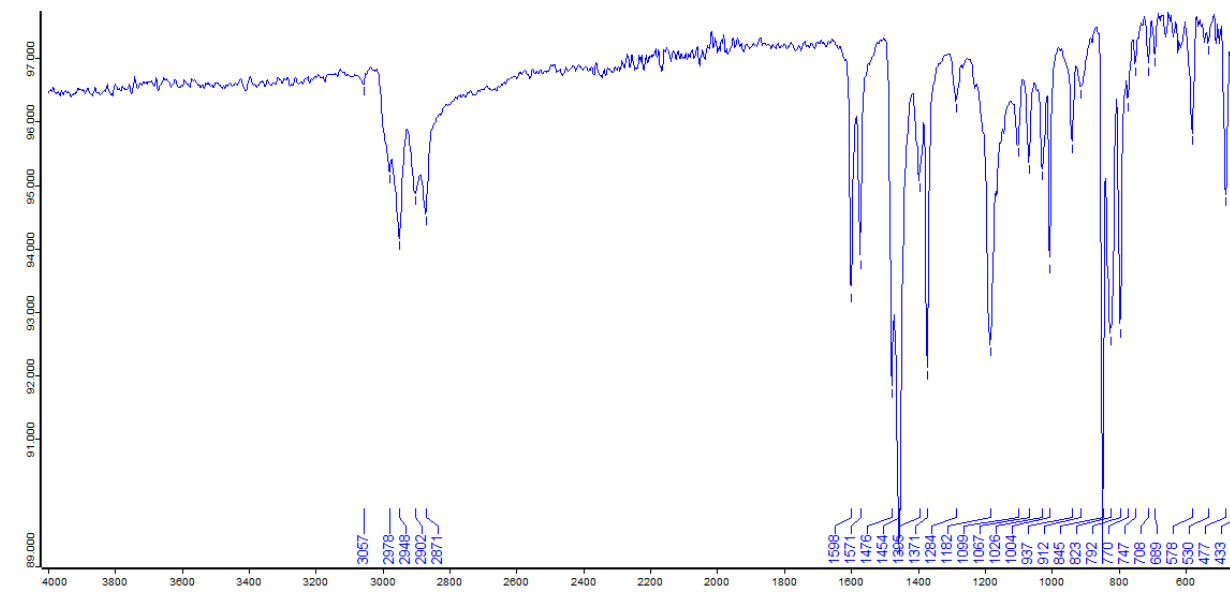
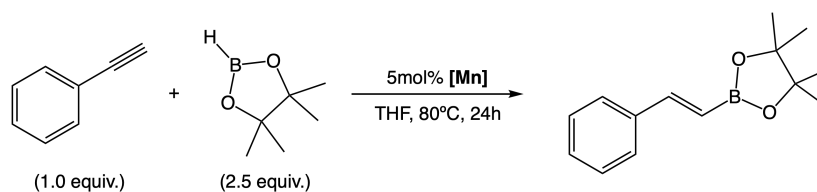


Figure S1. IR spectrum (ATR) of **Mn3**.

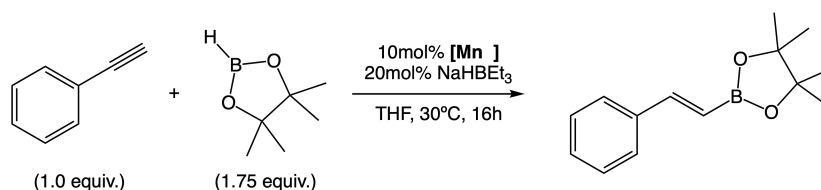
3. General Catalytic Procedures



3.1 General procedure for functionalization of terminal alkynes with HBPIN employing Mn precatalysts.

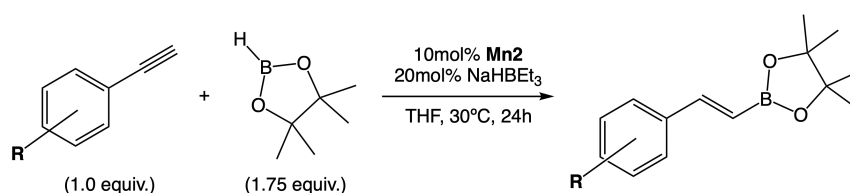
In an argon-filled glovebox a J. Young flask was charged with a magnetic stir bar and the reagents in the following order: **Mn** precatalyst (0.025 mmol), THF (0.76 mL), phenylacetylene (55 μ L, 0.5mmol), HBPIN (181 μ L, 0.88 mmol). The tube was sealed and

the resulting mixture was stirred at 80 °C for 24 hours. The reaction was quenched by exposing the reaction mixture to open atmosphere. Then the crude reaction was passed through a Pasteur pipette with a glass filter paper plug. The mixture was diluted with THF then analyzed by GC chromatography and NMR spectroscopy without additional purification.



3.2 General procedure for the hydroboration of terminal alkynes with HBPiN employing in situ activated Mn precatalysts.

In an argon-filled glovebox a J. Young flask was charged with a magnetic stir bar and the reagents in the following order: **Mn** precatalyst (0.025 mmol), THF (0.77 mL), phenylacetylene (55 μL , 0.5 mmol), and HBPiN (127 μL , 0.88 mmol) and NaHBET₃ (50 μL of a 1.0 M solution in THF, 0.05 mmol). The tube was sealed and the resulting mixture was stirred at 30 °C for 16 hours. The reaction was quenched by exposing the reaction mixture to open atmosphere. Then the crude reaction was passed through a Pasteur pipette with a glass filter paper plug. The mixture was diluted with THF then analyzed by GC chromatography and NMR spectroscopy without additional purification.

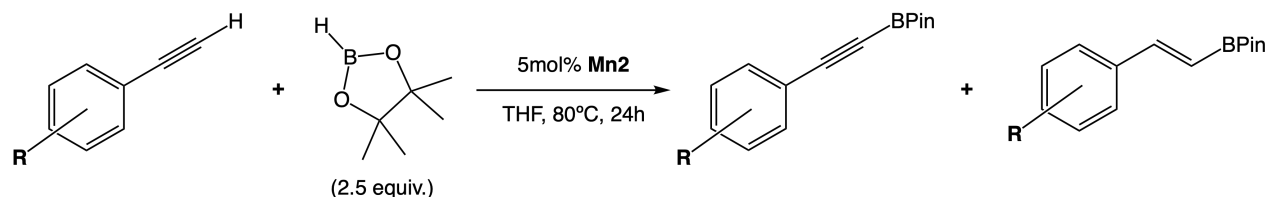


3.3 General procedure for the hydroboration of terminal alkynes employing in situ activated Mn₂ as precatalyst.

In an argon-filled glovebox a J. Young flask was charged with a magnetic stir bar and the reagents in the following order: **Mn₂** (11.6 mg, 0.025 mmol), THF (0.35 mL), terminal alkyne (0.25 mmol), HBPiN (64 μL , 0.44 mmol) and NaHBET₃ (50 μL of a 1.0 M solution in THF, 0.05 mmol). The tube was sealed and the resulting mixture was stirred at 30 °C for 24 hours. The reaction was quenched by exposing the mixture to open atmosphere. Then the crude reaction was passed through a Pasteur pipette with a glass filter paper

plug. The mixture was diluted with THF then analyzed by GC and NMR spectroscopy without additional purification.

4. Efficiency of Mn2 for the functionalization of terminal alkynes with HBPIn



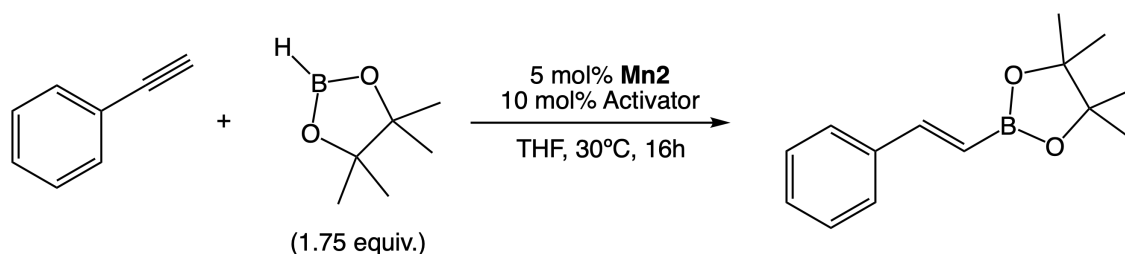
R = H, **1**, 23% Conversion
 R = 4-F, **2**, 24% Conversion
 R = 3-F, **3**, 52% Conversion
 R = 2-F, **4**, 51% Conversion

R = H, **1a**, <5% Yield
 R = 4-F, **2a**, 15% Yield
 R = 3-F, **3a**, 19% Yield
 R = 2-F, **4a**, 45% Yield

R = H, **1b**, 14% Yield
 R = 4-F, **2b**, 7% Yield
 R = 3-F, **3b**, N.D.
 R = 2-F, **4b**, N.D.

In an argon-filled glovebox a J. Young flask was charged with a magnetic stir bar and the reagents in the following order: **Mn2** (11.6 mg, 0.025 mmol), THF (0.77 mL), terminal alkyne (0.5 mmol), and HBPIn (181 μL , 1.3 mmol). The tube was sealed and the resulting mixture was stirred at 80 $^\circ\text{C}$ for 24 hours. The reaction was quenched by exposing the reaction mixture to open atmosphere. Then the crude reaction was passed through a Pasteur pipette with a glass filter paper plug. The mixture was diluted with THF then analyzed by GC chromatography and NMR spectroscopy without additional purification. Yield and conversion for substrate **1** was determined by GC employing mesitylene as internal standard. Yields and conversions for substrates **2-4** were determined by ^{19}F NMR spectroscopy employing 1,4-difluorobenzene as internal standard.

5. Optimization of the Conditions for the Hydroboration of Terminal Alkynes Employing Mn2 as Precatalyst

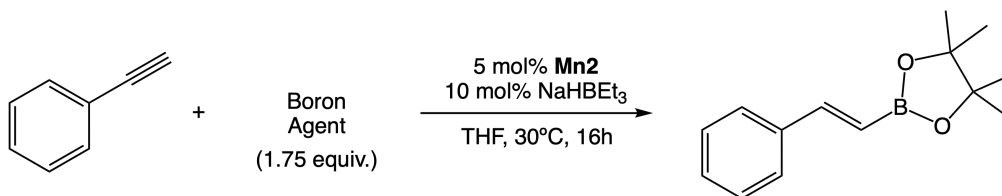


5.1 Optimization of the activator

Entry	Activator	Conversion (%)	Yield (%)
1	NaHBET ₃	91	78
2	MeLi	41	<5
3	PhLi	<5	<5
4	KOtBu	86	<5

Yields and conversions were determined by GC employing mesitylene as internal standard.

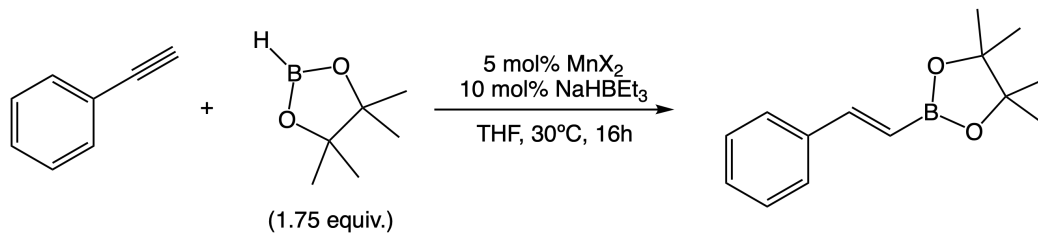
Table S1. Evaluation of the efficiency of different activators.



5.2 Optimization of the borylating agent

Entry	Borylating agent	Conversion (%)	Yield (%)
1	HBPIn	91	78
3	HBDan	36	<5
4	B ₂ Pin ₂	53	<5

Table S2. Evaluation of the efficiency of different borylating agents.



5.3 Evaluation of the catalytic efficiency of *in-situ* formed Mn precatalysts: The catalytic reactions were conducted following the general catalytic procedure described in section 3.2, employing 5 mol% of MnX_2 (X = Cl, 3.1 mg, 0.025 mmol; X = Br, 5.4 mg, 0.025 mmol; X = OAc, 4.3 mg, 0.025 mmol; X = OTf, 8.8 mg, 0.025 mmol), 5 mol% of $i\text{PrPNP}$ (17 mg, 0.05 mmol) phenylacetylene (55 μL , 0.5 mmol) and THF (0.3 mL).

Entry	X	Conversion (%)	Yield 1b (%)
1	Cl	97	74
2	Br	54	18
3	OAc	52	<5
4	OTf	49	<5

Table S3. Evaluation of the catalyst efficiency of *in-situ* formed precatalysts from different MnX_2 salts and $i\text{PrPNP}$.

Note: We hypothesize that the $\text{Mn}(\text{OAc})_2$, $\text{Mn}(\text{OTf})_2$ and MnBr_2 salts fail on efficiently generating the catalytically active species. In the cases of $\text{Mn}(\text{OAc})_2$ and $\text{Mn}(\text{OTf})_2$, we hypothesize that the corresponding $[\text{Mn}(i\text{PrPNP})\text{X}_2]$ precatalysts cannot be accessed under the reaction conditions, based on previous synthetic efforts in our lab. In the case of the MnBr_2 , however, we hypothesize that the generation of the catalytically active species upon *in situ* activation with NaHBET_3 could be inefficient, as complexes containing the MnCl_2 and MnBr_2 fragments with other pincer ligands have been reported and are stable (see references in our previous work at *Inorg. Chem. Front.* **2023**, 10, 6067-6076).

5.4 Optimization of the order of addition of the reagents

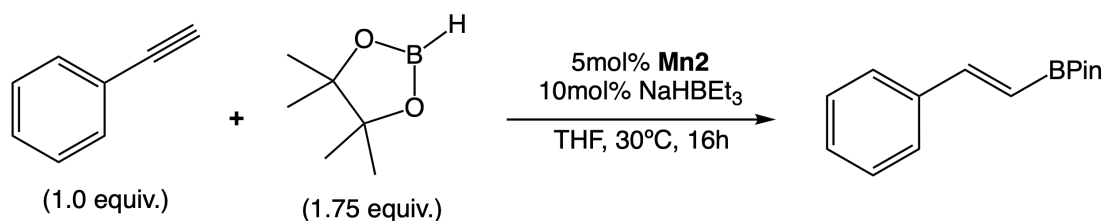
Entry	Conditions	Conversion (%)	Yield 1b (%)
1	A	91	78
2	B	96	44
3	C	60	<5

Table S4. Optimization of order of addition of the reagents.

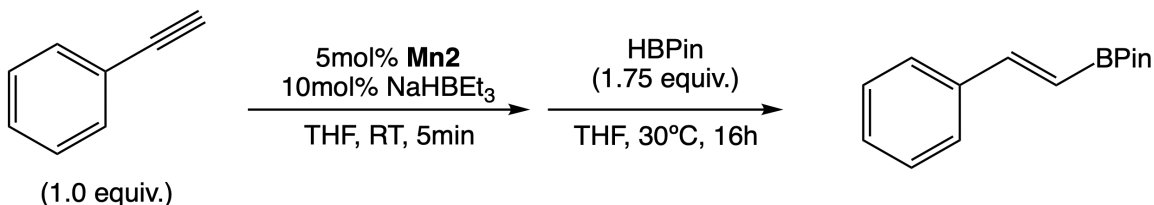
A = Alkyne, HBPIn, NaHBET₃ last

B = Alkyne, NaHBET₃, HBPIn last

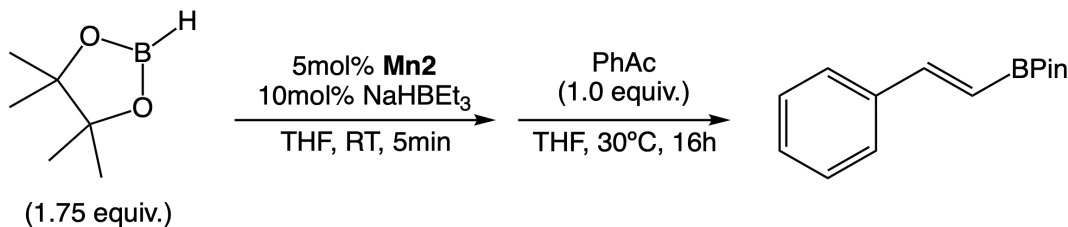
C = HBPIn, NaHBET₃, Alkyne last



Conditions A: In an argon-filled glovebox, a J. Young flask was charged with **Mn2** (11.6 mg, 0.25 mmol), phenylacetylene (55 μ L, 0.5 mmol), HBPIn (127 μ L, 0.875 mmol), and a stir bar. The mixture was promptly diluted with THF (0.77 mL) and stirred yielding a pale-yellow solution. While stirring, NaHBET₃ (50 μ L of a 1.0 M solution in THF, 0.05 mmol) was added dropwise to the THF solution whereby the solution underwent a color transition to become dark maroon. The J. Young flask was immediately sealed and placed in an oil bath for 16 h at 30 °C while stirring. The reaction was quenched via exposure to open atmosphere. The crude reaction mixture was passed through a Pasteur pipette plugged with a glass filter paper and then analyzed by GC chromatography without additional purification affording (*E*)-4,4,5,5-tetramethyl-2-(styryl)-1,3,2-dioxaborolane in a 78% crude yield determined by GC employing mesitylene as internal standard.

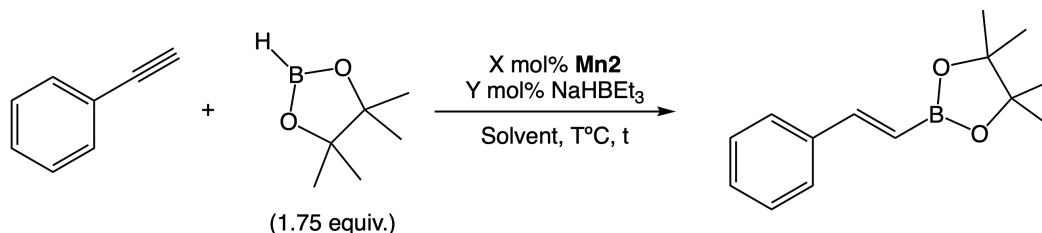


Conditions B: In an argon-filled glovebox a J. Young flask was charged with **Mn₂** (11.6 mg, 0.25 mmol), phenylacetylene (55 μ L, 0.5 mmol), and a stir bar. The mixture was diluted with THF (0.77mL) and stirred. The solution was chilled to -20 °C and NaHBEt₃ (50 μ L of a 1.0M solution in THF, 0.05 mmol) was added dropwise. Stirring for 5 minutes resulted in a color change from yellow to dark maroon. HBPin (127 μ L, 0.875mmol) was subsequently added to the solution and the J. Young flask was immediately sealed and placed in an oil bath for 16 h at 30 °C while stirring. The reaction was quenched via exposure to open atmosphere. The crude reaction mixture was passed through a Pasteur pipette plugged with a glass filter paper and then analyzed by GC chromatography without additional purification affording (*E*)-4,4,5,5-tetramethyl-2-(styryl)-1,3,2-dioxaborolane in a 44% crude yield determined by GC employing mesitylene as internal standard.



Conditions C: In an argon-filled glovebox a J. Young flask was charged with **Mn₂** (11.6 mg, 0.25 mmol), HBPin (127 μ L, 0.875 mmol), and a stir bar. The mixture was diluted with THF (0.77mL) and stirred yielding a pale-yellow solution. The solution was chilled to -20 °C and NaHBEt₃ (50 μ L of a 1.0 M solution in THF, 0.05 mmol) was added dropwise. Stirring for 5 minutes resulted in a color change from yellow to dark maroon. Phenylacetylene (55 μ L, 0.875mmol) was subsequently added to the solution and the J. Young flask was immediately sealed and placed in an oil bath for 16 h at 30 °C while stirring. The reaction was quenched via exposure to open atmosphere. The crude reaction mixture was passed through a Pasteur pipette plugged with a glass filter paper and then analyzed by GC chromatography without additional purification affording (*E*)-

4,4,5,5-tetramethyl-2-(styryl)-1,3,2-dioxaborolane in <5% crude yield determined by GC employing mesitylene as internal standard.



5.5 Optimization of the reaction conditions: The optimization of the reaction conditions afforded the % conversion and % yield reported in Table S5. All the catalytic reactions were conducted following the general catalytic procedure described in 3.2 and yields were calculated utilizing GC employing mesitylene as internal standard.

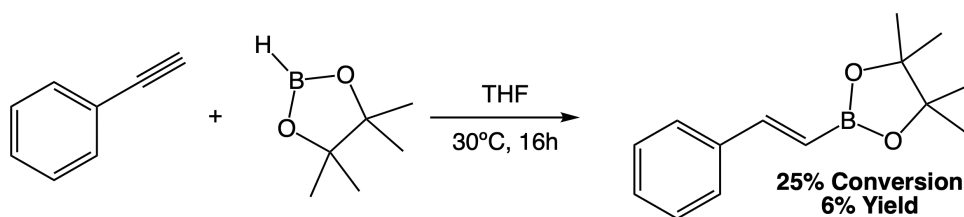
Entry	Molarity	Catalyst Loading (mol%)	Equiv. of HBPIn	T (°C)	Solvent	t (h)	% Conversion	% Yield
1	0.5	5	1	RT	THF	24	78%	28%
2	0.5	5	1	30	THF	24	94%	54%
3	0.5	5	1	40	THF	24	98%	54%
4	0.5	5	1	50	THF	24	>99%	47%
5	0.5	5	1	30	THF	24	94%	54%
6	0.5	5	1.2	30	THF	24	92%	50%
7	0.5	5	1.5	30	THF	24	93%	65%
8	0.5	5	1.75	30	THF	24	93%	75%
10	0.5	5	2	30	THF	24	97%	57%
11	0.5	5	1.75	30	Acetonitrile	24	99%	20%
12	0.5	5	1.75	30	Methanol	24	0%	0%
13	0.5	5	1.75	30	Toluene	24	0%	0%
14	0.25	5	1.75	30	THF	24	80%	79%
15	1.0	5	1.75	30	THF	24	>99%	48%
16	0.5	3	1.75	30	THF	24	>99%	24%

17	0.5	10	1.75	30	THF	24	>99%	86%
18	0.5	5	1.75	30	THF	16	98%	78%
19	0.5	5	1.75	30	THF	48	>99%	73%
20	0.5	10	1.75	RT	THF	168	98%	49%

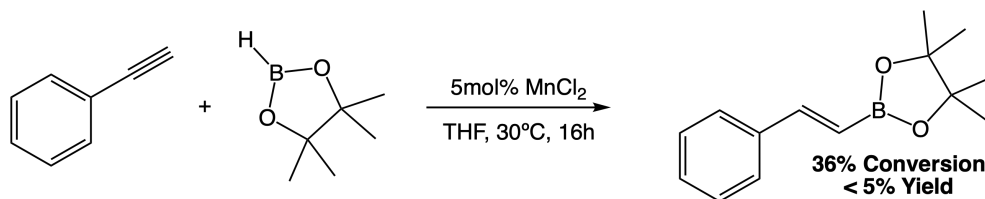
Table S5. Optimization of catalytic conditions.

6. Control Experiments

The control experiments were carried out following the general catalytic procedure described in section 3.2.

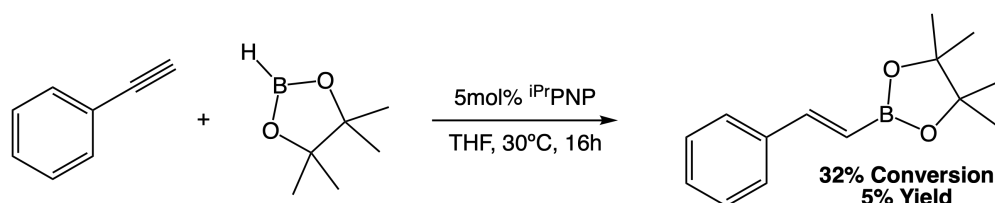


6.1 Reaction of phenylacetylene with HBPIn. In an argon-filled glovebox a J. Young flask was charged with a magnetic stir bar, phenylacetylene (55 μ L, 0.50 mmol), THF (0.77 mL) and HBPIn (127 μ L, 0.875 mmol). The tube was sealed and the resulting mixture was stirred at 30 °C for 16 hours. The reaction was quenched via exposure to open atmosphere. The crude reaction mixture was passed through a Pasteur pipette plugged with a glass filter paper and then analyzed by GC chromatography without additional purification. Conversion: 25%; Yield: 6%.

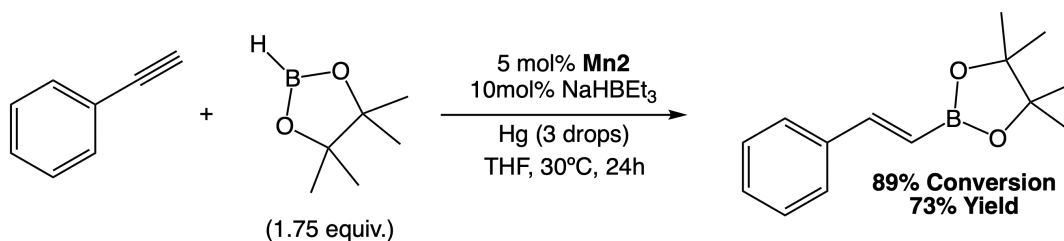


6.2 Reaction of phenylacetylene with HBPIn in the presence of 5 mol% of $MnCl_2$. In an argon-filled glovebox a J. Young flask was charged with a magnetic stir bar, phenylacetylene (55 μ L, 0.50 mmol), THF (0.77 mL), HBPIn (127 μ L, 0.875 mmol) and

MnCl₂ (3.2 mg, 0.025 mmol). The tube was sealed and the resulting mixture was stirred at 30 °C for 16 hours. The reaction was quenched via exposure to open atmosphere. The crude reaction mixture was passed through a Pasteur pipette plugged with a glass filter paper and then analyzed by GC chromatography without additional purification. Conversion: 36%; Yield: <5%.



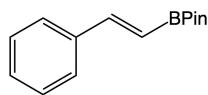
6.3 Reaction of phenylacetylene with HBPiPr₂ in the presence of 5 mol% of iPrPNP. In an argon-filled glovebox a J. Young flask was charged with a magnetic stir bar, phenylacetylene (55 μL, 0.50 mmol), THF (0.77 mL), HBPiPr₂ (127 μL, 0.875 mmol) and 2,6-bis((diisopropylphosphino)methyl)pyridine (iPrPNP, 8.5 mg, 0.025 mmol). The tube was sealed and the resulting mixture was stirred at 30 °C for 16 hours. The reaction was quenched via exposure to open atmosphere. The crude reaction mixture was passed through a Pasteur pipette plugged with a glass filter paper and then analyzed by GC chromatography without additional purification. Conversion: 32%; Yield: 5%.



6.4 Catalytic reaction in the presence of Hg drops. In an argon-filled glovebox a J. Young flask was charged with a magnetic stir bar and the reagents in the following order- Mn₂ (11.6 mg, 0.025 mmol), phenylacetylene (55 μL, 0.5 mmol), THF (0.77 mL), HBPiPr₂ (127 μL, 0.875 mmol), NaHBET₃ (50 μL of a 1.0 M solution in THF, 0.05 mmol) and three drops of Hg. The tube was sealed and the resulting mixture was stirred at 30 °C for 24 hours. The reaction was quenched via exposure to open atmosphere. The crude reaction

mixture was passed through a Pasteur pipette plugged with a glass filter paper and then analyzed by GC chromatography without additional purification. Conversion: 89%; Yield: 73%.

7. Characterization of alkenylboronate esters



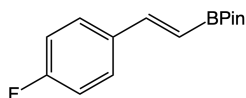
(E)-4,4,5,5-Tetramethyl-2-styryl-1,3,2-dioxaborolane (1b). The compound was prepared according to the general procedure using phenylacetylene (55 μ L, 0.5 mmol) as the terminal alkyne. Yield (crude yield): 86%

$^1\text{H NMR}$ (400 MHz, CDCl_3 , 25 $^\circ\text{C}$): δ 7.49 (d, J = 7.2 Hz, 2H), 7.43 (d, 1H), 7.32 (dt, 3H), 6.16 (d, 1H), 1.32 (s, 12H).

$^{13}\text{C}\{^1\text{H}\}$ NMR (100 MHz, CDCl_3 , 25 $^\circ\text{C}$): δ 149.6, 137.6, 129.0, 128.7, 127.2, 83.5, 24.9.

$^{11}\text{B NMR}$ (128 MHz, CDCl_3 , 25 $^\circ\text{C}$): δ 30.1.

The spectroscopic data matched that previously reported.⁷



2-[(1E)-2-(4-Fluorophenyl)ethenyl]-4,4,5,5-tetramethyl-1,3,2-dioxaborolane (2b).

The compound was prepared according to the general procedure using 4-fluorophenylacetylene (29 μ L, 0.25 mmol) as the terminal alkyne. Yield (crude yield): 18%

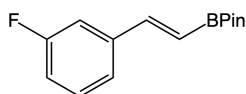
$^1\text{H NMR}$ (400 MHz, CDCl_3 , 25 $^\circ\text{C}$): δ 7.47- 7.44 (m, 2H), 7.37 (d, 1H), 7.03- 6.99 (m, 2H), 6.10 (d, J = 18.4 Hz, 1H), 1.31 (s, 12H).

$^{13}\text{C}\{^1\text{H}\}$ NMR (100 MHz, CDCl_3 , 25 $^\circ\text{C}$): δ 162.0, 148.2, 133.8, 128.8, 115.6, 83.5, 24.9

$^{11}\text{B NMR}$ (128 MHz, CDCl_3 , 25 $^\circ\text{C}$): δ 30.3.

$^{19}\text{F NMR}$ (376 MHz, CDCl_3 , 25 $^\circ\text{C}$): δ -112.41.

The spectroscopic data matched that previously reported.⁷



2-[(1E)-2-(3-Fluorophenyl)ethenyl]-4,4,5,5-tetramethyl-1,3,2-dioxaborolane (3b).

The compound was prepared according to the general procedure using 3-fluorophenylacetylene (29 μ L, 0.25 mmol) as the terminal alkyne. Yield (isolated yield): 10% (6.2 g).

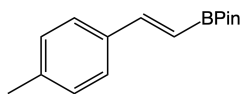
^1H NMR (400 MHz, CDCl_3 , 25°C): δ 7.37 (d, 1H), 7.30-7.16 (m, 3H), 6.98 (dt, 1H), 6.18 (d, 1H), 1.31 (s, 12H).

$^{13}\text{C}\{^1\text{H}\}$ NMR (100 MHz, CDCl_3 , 25°C): δ 161.9, 148.2, 140.0, 130.1, 123.1, 115.8, 113.4, 83.6, 24.9.

^{11}B NMR (128 MHz, CDCl_3 , 25°C): δ 30.1.

^{19}F NMR (376 MHz, CDCl_3 , 25°C): δ -113.44.

The spectroscopic data matched that previously reported.⁸



4,4,5,5-Tetramethyl-2-[(1E)-2-(4-methylphenyl)ethenyl]-1,3,2-dioxaborolane (4b).

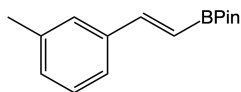
The compound was prepared according to the general procedure using 1-Ethynyl-4-methylbenzene (32 μ L, 0.25 mmol) as the terminal alkyne. Yield (crude yield): 78%

^1H NMR (400 MHz, CDCl_3 , 25°C): δ 7.41-7.36 (m, 3H), 7.16 (d, 2H), 6.14 (d, 1H), 2.35 (s, 3H), 1.32 (s, 12H).

$^{13}\text{C}\{^1\text{H}\}$ NMR (100 MHz, CDCl_3 , 25°C): δ 149.6, 139.1, 134.9, 129.4, 127.2, 83.4, 24.9, 21.4

^{11}B NMR (128 MHz, CDCl_3 , 25°C): δ 30.3.

The spectroscopic data matched that previously reported.⁷



4,4,5,5-Tetramethyl-2-[(1E)-2-(3-methylphenyl)ethenyl]-1,3,2-dioxaborolane (5b).

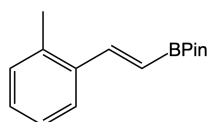
The compound was prepared according to the general procedure using 1-Ethynyl-3-methylbenzene (32 μ L, 0.25 mmol) as the terminal alkyne. Yield (crude yield): 68 %

¹H NMR (400 MHz, CDCl₃, 25°C): δ 7.34 (d, 1H), 7.24- 7.22 (m, 2H), 7.16 (t, 1H), 7.05 (d, 1H), 6.11 (d, 1H), 2.28 (s, 3H), 1.25 (s, 12H).

¹³C{¹H} NMR (100 MHz, CDCl₃, 25°C): δ 149.8, 138.1, 137.6, 129.8, 128.6, 127.9, 124.3, 83.4, 24.9, 21.5.

¹¹B NMR (128 MHz, CDCl₃, 25°C): δ 30.3.

The spectroscopic data matched that previously reported.⁷



4,4,5,5-Tetramethyl-2-[(1E)-2-(2-methylphenyl)ethenyl]-1,3,2-dioxaborolane (6b).

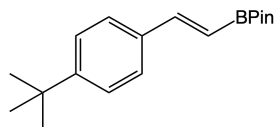
The compound was prepared according to the general procedure using 1-Ethynyl-2-methylbenzene (32 μL, 0.25 mmol) as the terminal alkyne. Yield (crude yield): <5 %

¹H NMR (400 MHz, CDCl₃, 25°C): δ 7.67 (d, 1H), 7.56 (d, 1H), 7.19–7.17 (m, 3H), 6.10 (dd, 1H), 2.41 (s, 3H), 1.33 (s, 12H).

¹³C{¹H} NMR (100 MHz, CDCl₃, 25°C): δ 147.2, 136.8, 136.4, 130.5, 128.7, 126.2, 125.9, 83.4, 24.9, 19.9.

¹¹B NMR (128 MHz, CDCl₃, 25°C): δ 30.5.

The spectroscopic data matched that previously reported.⁷



2-[(1E)-2-[4-(1,1-Dimethylethyl)phenyl]ethenyl]-4,4,5,5-tetramethyl-1,3,2-

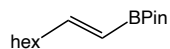
dioxaborolane (7b). The compound was prepared according to the general procedure using 1-(Tert-butyl)-4-ethynylbenzene (45 μL, 0.25 mmol) as the terminal alkyne. Yield (crude yield): 89 %

¹H NMR (400 MHz, CDCl₃, 25°C): δ 7.45-7.42 (m, 3H), 7.38-7.36 (m, 2H), 6.16 (d, 1H), 1.32 (s, 21H).

¹³C{¹H} NMR (100 MHz, CDCl₃, 25°C): δ 152.2, 149.5, 134.9, 126.9, 125.6, 83.4, 34.8, 31.4, 24.9.

¹¹B NMR (128 MHz, CDCl₃, 25°C): δ 30.3.

The spectroscopic data matched that previously reported.⁷



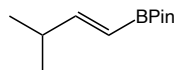
4,4,5,5-Tetramethyl-2-(1E)-1-octen-1-yl-1,3,2-dioxaborolane (8b). The compound was prepared according to the general procedure using 1-Octyne (36 μ L, 0.25 mmol) as the terminal alkyne. Yield (crude yield): 58 %

¹H NMR (400 MHz, CDCl₃, 25°C): δ 6.64 (dt, 1H), 5.43 (d, 1H), 2.14-2.12 (m, 2H), 1.40-1.38 (m, 2H), 1.28-1.25 (m, 18H), 0.87-0.84 (m, 3H).

¹³C{¹H} NMR (100 MHz, CDCl₃, 25°C): δ 154.9, 83.0, 35.9, 31.7, 29.0, 28.3, 24.9, 24.9, 22.7, 14.2.

¹¹B NMR (128 MHz, CDCl₃, 25°C): δ 29.6.

The spectroscopic data matched that previously reported.⁹



4,4,5,5-Tetramethyl-2-[(1E)-3-methyl-1-buten-1-yl]-1,3,2-dioxaborolane (9b). The compound was prepared according to the general procedure using 3-Methyl-1-butyne (26 μ L, 0.25 mmol) as the terminal alkyne. Yield (crude yield): 66 %

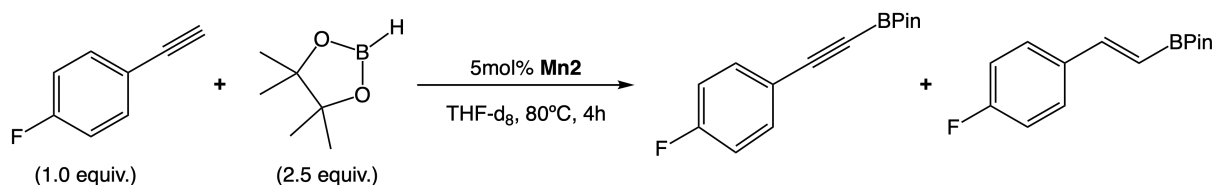
¹H NMR (400 MHz, CDCl₃, 25°C): δ 1.01 (d, 6H), 1.26 (s, 12H), 2.35–2.33 (m, 1H), 5.40 (dd, 1H), 6.64 (dd, 1H).

¹³C{¹H} NMR (100 MHz, CDCl₃, 25°C): δ 21.5, 24.9, 33.7, 83.1, 161.1.

¹¹B NMR (128 MHz, CDCl₃, 25°C): δ 30.2.

The spectroscopic data matched that previously reported.¹⁰

8. NMR Monitoring of Catalytic and Stoichiometric Reactions.



8.1 Qualitative NMR monitoring of the functionalization of 4-fluorophenylacetylene with HBPIn employing 5 mol% of Mn₂ as precatalyst.

In an argon-filled glovebox, 4-fluorophenylacetylene (23 μ L, 0.2 mmol) and HBPIn (73 μ L, 0.5 mmol) were transferred into a J. Young NMR tube with 0.18 mL of THF-d₈. The tube was sealed, brought out of the glovebox and the ¹H, ¹⁹F, and ¹¹B NMR spectra were registered. The J. Young NMR tube was brought back into the glovebox and **Mn₂** (9.3 mg, 0.02 mmol) was added to the solution. The tube was sealed, shaken to fully dissolve **Mn₂**, brought out of the glovebox and the ¹H, ¹⁹F, ¹¹B, and ³¹P NMR spectra were registered at room temperature. The headspace was evacuated by a freeze-pump-thaw cycle. The reaction was monitored by ¹H, ¹⁹F, ¹¹B, and ³¹P NMR spectroscopy at 80°C for 4 hours.

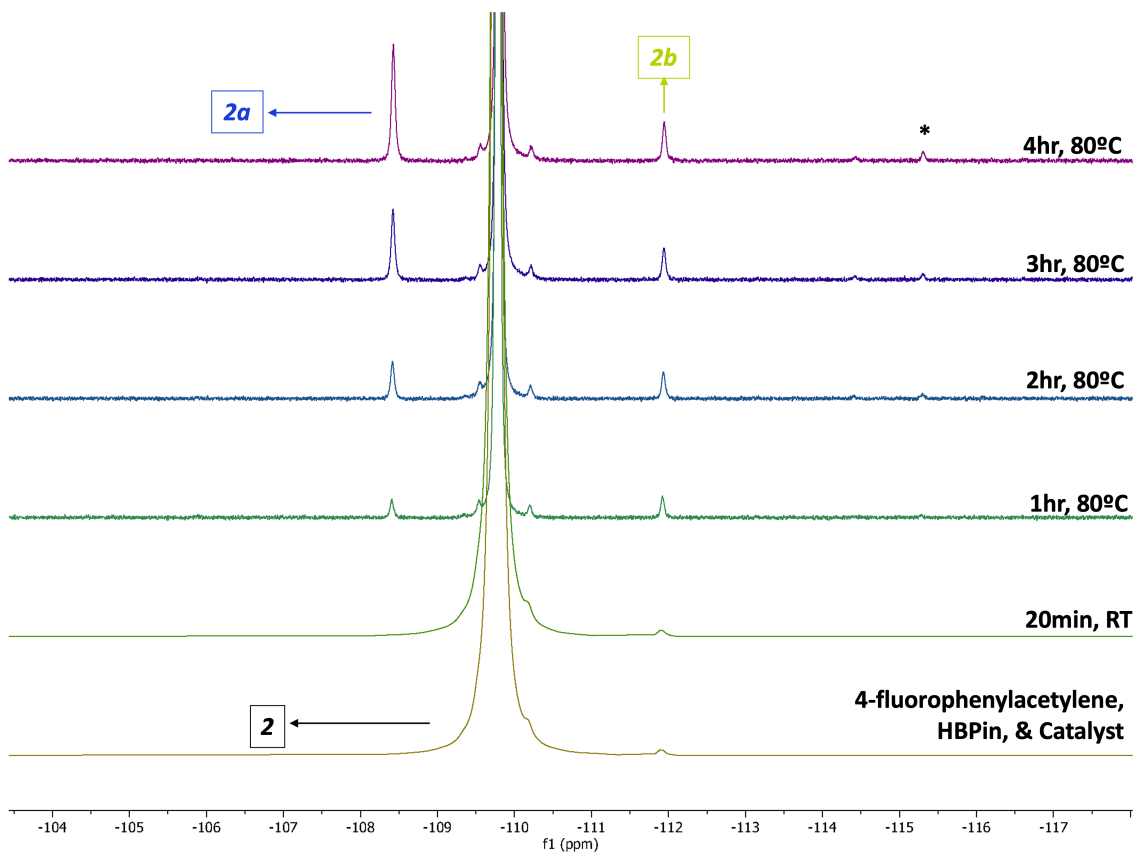


Figure S2. ^{19}F NMR spectra of the catalytic functionalization reaction in THF- d_8 at 80°C.

(* = Unidentified Products)

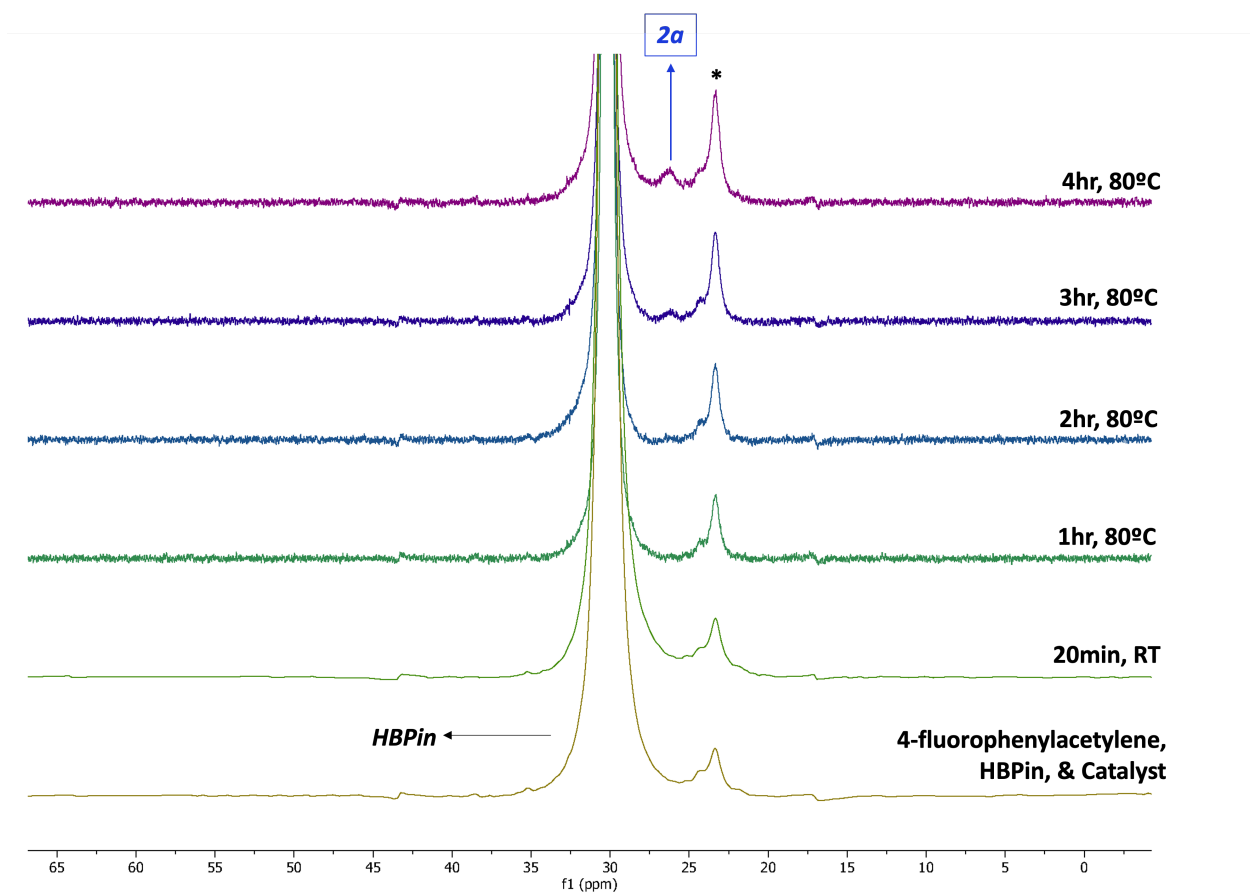


Figure S3. ^{11}B NMR spectra of the catalytic functionalization reaction in THF-d_8 at 80°C .

(* = Unidentified Impurity present in HBPIn)

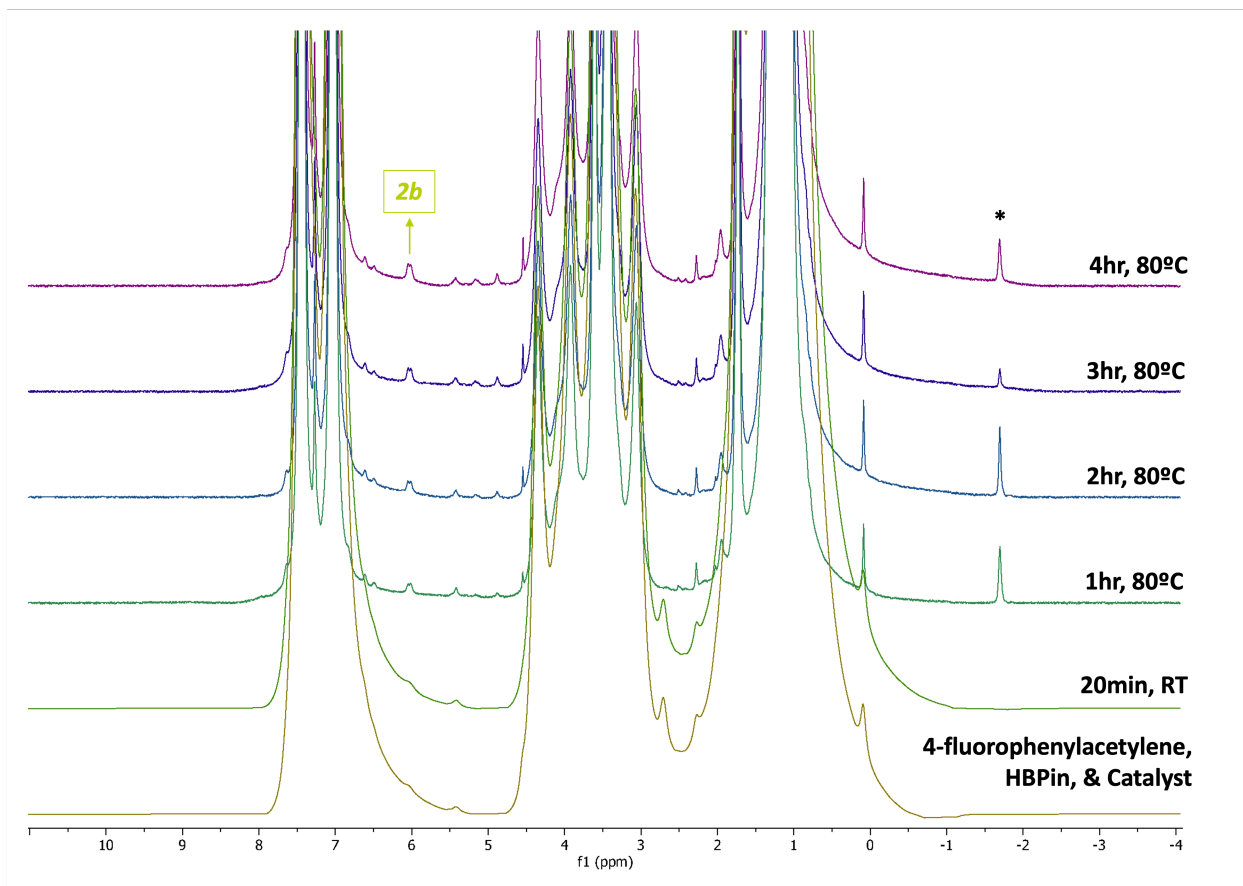


Figure S4. ¹H NMR spectra of the catalytic functionalization reaction in THF-d₈ at 80°C.

(* = Unidentified Products)

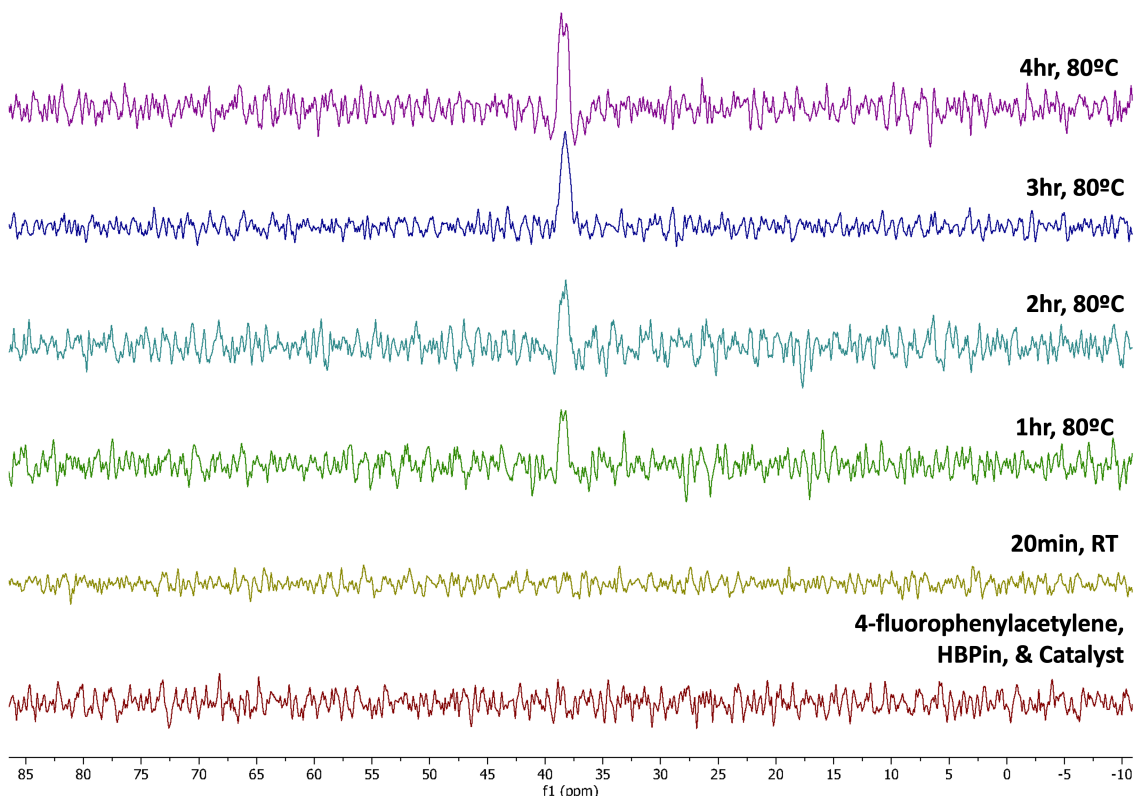
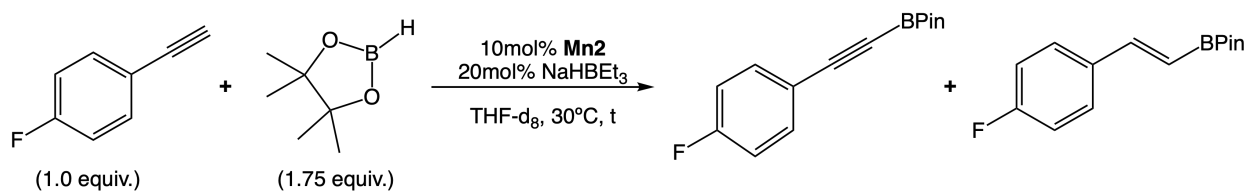


Figure S5. ^{31}P NMR spectra of the catalytic functionalization reaction in THF-d_8 at 80°C .



8.2 Quantitative NMR monitoring of the hydroboration of 4-fluorophenylacetylene with HBPIn employing 10 mol% of Mn2 / 20 mol% of NaHBET₃ as precatalyst. 4-fluorophenylacetylene (23 μL , 0.20 mmol), HBPIn (51 μL , 0.35 mmol), and 1,4-difluorobenzene (5 μL , 0.048 mmol, internal standard) and THF-d_8 (0.28 mL) were added to a J. Young NMR tube. The ^1H , ^{19}F , and ^{11}B NMR spectra were of the starting reagents was registered. The **Mn2** complex (9.3 mg, 0.02 mmol) was loaded into a 2 mL vial and the solution of the previous reagents in THF-d_8 was transferred over. The resulting mixture was chilled at -20°C for 10 minutes. In a separate 2mL vial, NaHBET_3 (40 μL of a

1.0 M solution in THF, 0.04 mmol) was added and the volatiles were removed under vacuum for 60 minutes. The resulting oil was dissolved in THF- d_8 (0.04 mL) and added to the previously chilled mixture in the 2 mL vial. A color change from yellow to dark maroon was observed and solid precipitated. The resulting mixture was filtered through a pipette with a glass filter paper plug into a J. Young NMR tube that was sealed and brought out of the glovebox. The reaction was monitored by ^1H , ^{19}F , ^{11}B , and ^{31}P NMR spectroscopy at 30 °C for 19 hours (see Figure S6). No signals attributable to diamagnetic manganese species were observed in the NMR spectra, however, signals attributable to the hydroboration product (**1b**, **34% Yield after 16h**), the C-H borylation product (**1a**, **4% Yield after 16h**) and the semihydrogenation product (**1c**, **<5% Yield after 16h**) were identified in the ^1H and ^{19}F NMR spectra.

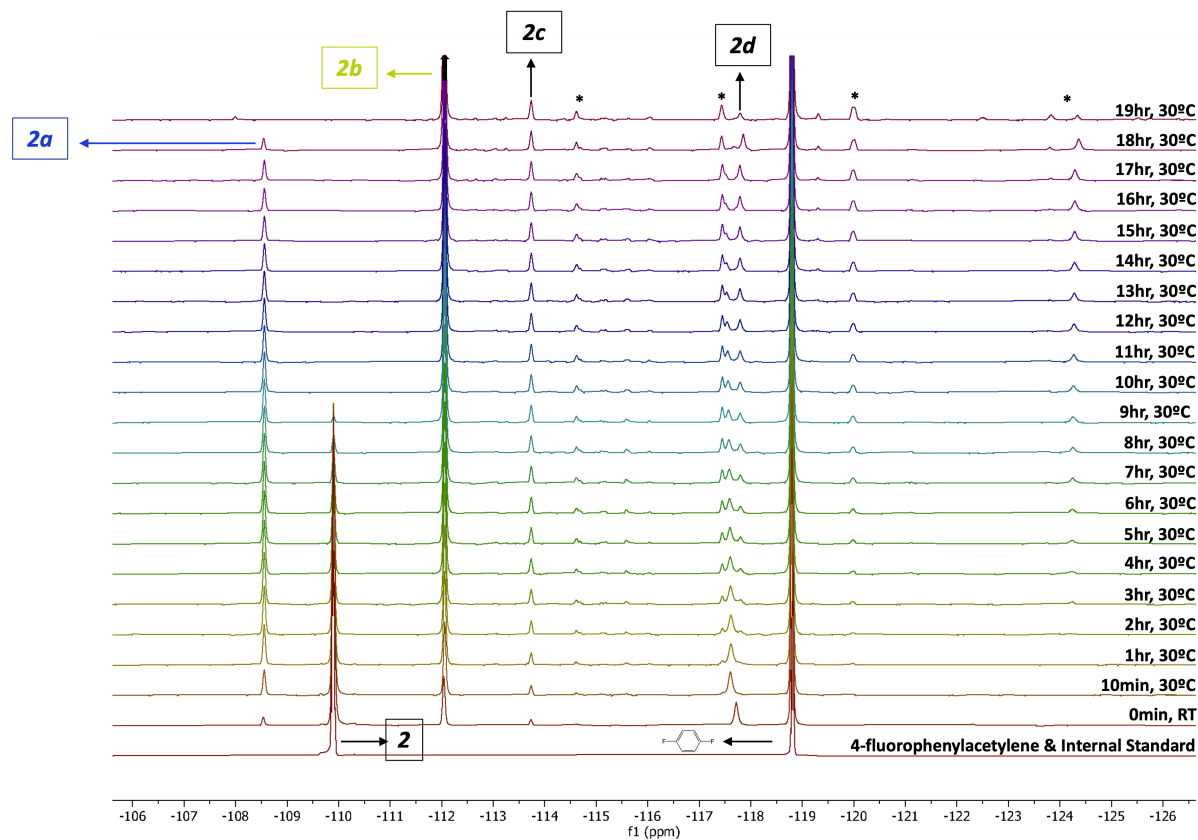


Figure S6. ^{19}F NMR spectra of catalytic hydroboration reaction in THF- d_8 at 30°C, using 1,4-difluorobenzene as internal standard. (* = Unidentified Products)

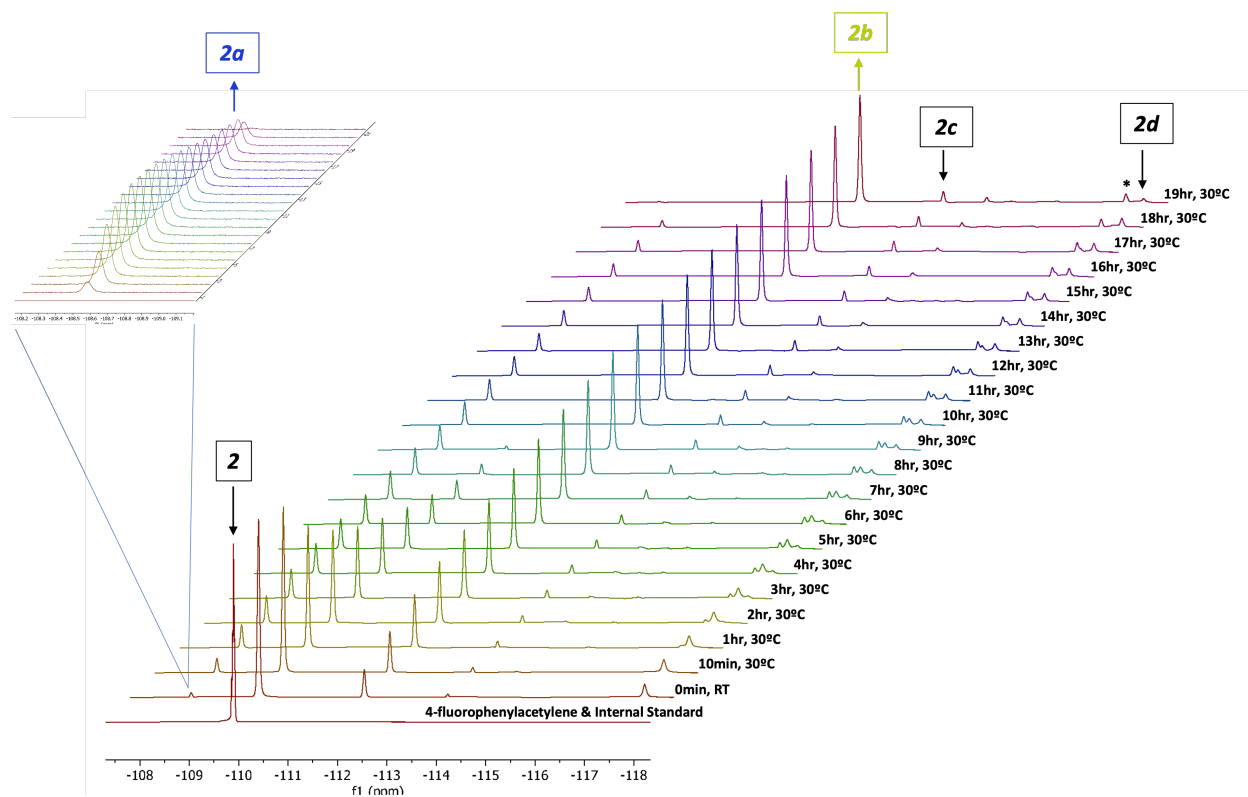


Figure S7. Zoomed in ^{19}F NMR spectra of catalytic hydroboration reaction in THF-d_8 at 30°C, using 1,4-difluorobenzene as internal standard. (* = Unidentified Products)

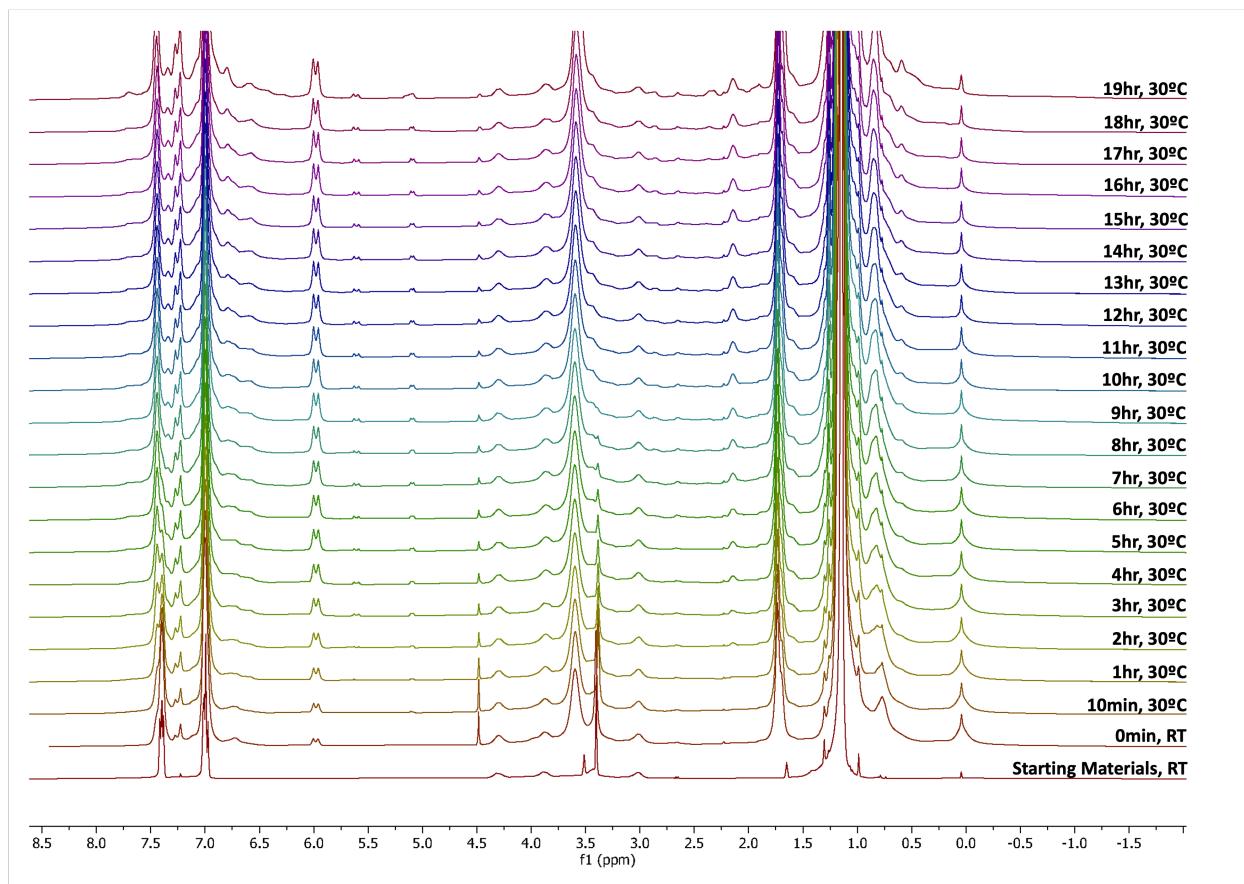


Figure S8. ¹H NMR spectra of catalytic hydroboration reaction in THF-d₈ at 30°C, using 1,4-difluorobenzene as internal standard

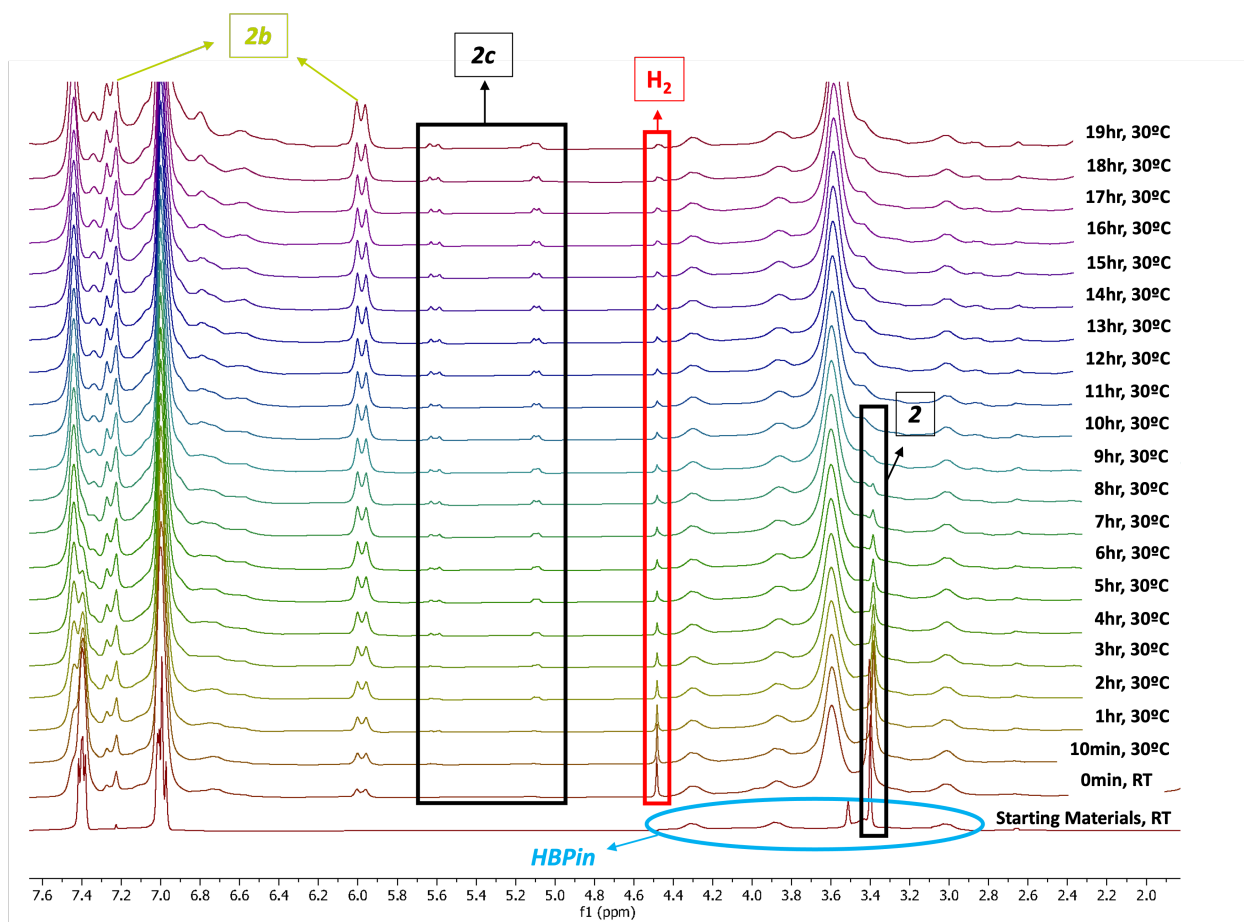


Figure S9. Zoomed in ^1H NMR spectra of catalytic hydroboration reaction in THF-d_8 at 30°C , using 1,4-difluorobenzene as internal standard.

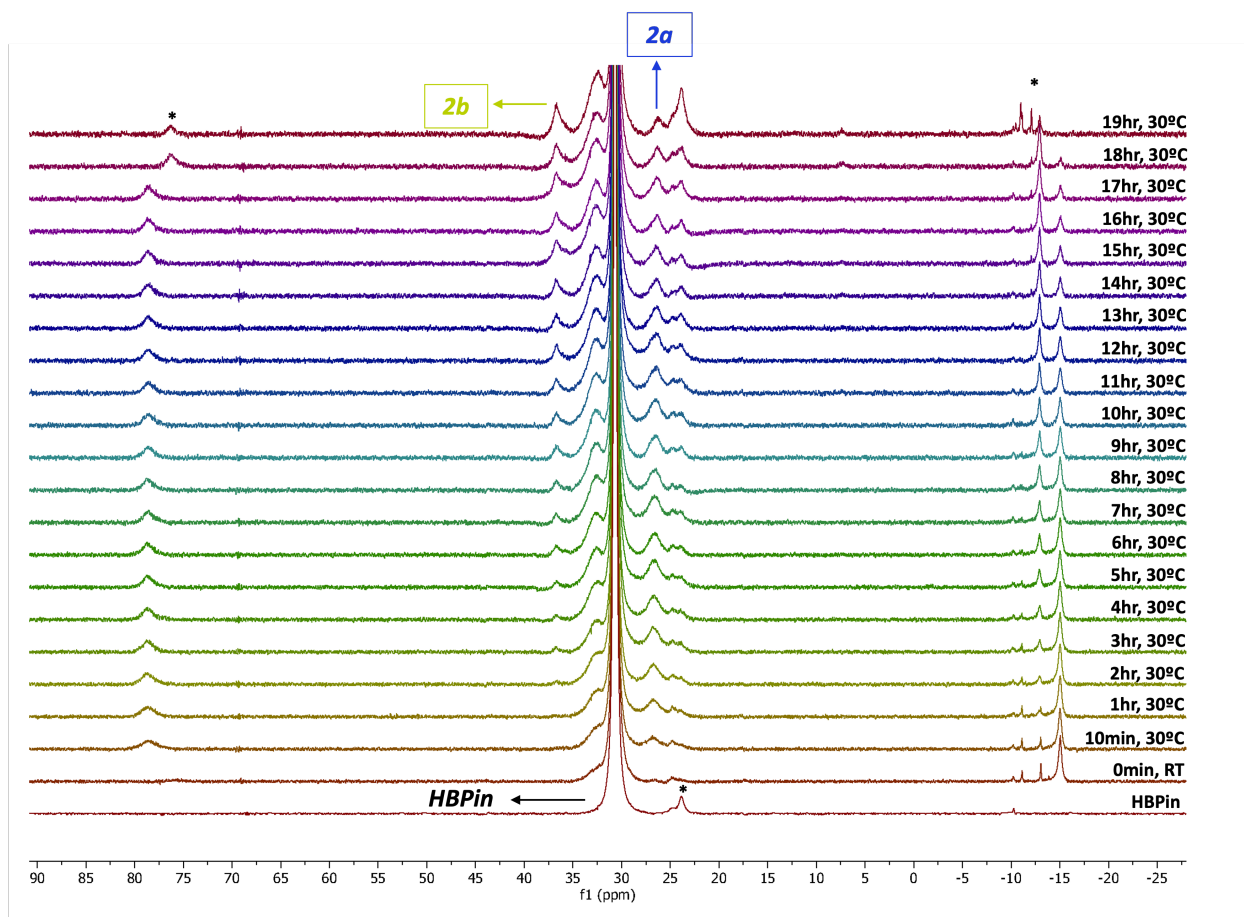


Figure S10. ^{11}B NMR spectra of catalytic hydroboration reaction in THF-d_8 at 30°C , using 1,4-difluorobenzene at internal standard. (* = Unidentified Products)

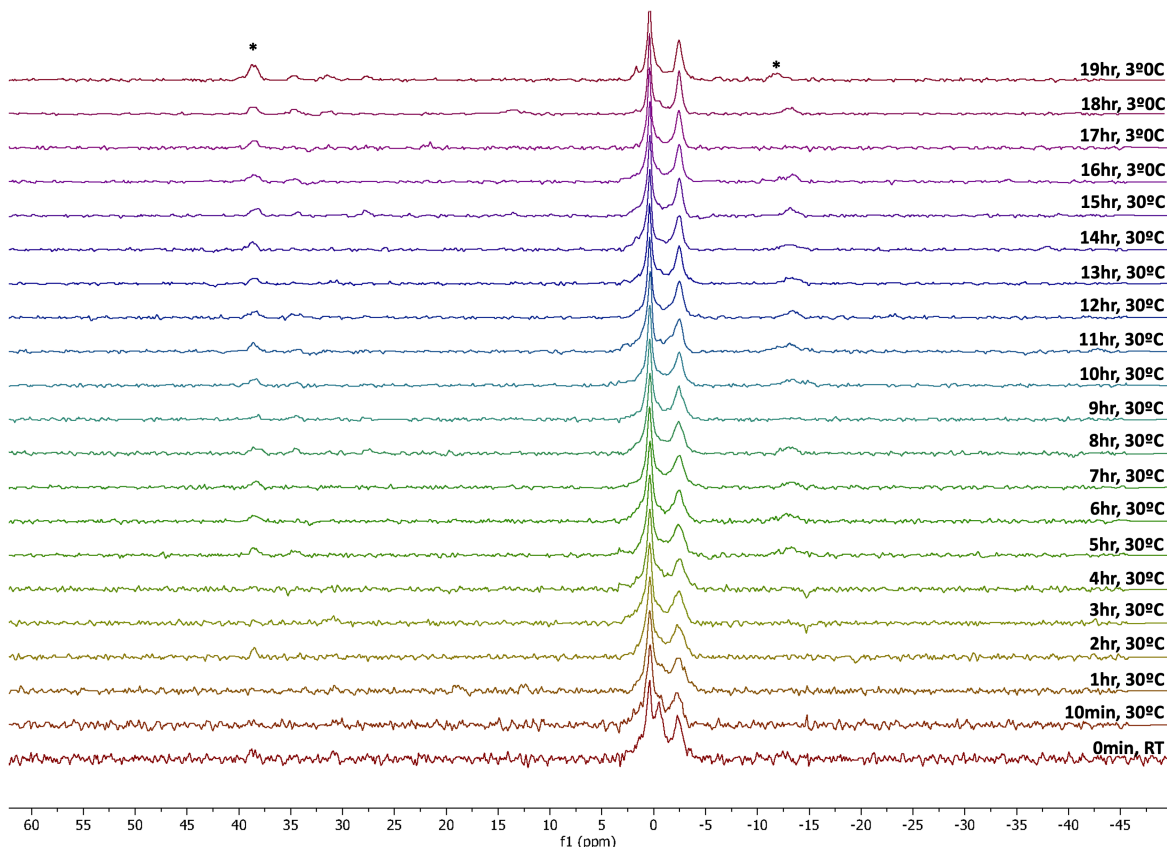
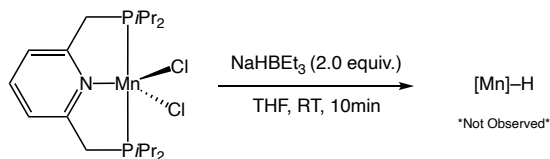


Figure S11. ^{31}P NMR spectra of catalytic hydroboration reaction in THF-d_8 at 30°C , using 1,4-difluorobenzene as internal standard. (* = Unidentified Products)



8.3 Reaction of Mn2 with 2 equiv of NaHBET_3 .

In an argon-filled glovebox a scintillation vial was charged with a stir bar and **Mn2** (75 mg, 0.16 mmol) and THF (3 mL). The resulting yellow solution was chilled to -20°C and NaHBET_3 (0.32 mL of a 1.0 M solution in THF, 0.32 mmol) was added dropwise to the solution with vigorous stirring. The solution underwent a color change from yellow to dark maroon. After 10 minutes of stirring at room temperature, precipitation of solid was observed. The volatiles were removed *in vacuo* yielding a mixture a brown oil that was

redissolved in toluene-d₈ (0.4 mL), filtered through pippete with a glass filter paper plug to a J. Young NMR tube.

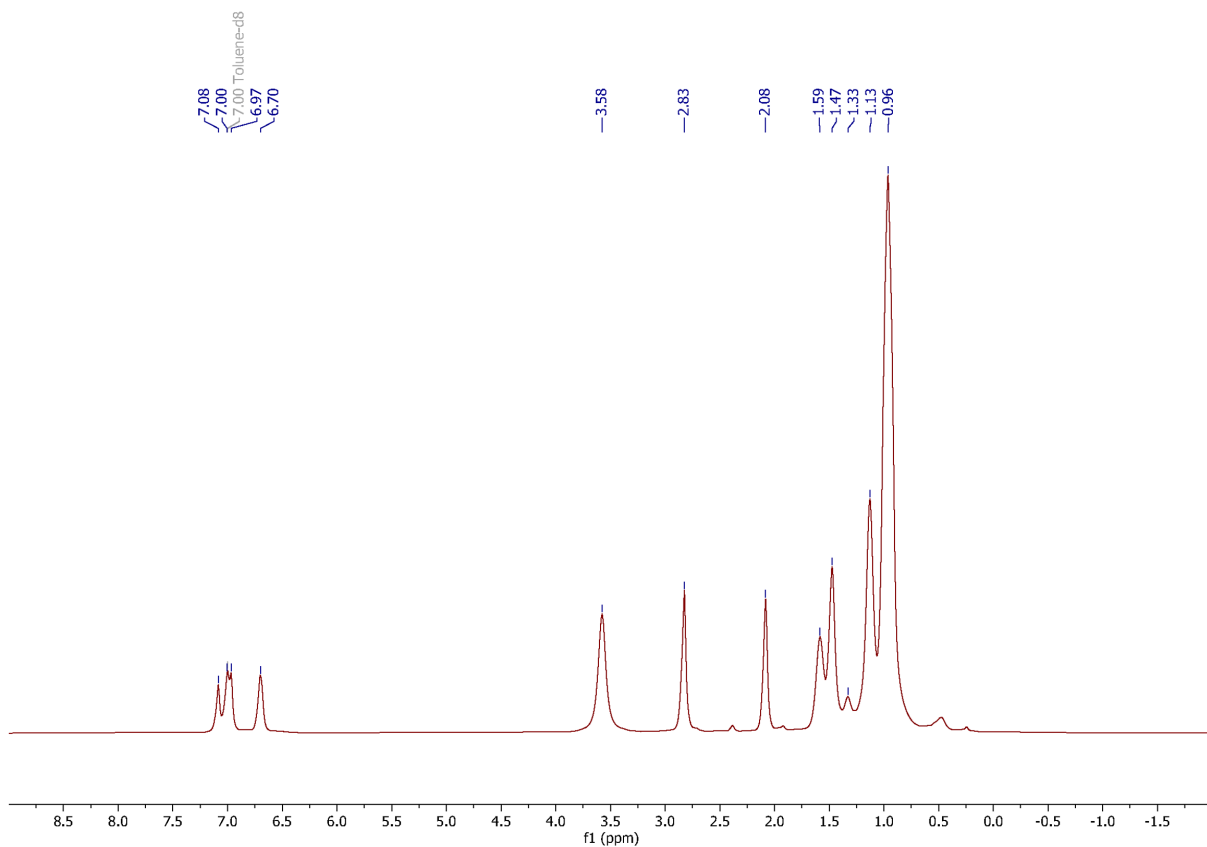


Figure S12. Crude ¹H NMR spectrum NaHBET₃ in toluene-d₈ of the reaction of **Mn2** with 2 equiv. of NaHBET₃.

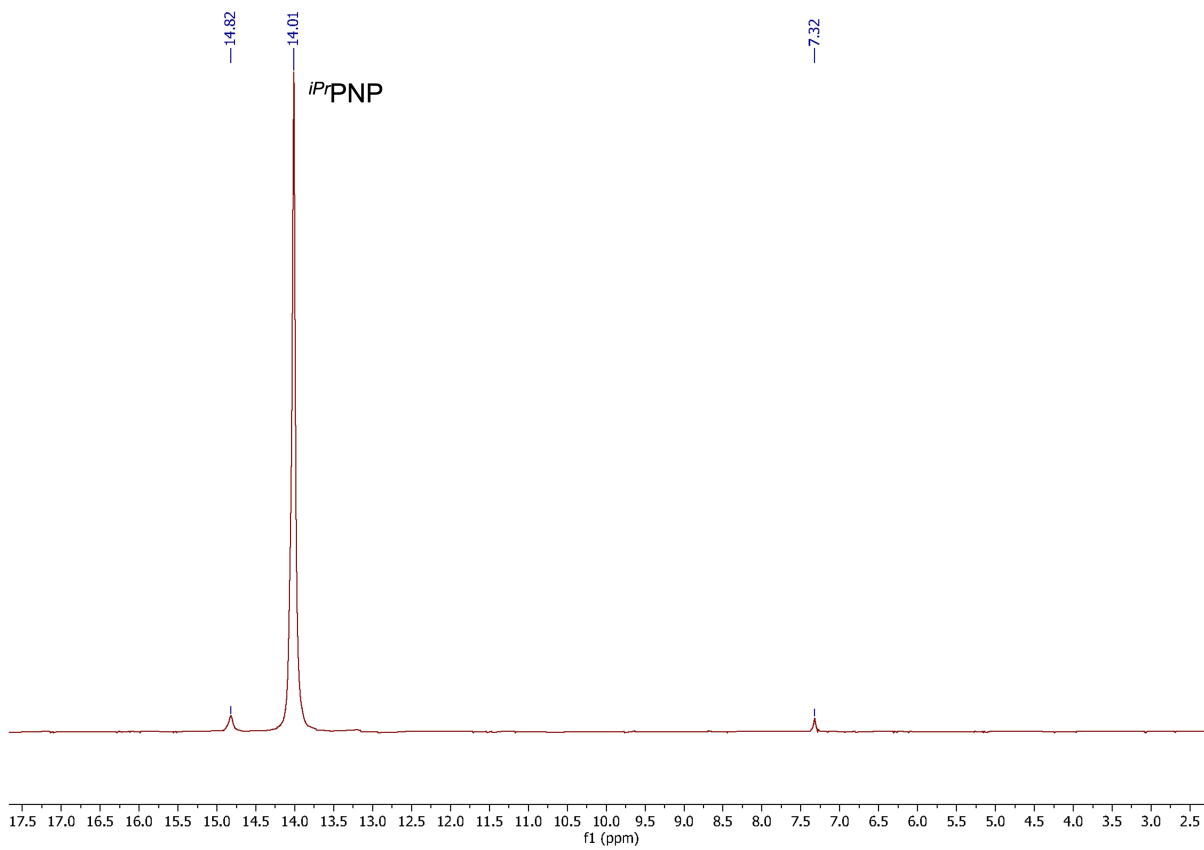
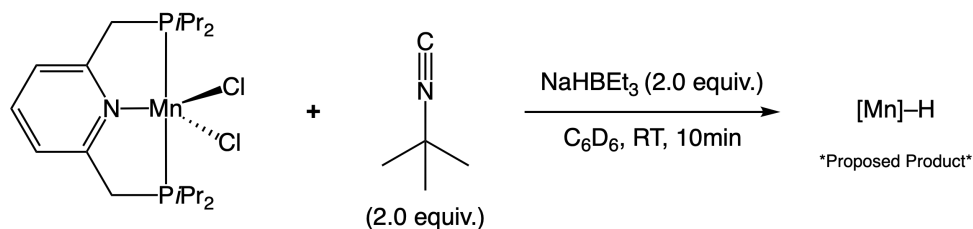


Figure S13. Crude ^{31}P NMR spectrum NaHBET_3 in toluene- d_8 of the reaction of **Mn2** with 2 equiv. of NaHBET_3 .



8.4 Reaction of Mn2 with 2 equiv of NaHBET_3 in the presence of 2 equiv of $t\text{BuCN}$:

In an argon-filled glovebox a 2 mL vial was charged with a stir bar, **Mn2** (15 mg, 0.032 mmol), C_6D_6 (0.25 mL) and *tert*-butyl isocyanide (7.2 μL , 0.064 mmol) and was chilled to $-20\text{ }^\circ\text{C}$. In a separate 2mL vial, NaHBET_3 (64 μL of a 1.0 M solution in THF, 0.064 mmol) was added and the volatiles were removed under vacuum for 60 minutes. The resulting oil was dissolved in C_6D_6 (0.10 mL) and added to the previously chilled mixture in the 2 mL vial. The resulting solution was added dropwise to the chilled C_6D_6 solution resulting in a color change from yellow to dark marron and the precipitation of solid. After stirring

for 10 minutes at room temperature, the resulting mixture was filtered through a pipette with a glass filter paper plug and analyzed by ^1H and ^{31}P NMR spectroscopy.

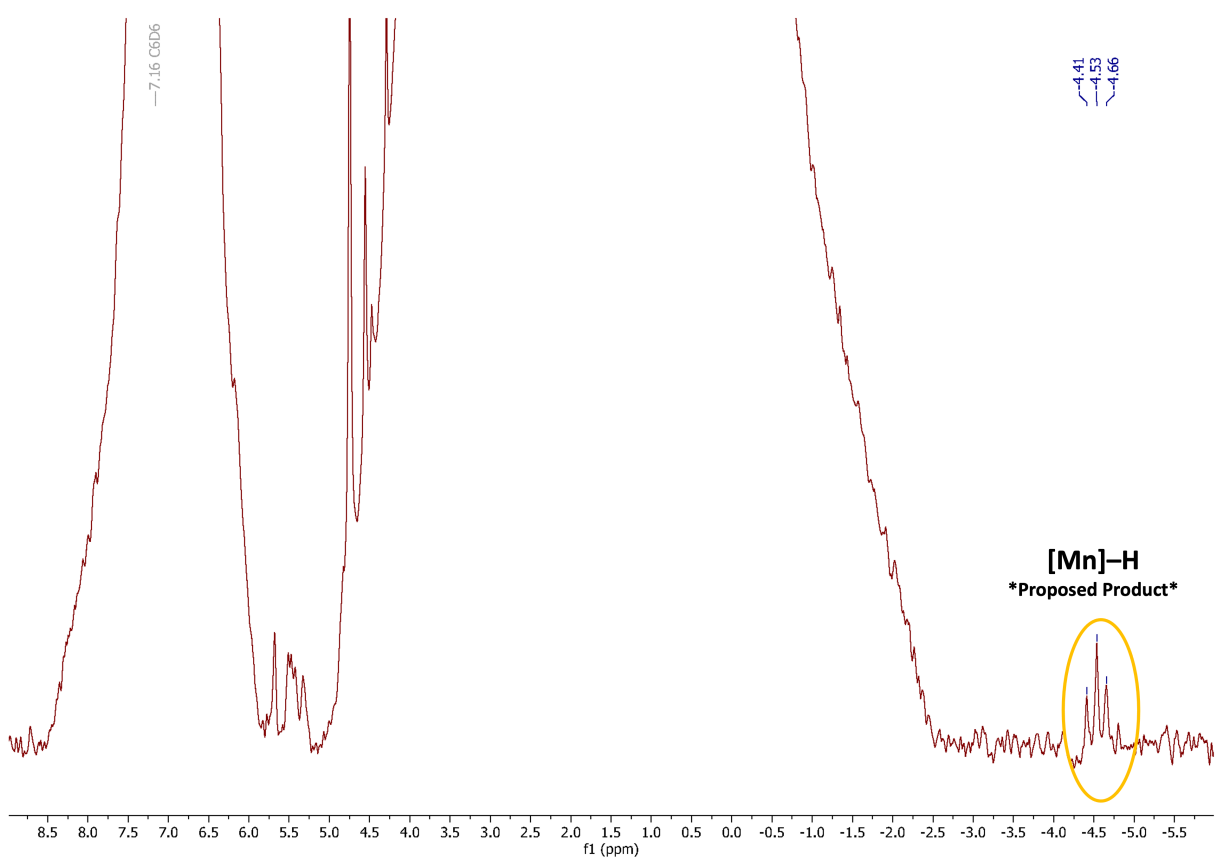


Figure S14. Crude ^1H NMR spectrum NaHBET_3 in C_6D_6 of the reaction of **Mn2** with 2 equiv. of NaHBET_3 in the presence of 2 equiv. of tBuCN in C_6D_6

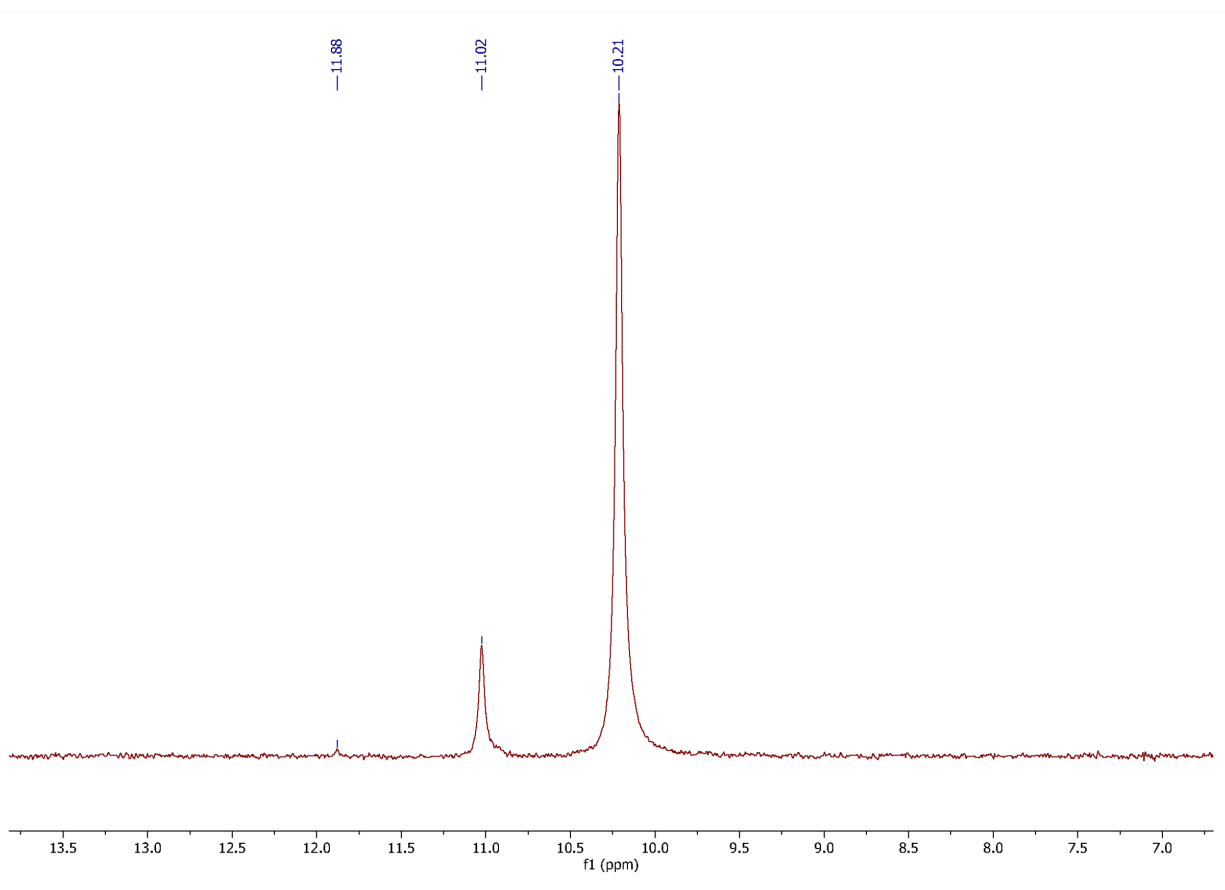
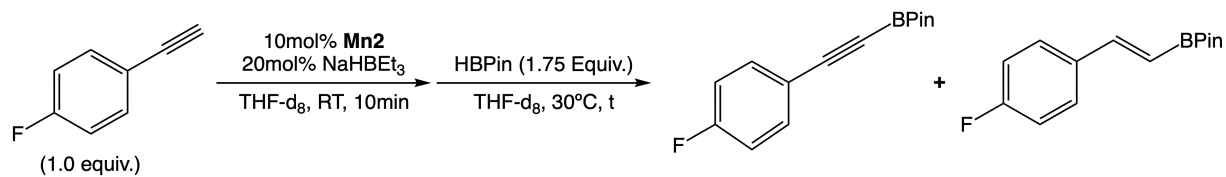


Figure S15. Crude ³¹P NMR spectrum NaHBEt₃ in C₆D₆ of the reaction of **Mn2** with 2 equiv. of NaHBEt₃ in the presence of 2 equiv. of tBuCN in C₆D₆



8.5 Quantitative NMR monitoring of the reaction of **Mn2** / NaHBEt₃ with 4-fluorophenylacetylene followed by addition of HBPIn.

4-fluorophenylacetylene (23 μ L, 0.20 mmol), THF-d₈ (0.28 mL) and 1,4-difluorobenzene (5 μ L, 0.048mmol, internal standard) were mixed in a J. Young NMR tube and the ¹H and ¹⁹F NMR spectra were registered. The solution was then transferred to a 2 mL vial containing **Mn2** (9.3 mg, 0.02 mmol) and chilled to -20°C. In a separate 2 mL vial, NaHBEt₃ (40 μ L of a 1.0 M solution in THF, 0.04 mmol) was added and the volatiles were removed under vacuum for 60 minutes. The resulting oil was redissolved in THF-d₈ (0.04

mL) and added dropwise to the previously chilled. A color change from yellow to dark maroon was observed and solid precipitated. The resulting mixture was filtered through a pipette with a glass filter paper plug into a J. Young NMR tube, sealed, brought out of the glovebox and the ^1H , ^{19}F , and ^{31}P NMR spectra were registered. The tube was brought back into the glovebox, the solution was transferred into the previously used 2 mL vial and HBPIn (51 μL , 0.35 mmol) was added at room temperature. The solution was stirred for 5 minutes, filtered through a fiber glass paper to the J. Young NMR tube, and the ^1H , ^{11}B , ^{19}F , and ^{31}P NMR spectra were registered at room temperature. Afterwards, the mixture was heated up to 30 $^\circ\text{C}$ in the NMR spectrometer probe for 26 hours and the reaction was monitored by ^1H , ^{11}B , ^{19}F , and ^{31}P NMR spectroscopy. Signals attributable to the hydroboration product (**2b**, **9% Yield**), the C-H borylation product (**2a**, **12% Yield**) and the semihydrogenation product (**2c**, **6% Yield**) were identified in the ^1H and/or ^{19}F NMR spectra.

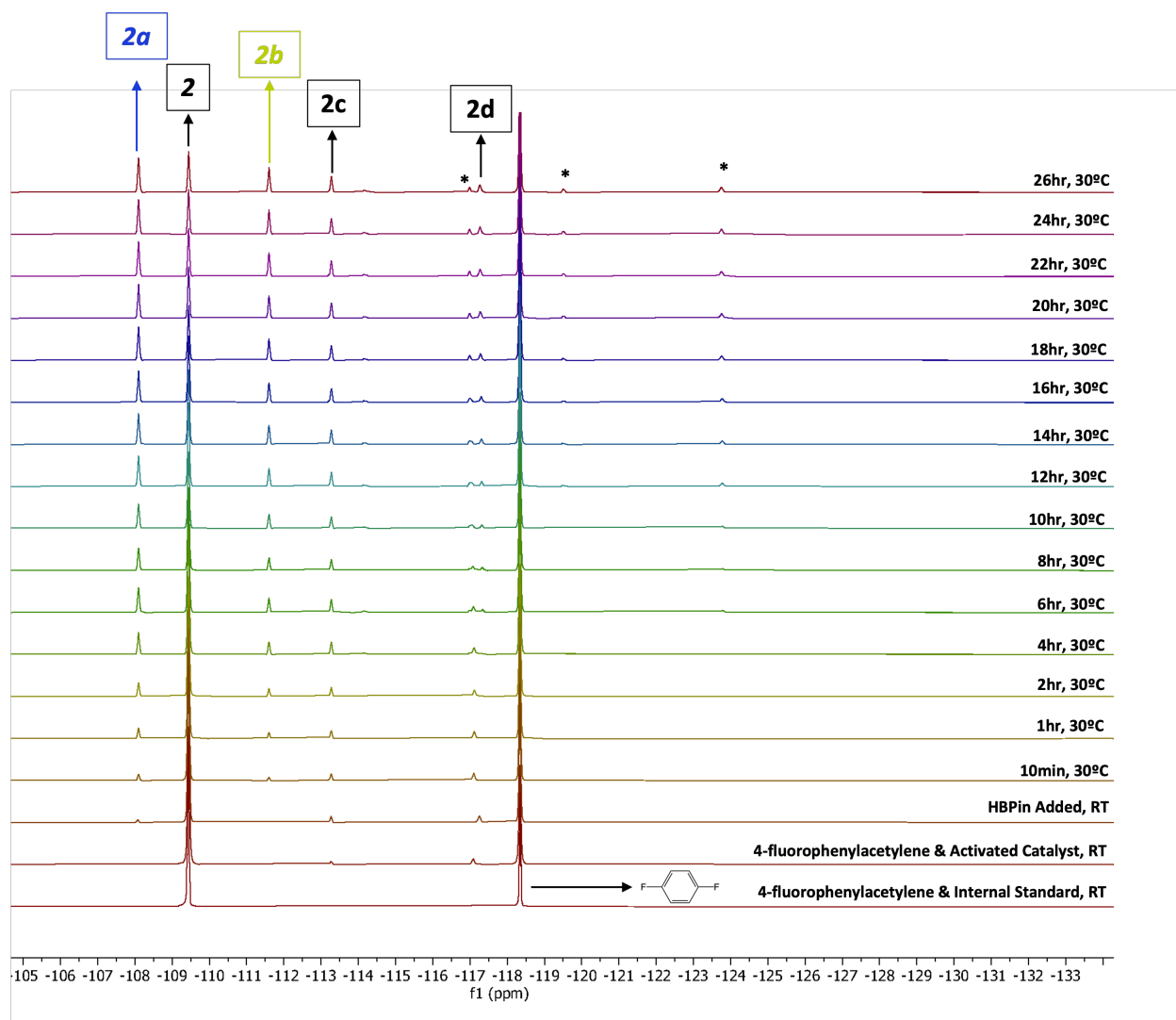


Figure S16. ¹⁹F NMR spectra of the reaction of **Mn²⁺** / NaHBET₃ with 4-fluorophenylacetylene followed by addition of HBPIn in THF-d₈, using 1,4-difluorobenzene as internal standard. (* = Unidentified Products)

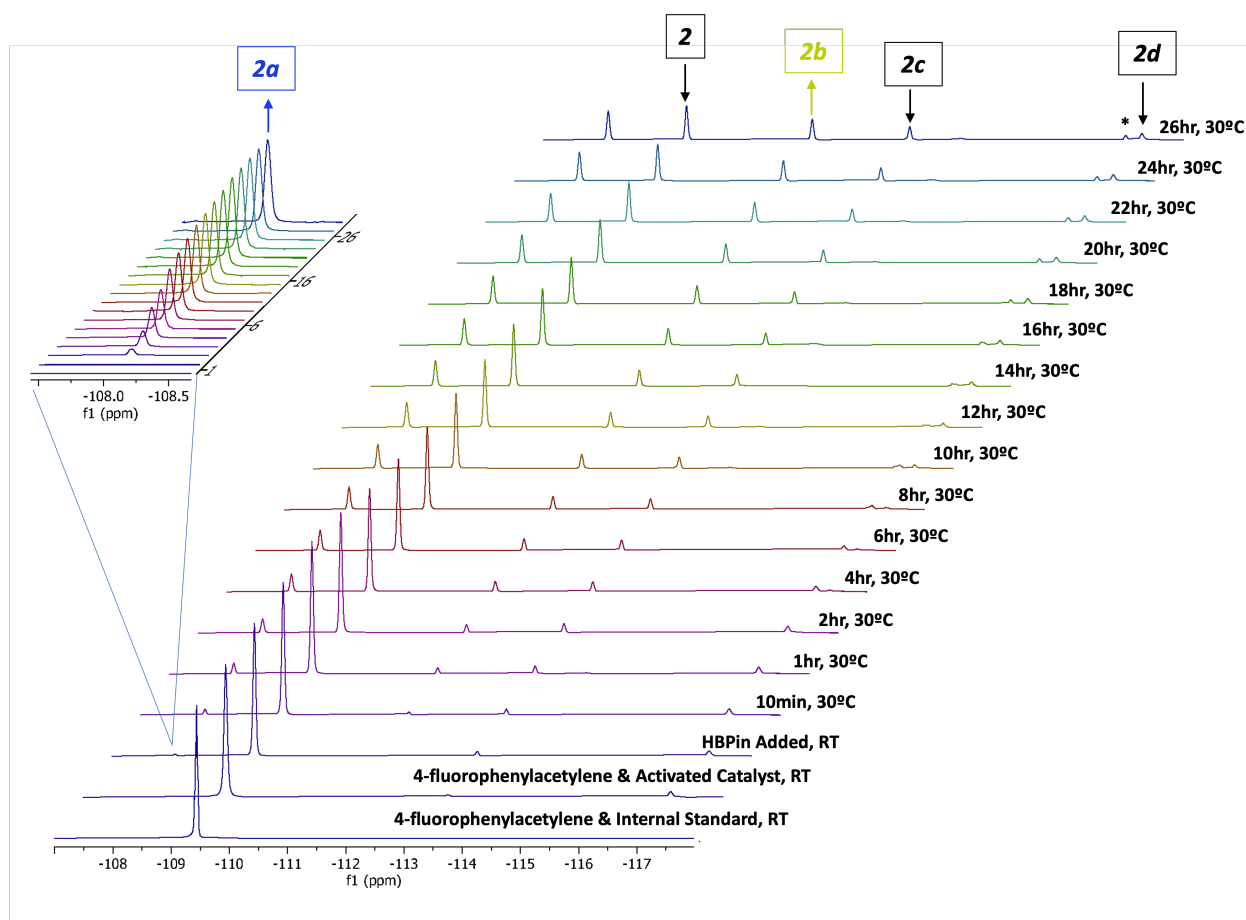


Figure S17. Zoomed in ^{19}F NMR spectra of the reaction of **Mn2** / NaHBET_3 with 4-fluorophenylacetylene followed by addition of HBPIn in THF-d_8 , using 1,4-difluorobenzene as internal standard. (* = Unidentified Products)

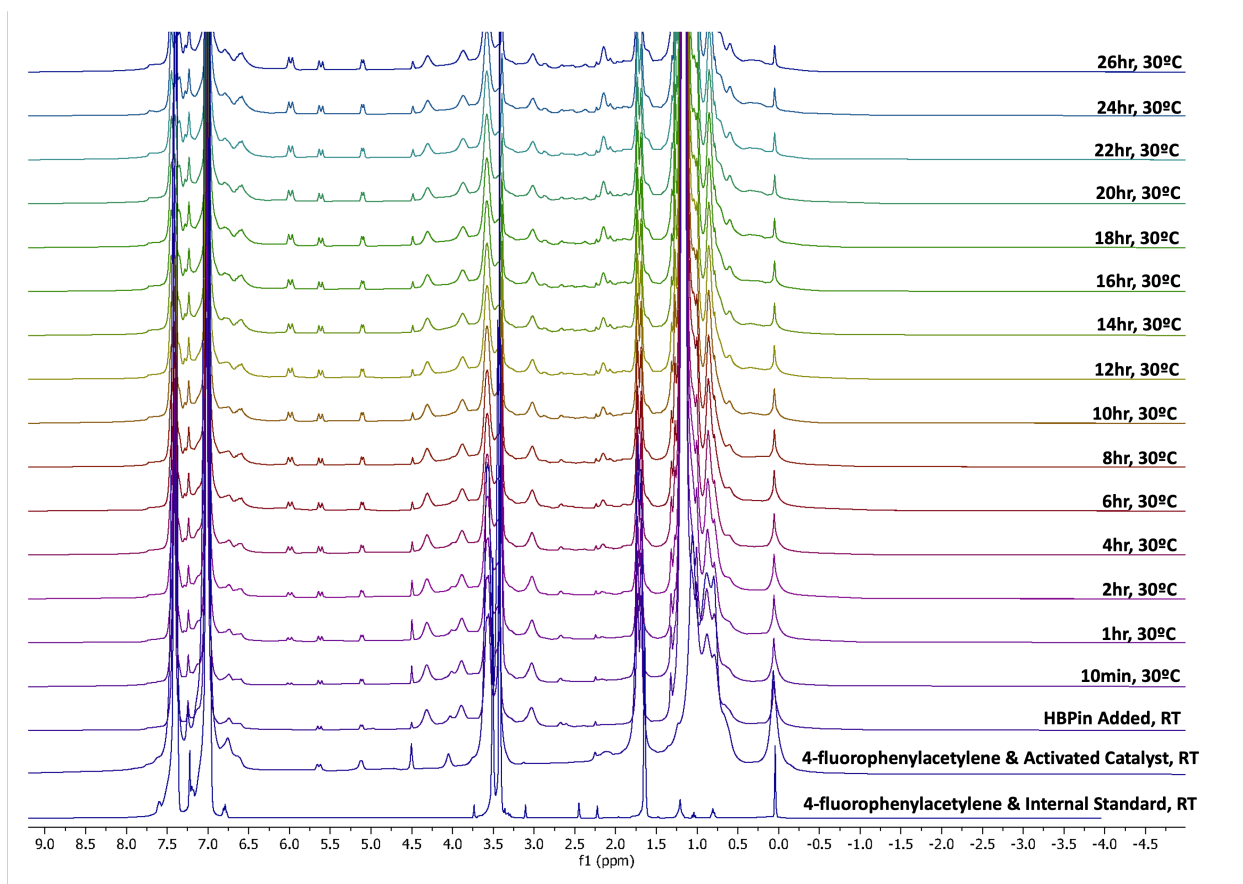


Figure S18. ¹H NMR spectra of the reaction of **Mn2** / NaHBET₃ with 4-fluorophenylacetylene followed by addition of HBPIn in THF-d₈, using 1,4-difluorobenzene as internal standard.

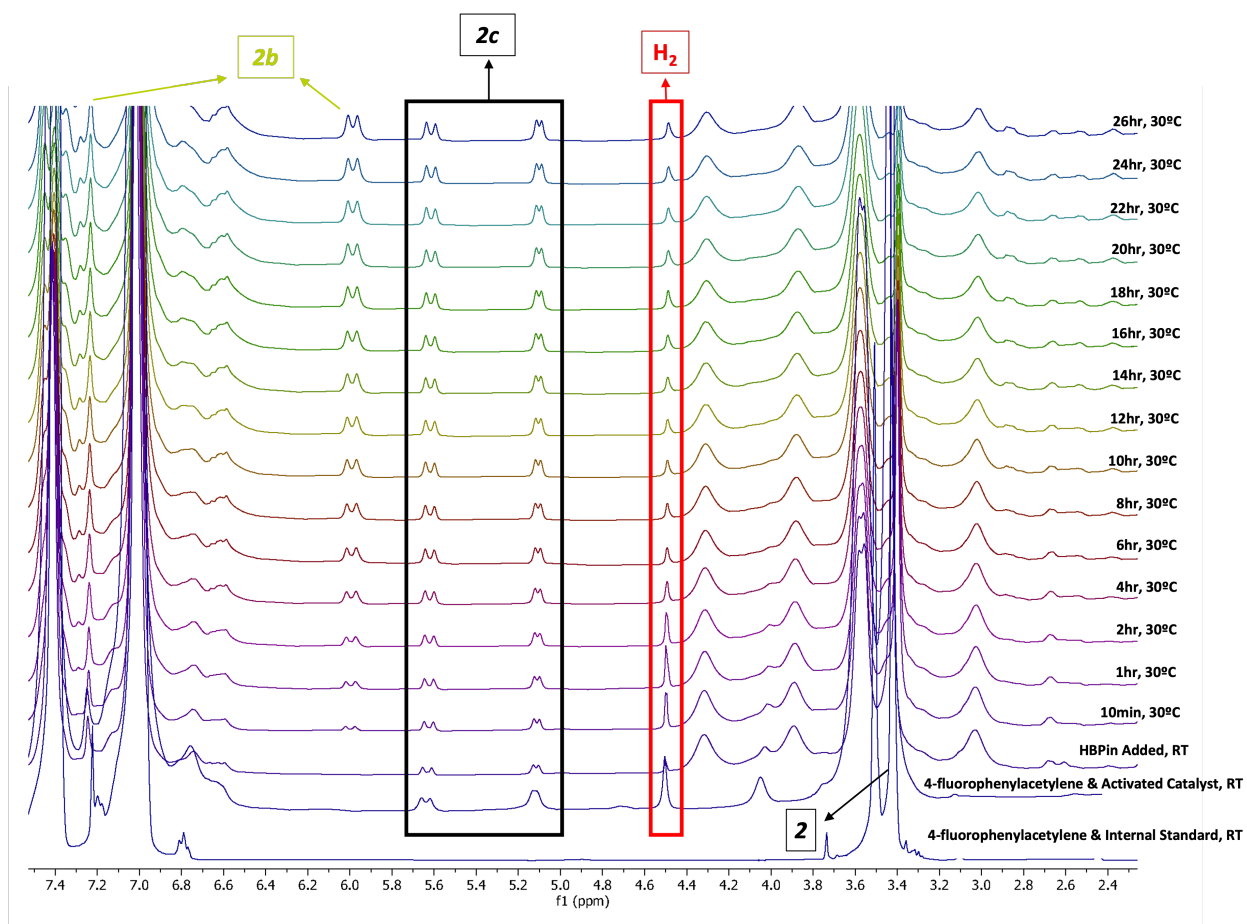


Figure 19. Zoomed in ^1H NMR spectra of the reaction of $\text{Mn}_2 / \text{NaHBET}_3$ with 4-fluorophenylacetylene followed by addition of HBPIn in THF-d_8 , using 1,4-difluorobenzene as internal standard. (* = Unidentified Products)

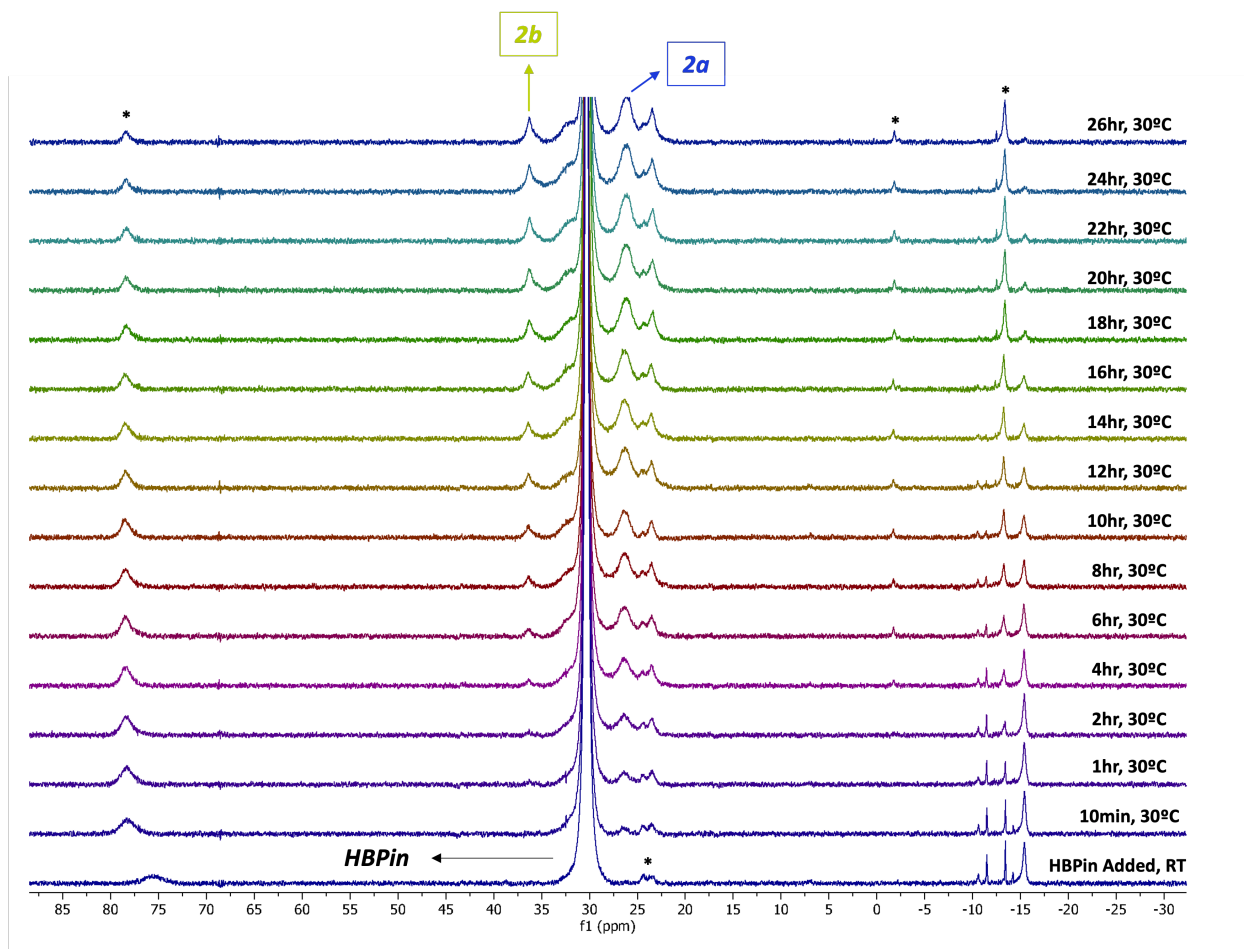


Figure S20. ^{11}B NMR spectra of the reaction of **Mn2** / NaHBEt_3 with 4-fluorophenylacetylene followed by addition of HBPIn in THF-d_8 , using 1,4-difluorobenzene as internal standard. (* = Unidentified Products)

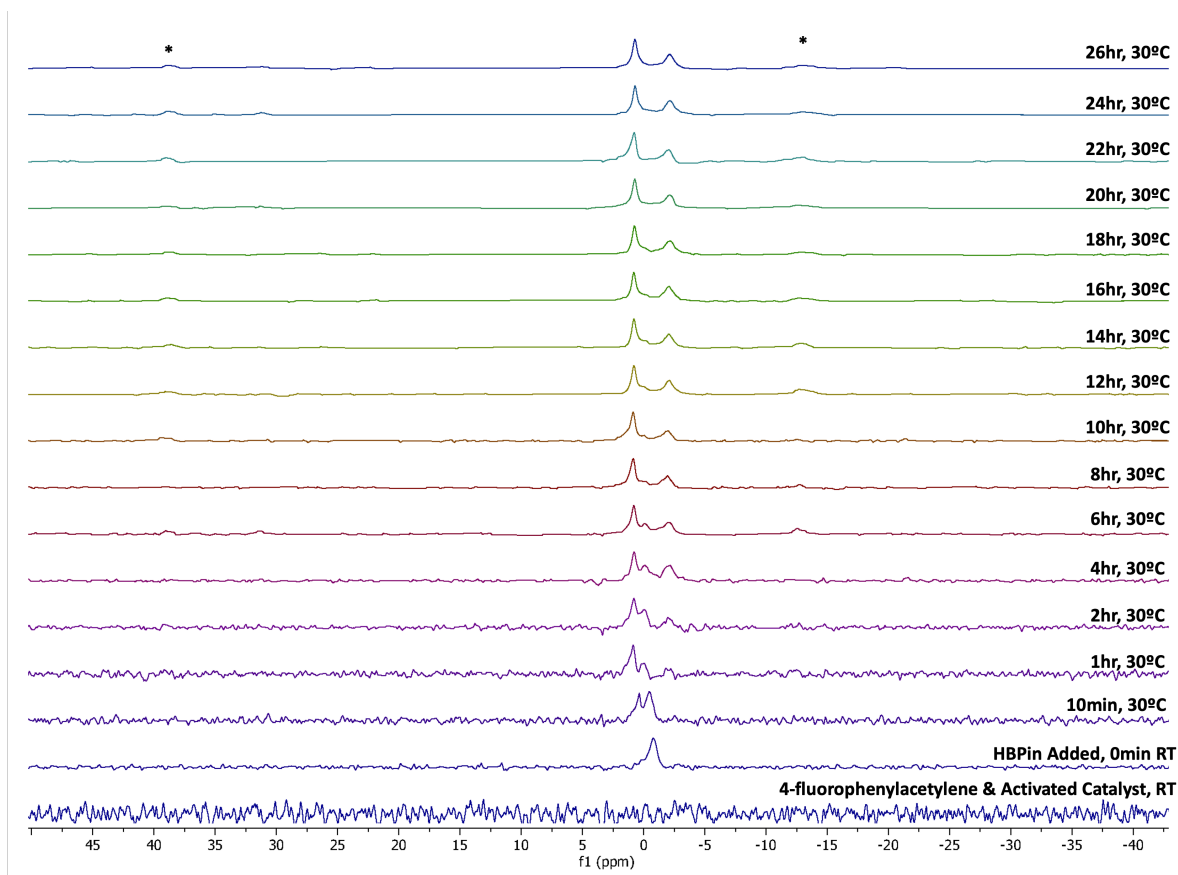
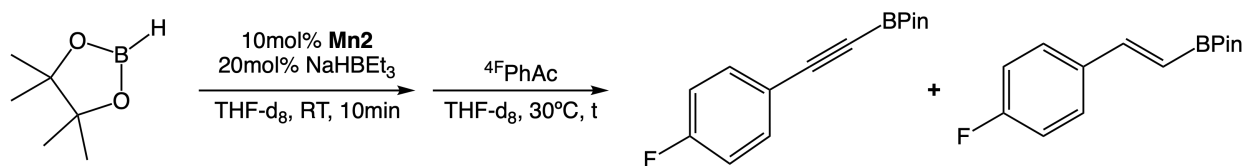


Figure S21. ^{31}P NMR spectra of the reaction of **Mn2** / NaHBET_3 with 4-fluorophenylacetylene followed by addition of HBPIn in THF-d_8 , using 1,4-difluorobenzene as internal standard. (* = Unidentified Products)



8.6 Quantitative NMR monitoring of the reaction of **Mn2** / NaHBET_3 with HBPIn followed by addition of 4-fluorophenylacetylene.

HBPIn (51 μL , 0.35 mmol), THF-d_8 (0.28 mL) and 1,4-difluorobenzene (5 μL , 0.048mmol, internal standard) were mixed in a J. Young NMR tube and the ^1H and ^{11}B NMR spectra were registered. The solution was then transferred to a 2 mL vial containing **Mn2** (9.3 mg, 0.02 mmol) and chilled to -20°C . In a separate 2 mL vial, NaHBET_3 (40 μL of a 1.0 M solution in THF, 0.04 mmol) was added and the volatiles were removed under vacuum for 60 minutes. The resulting oil was redissolved in THF-d_8 (0.04 mL) and added dropwise

to the previously chilled. A color change from yellow to dark maroon was observed and solid precipitated. The resulting mixture was filtered through a pipette with a glass filter paper plug into a J. Young NMR tube, sealed, brought out of the glovebox and the ^1H , ^{11}B , and ^{31}P NMR spectra were registered. The tube was brought back into the glovebox, the solution was transferred into the previously used 2 mL vial and 4-fluorophenylacetylene (23 μL , 0.2 mmol) was added at room temperature. The solution was stirred for 5 minutes, filtered through a fiber glass paper to the J. Young NMR tube, and the ^1H , ^{11}B , ^{19}F , and ^{31}P NMR spectra were registered at room temperature. Afterwards, the mixture was heated up to 30 $^\circ\text{C}$ in the NMR spectrometer probe for 26 hours and the reaction was monitored by ^1H , ^{11}B , ^{19}F , and ^{31}P NMR spectroscopy. Signals attributable to the hydroboration product (**2b**, <5% Yield), the C-H borylation product (**2a**, <5% Yield) and the semihydrogenation product (**2c**, <5% Yield) were identified in the ^1H and/or ^{19}F NMR spectra.

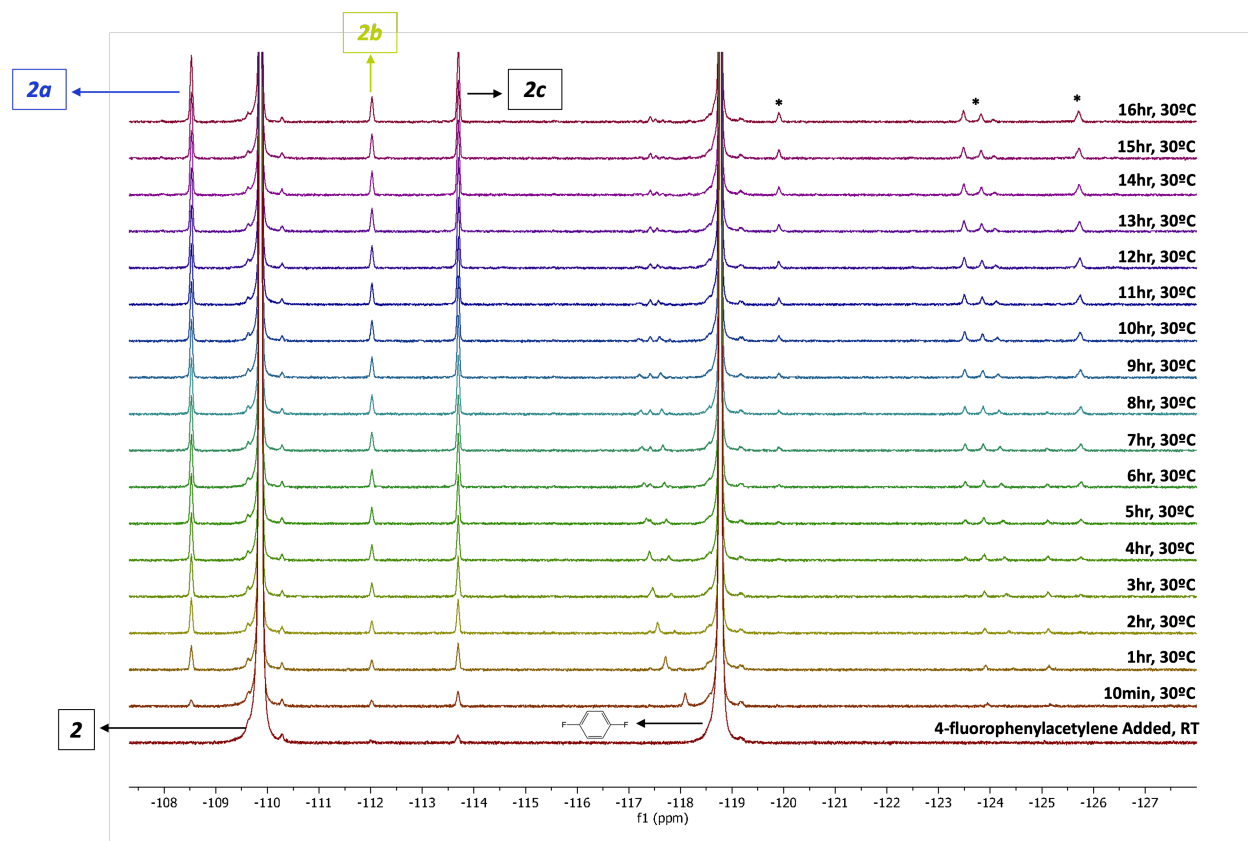


Figure S22. ^{19}F NMR spectra of the reaction of **Mn2** / NaHBET_3 with HBPIn followed by addition of 4-fluorophenylacetylene in THF-d_8 , using 1,4-difluorobenzene as internal standard. (* = Unidentified Products)

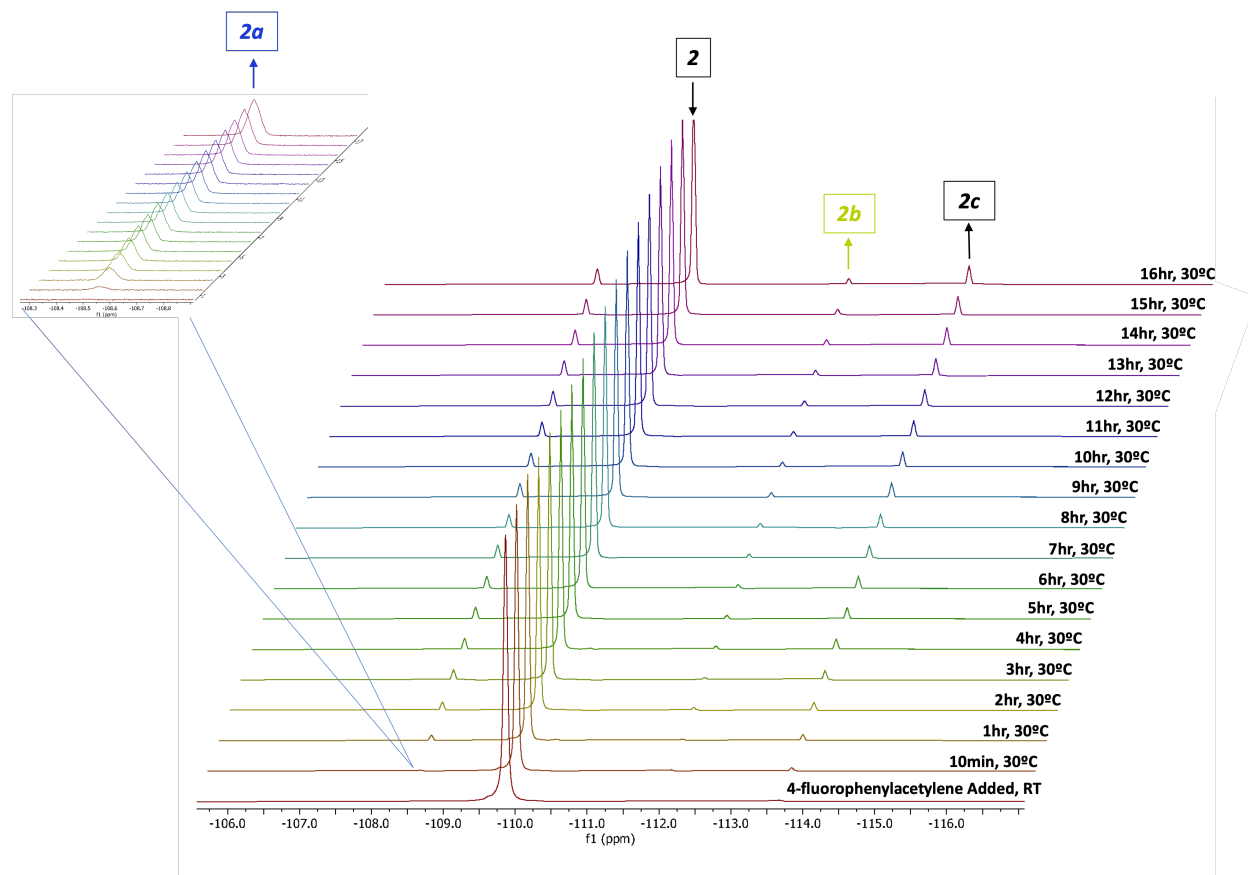


Figure S23. Zoomed in ^{19}F NMR spectra of the reaction of **Mn2** / NaHBEt_3 with HBPIn followed by addition of 4-fluorophenylacetylene in THF-d_8 , using 1,4-difluorobenzene as internal standard.

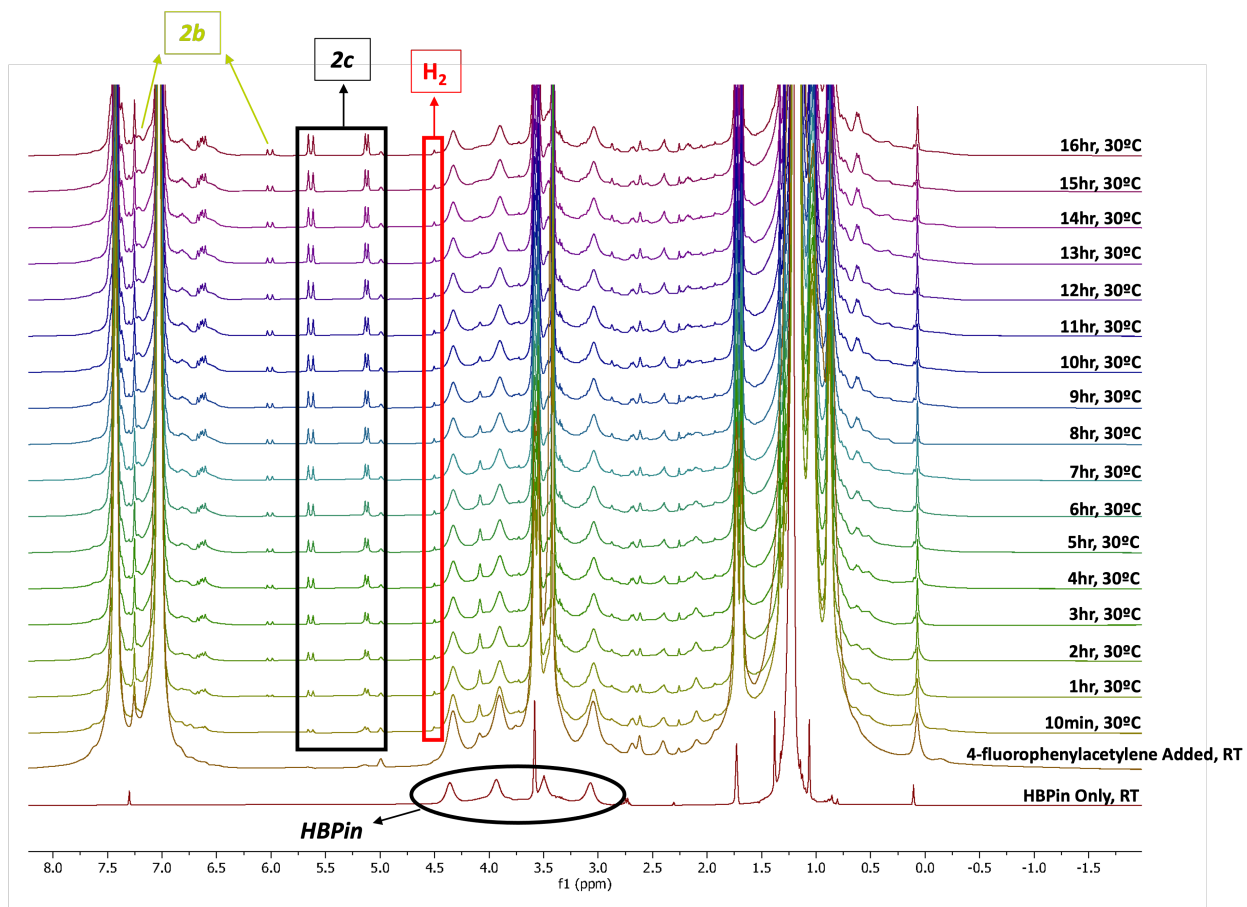


Figure S24. ^1H NMR spectra of the reaction of **Mn2** / NaHBET_3 with HBPIn followed by addition of 4-fluorophenylacetylene in THF-d_8 , using 1,4-difluorobenzene as internal standard.

(* = Unidentified Products)

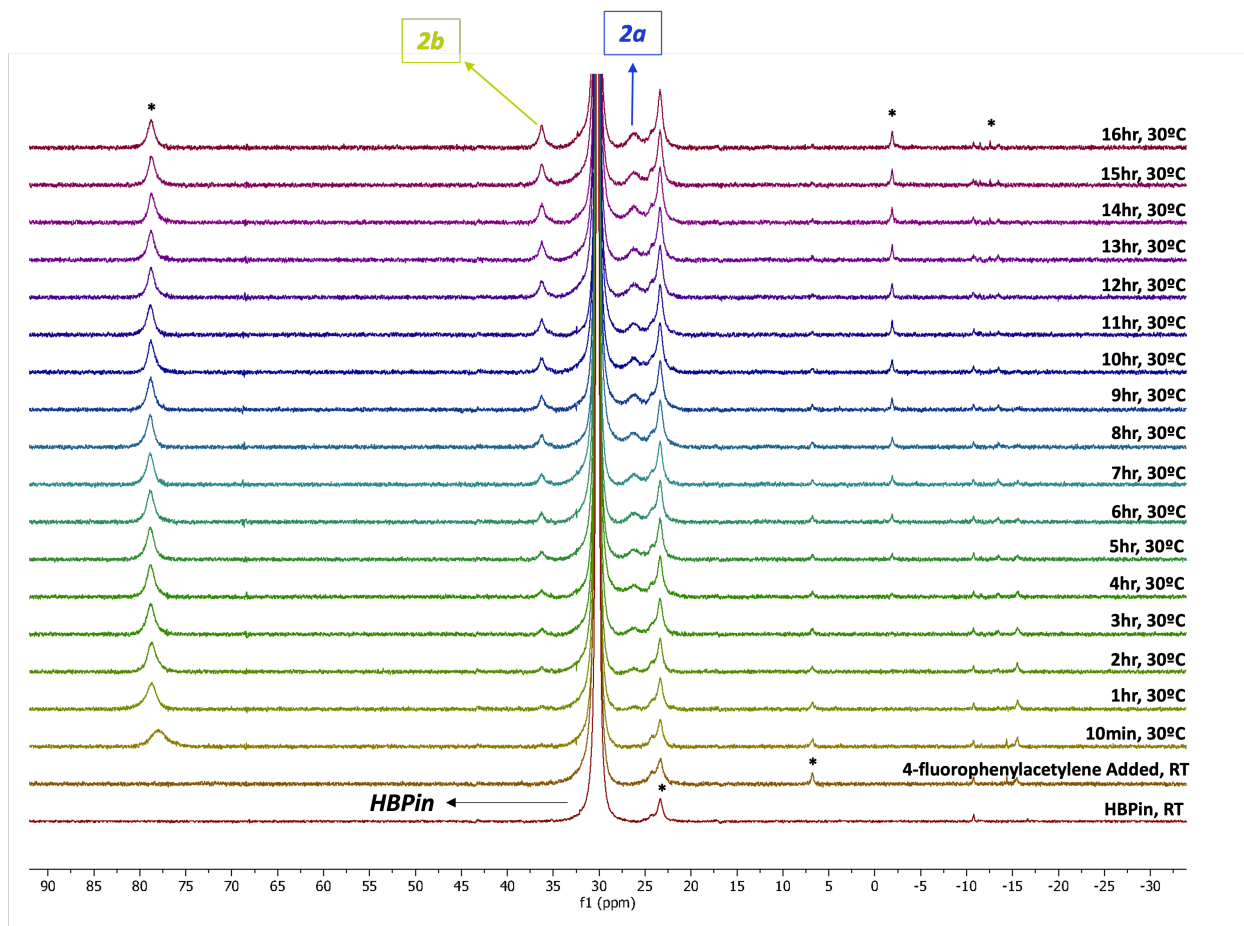


Figure S25. ^{11}B NMR spectra of the reaction of **Mn2** / NaHBET_3 with HBPIn followed by addition of 4-fluorophenylacetylene in THF-d_8 , using 1,4-difluorobenzene as internal standard.

(* = Unidentified Products)

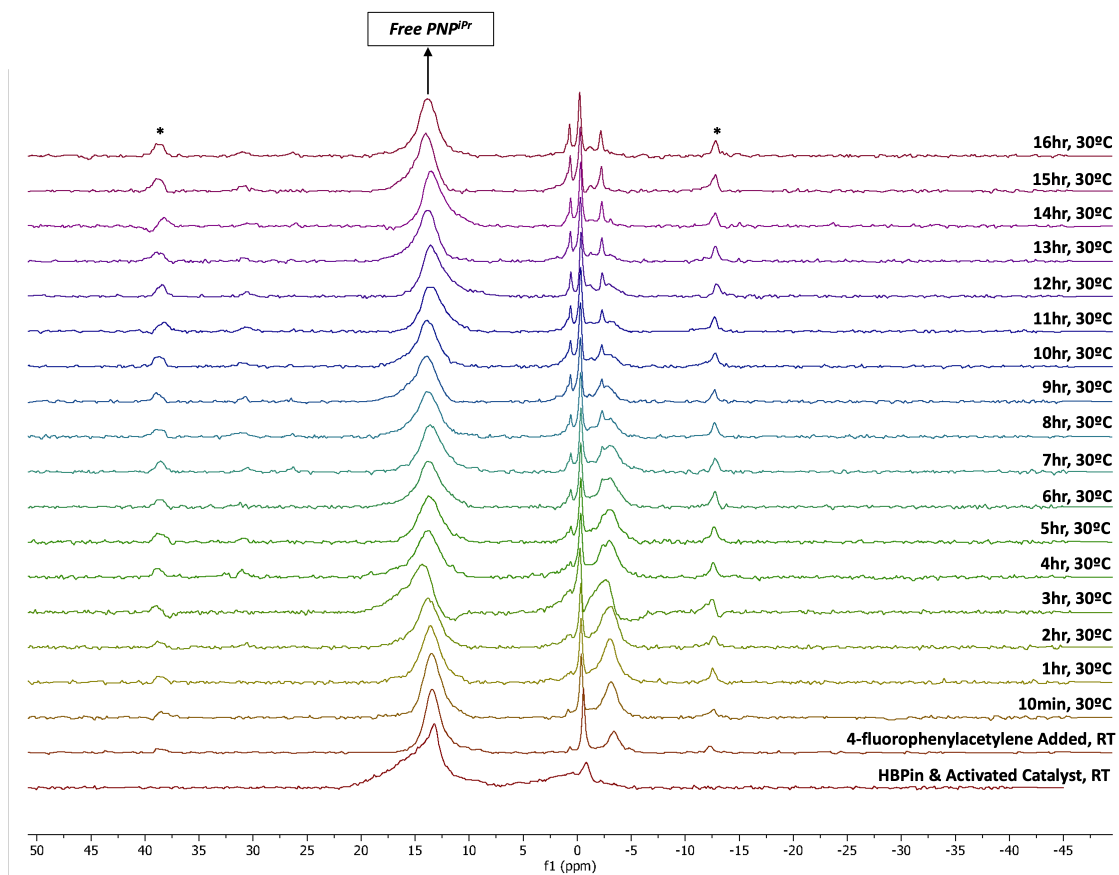


Figure S26. ^{31}P NMR spectra of the reaction of **Mn2** / NaHBET_3 with HBPIn followed by addition of 4-fluorophenylacetylene in THF-d_8 , using 1,4-difluorobenzene as internal standard.

(* = Unidentified Products)

9. NMR spectra of alkenylboronate esters

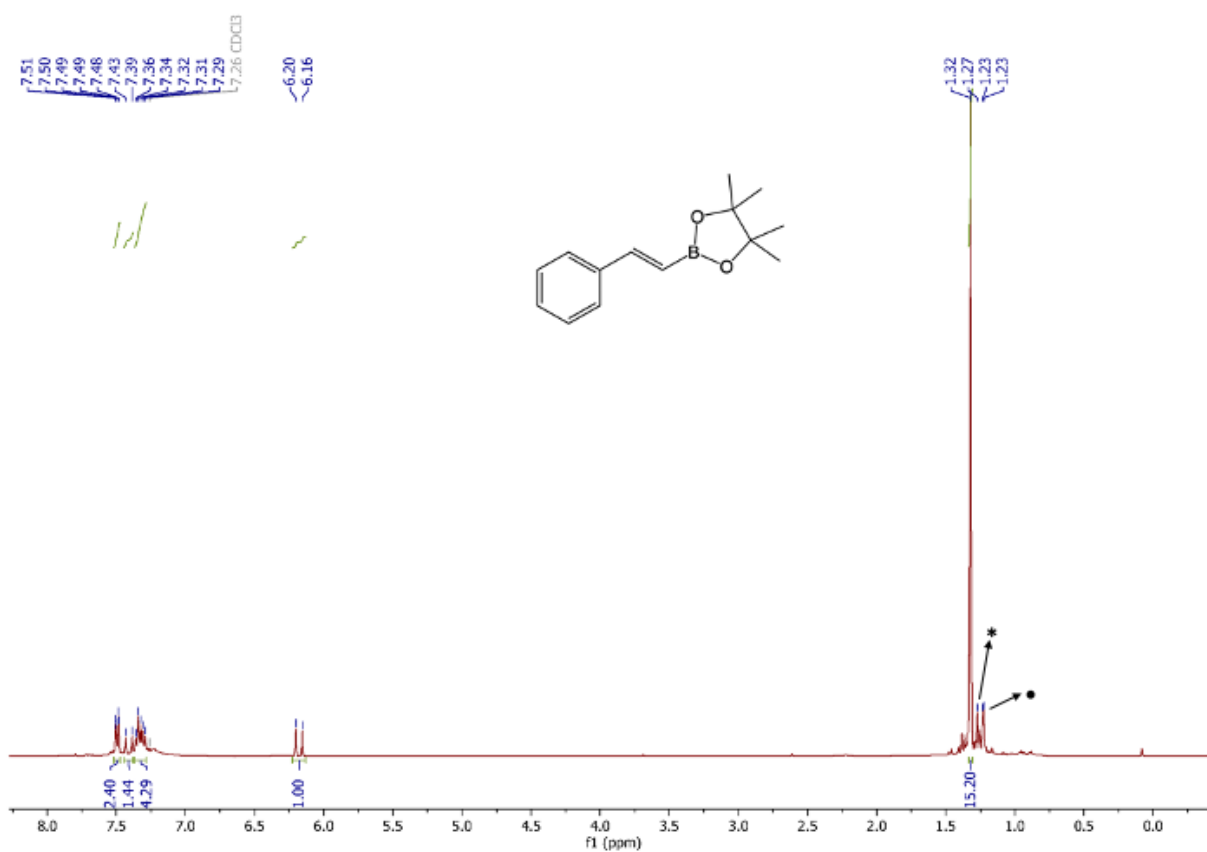


Figure S27: ¹H NMR (CDCl₃, 400MHz) of (*E*)-4,4,5,5-Tetramethyl-2-styryl-1,3,2-dioxaborolane

(• = Peak corresponding to C-H Borylated Product 1a, * = Unidentified Products)

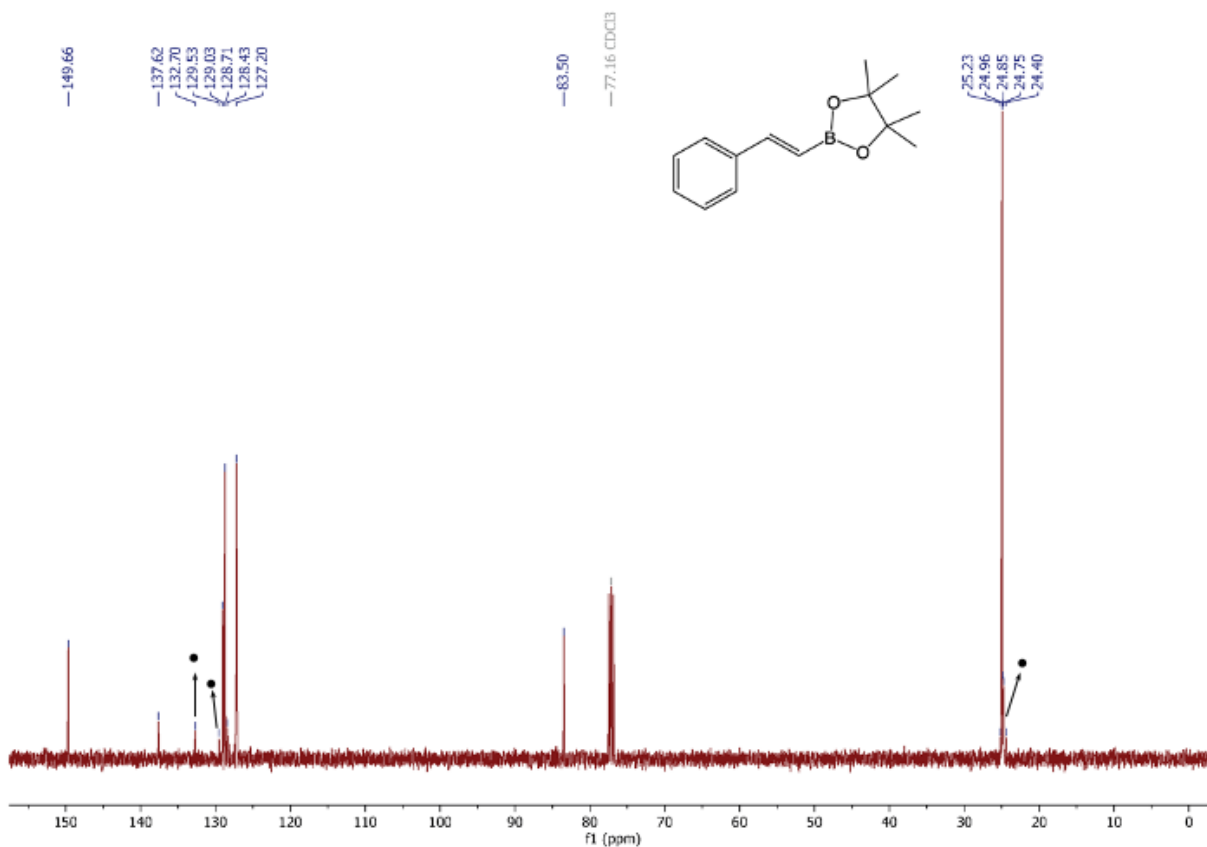


Figure S28: ^{13}C NMR (CDCl₃, 100MHz) of (*E*)-4,4,5,5-Tetramethyl-2-styryl-1,3,2-dioxaborolane (• = Peak corresponding to C-H Borylated Product 1a)

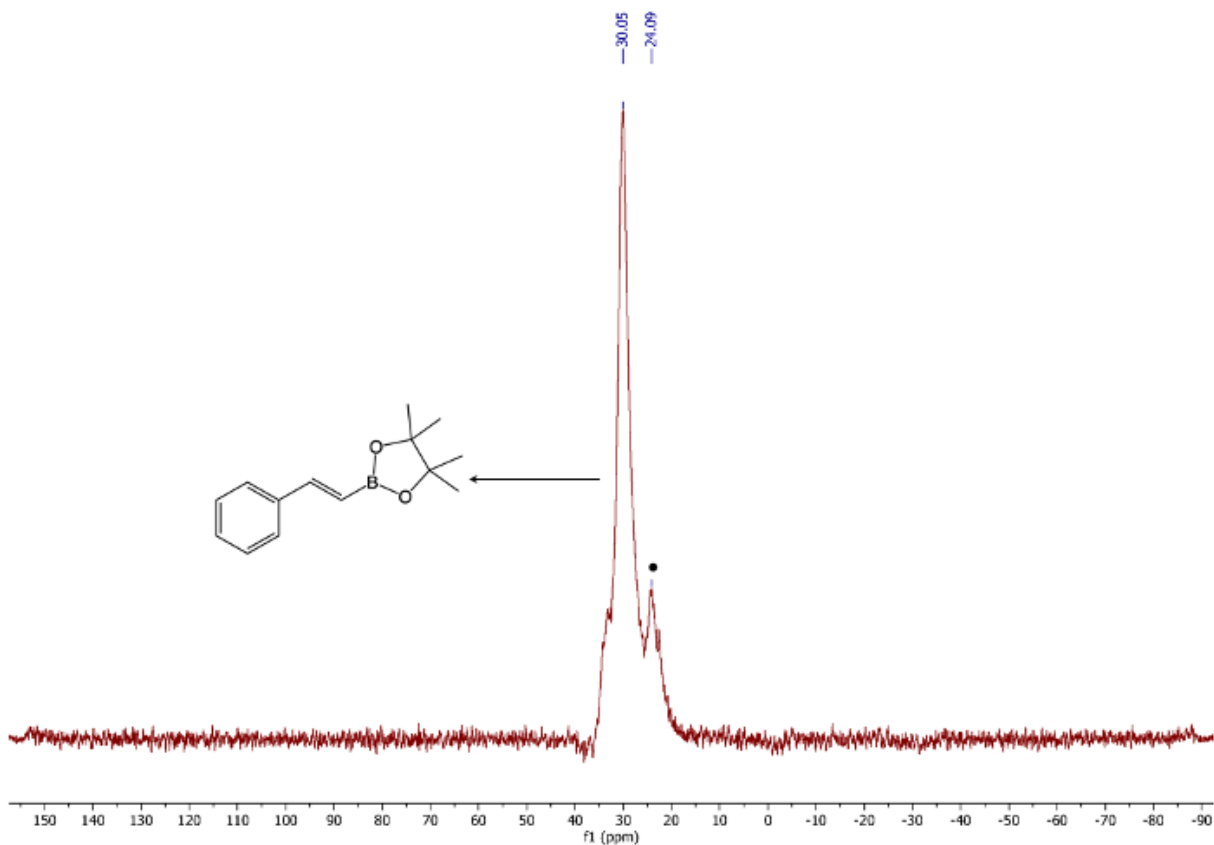


Figure S29: ^{11}B NMR (CDCl_3 , 128 MHz) of *(E)*-4,4,5,5-Tetramethyl-2-styryl-1,3,2-dioxaborolane (• = Peak corresponding to C-H Borylated Product 1a)

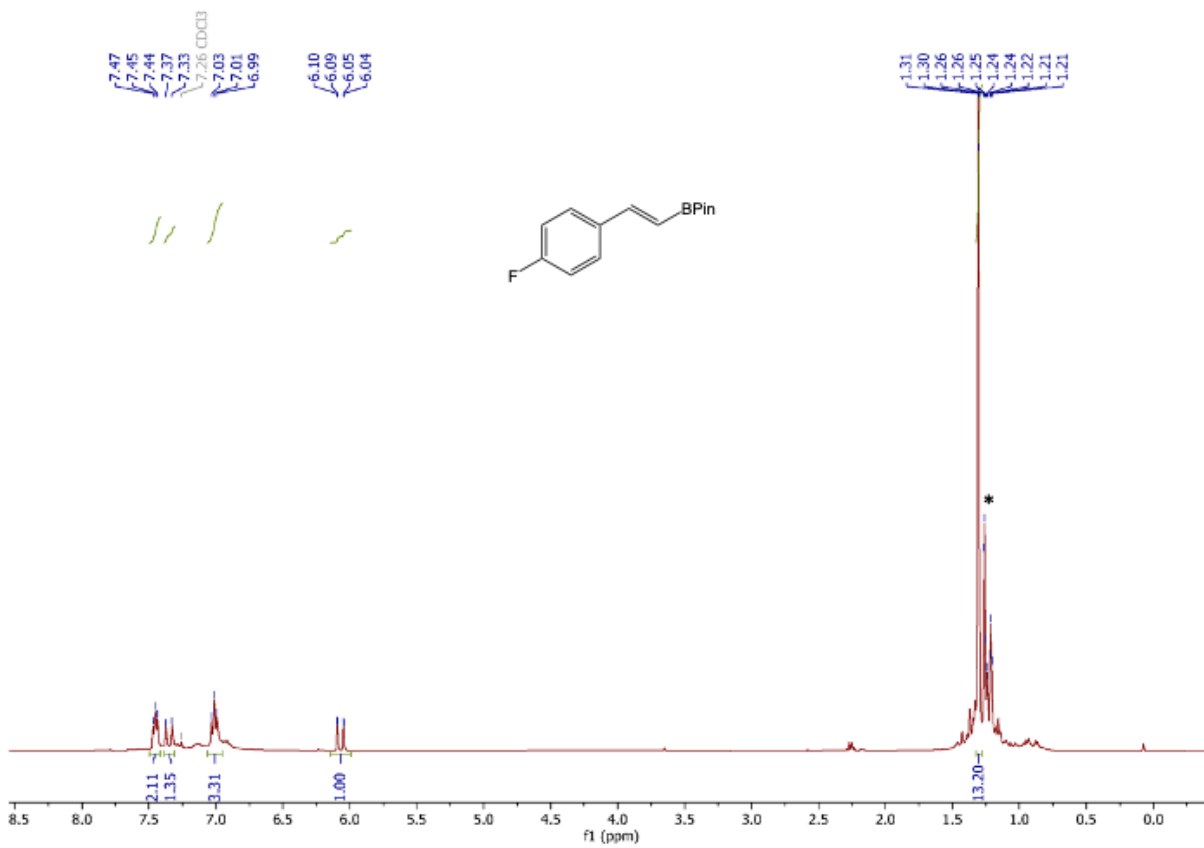


Figure S30: ¹H NMR (CDCl₃, 400MHz) of 2-[(1E)-2-(4-Fluorophenyl)ethenyl]-4,4,5,5-tetramethyl-1,3,2-dioxaborolane (* = Unidentified Products)

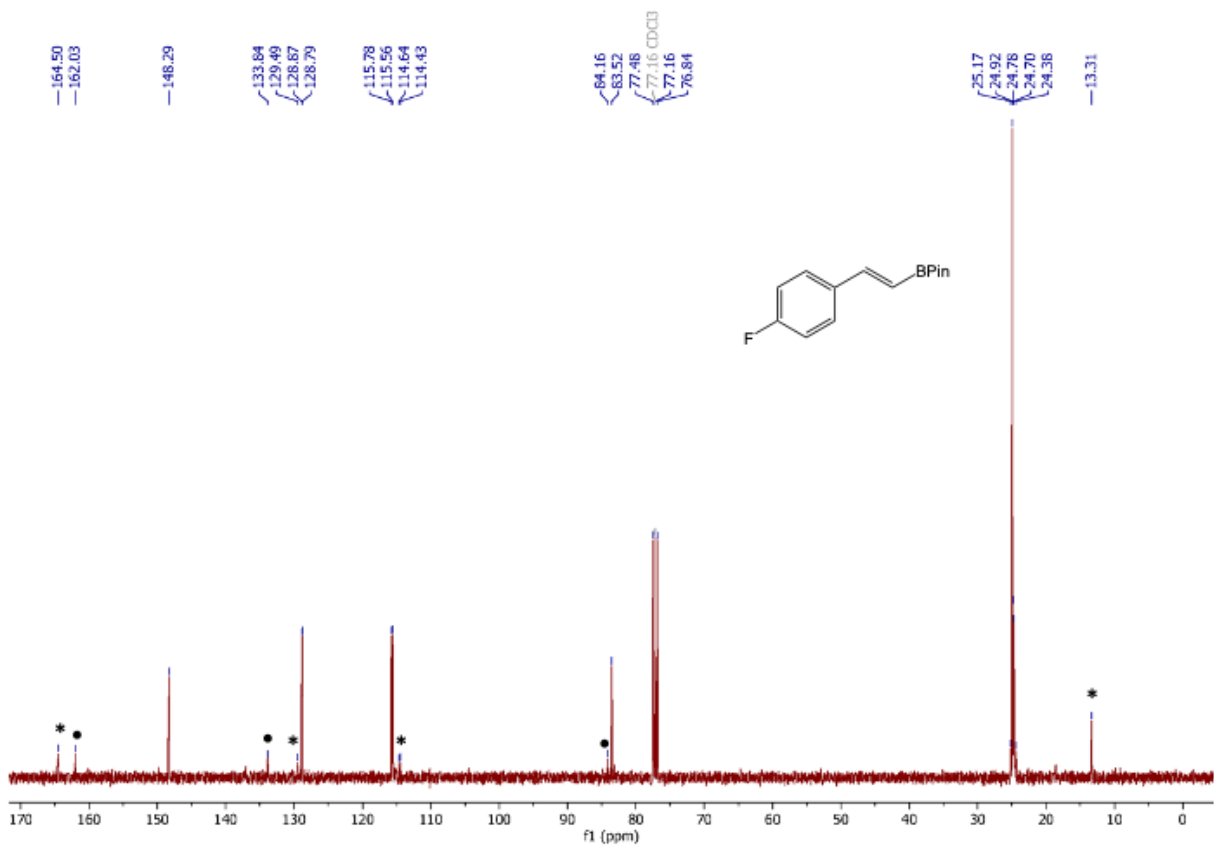


Figure S31: ^{13}C NMR (CDCl_3 , 100MHz) of 2-[(1*E*)-2-(4-Fluorophenyl)ethenyl]-4,4,5,5-tetramethyl-1,3,2-dioxaborolane (• = Peak corresponding to C-H Borylated Product 2a, * = Unidentified Products)

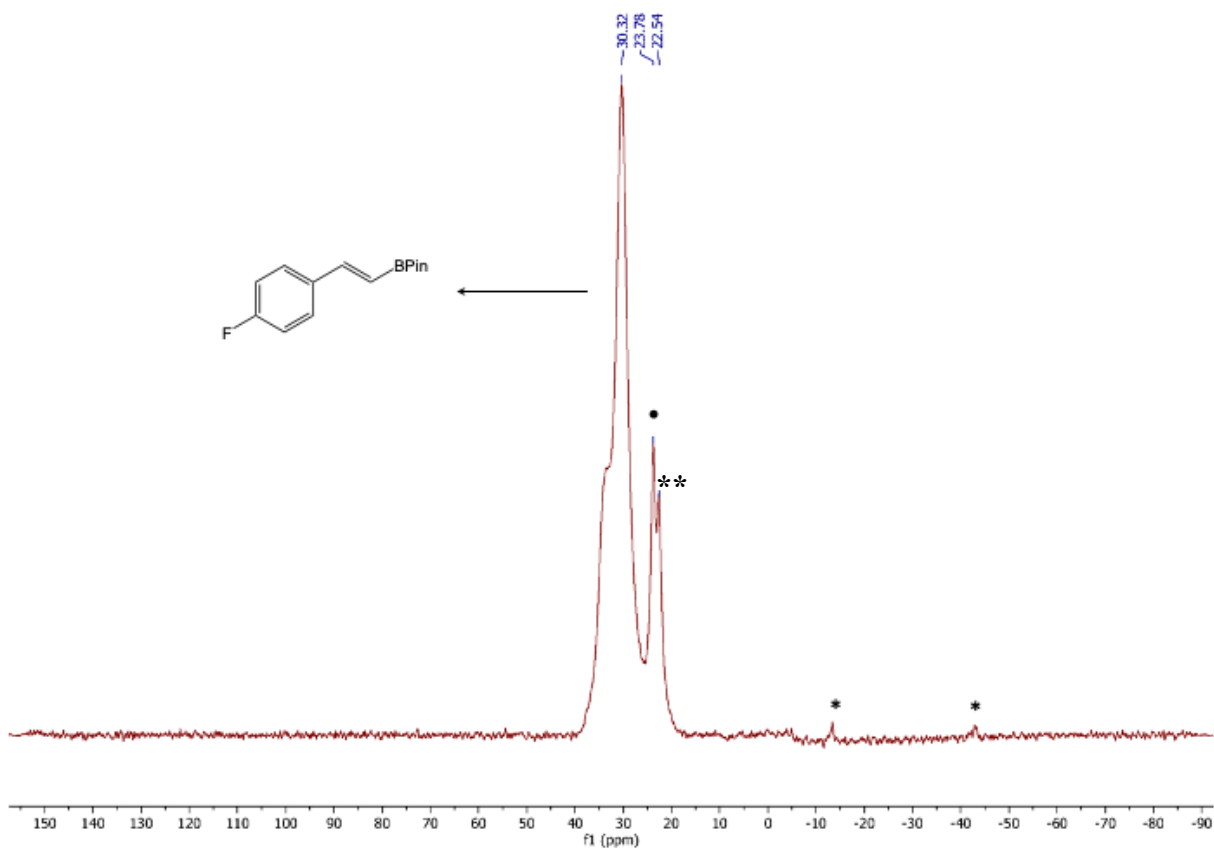


Figure S32: ^{11}B NMR (CDCl_3 , 128 MHz) of 2-[(1*E*)-2-(4-Fluorophenyl)ethenyl]-4,4,5,5-tetramethyl-1,3,2-dioxaborolane (• = Peak corresponding to C-H Borylated Product 2a, * = Unidentified Products, ** = Impurity from HBpin)

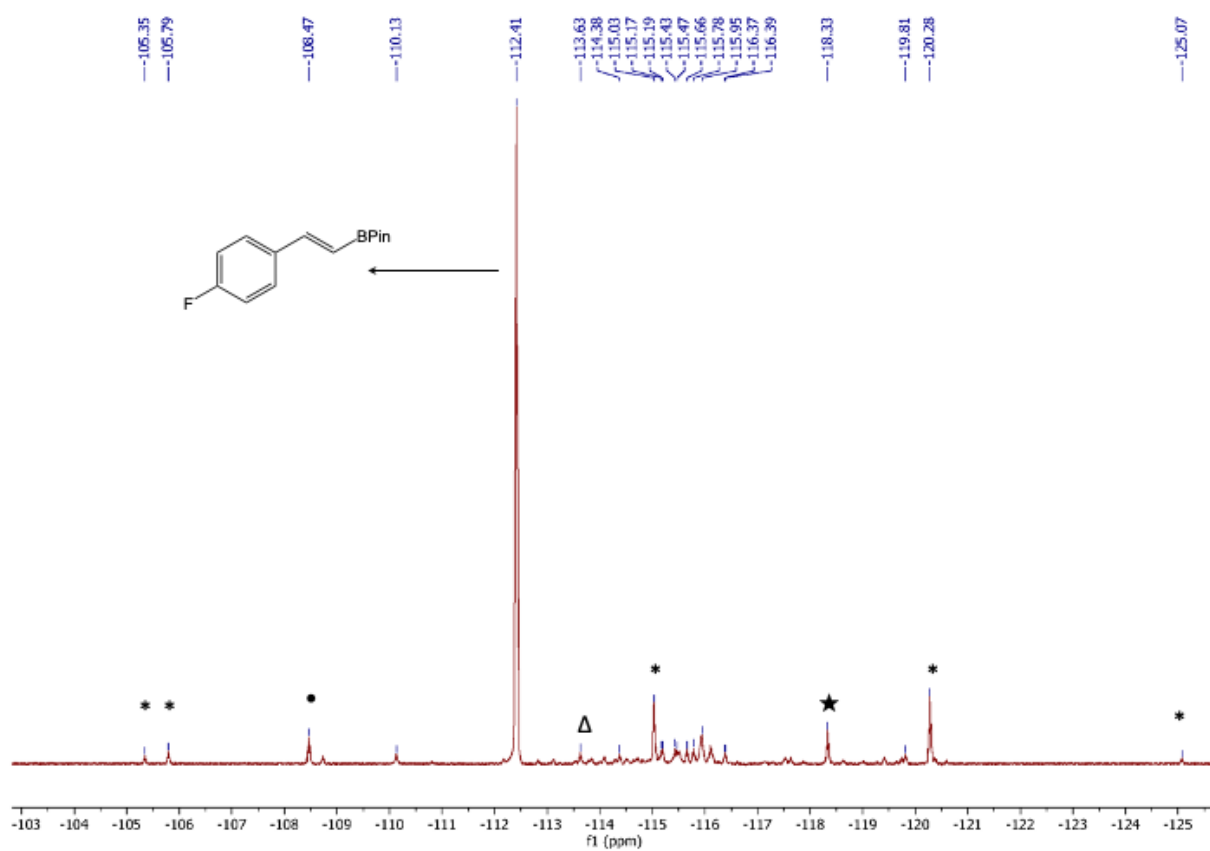


Figure S33: ^{19}F NMR (CDCl_3 , 376 MHz) of (2-[(1*E*)-2-(4-Fluorophenyl)ethenyl]-4,4,5,5-tetramethyl-1,3,2-dioxaborolane (• = Peak corresponding to C-H Borylated Product 2a, ★ = Peak corresponding to Semihydrogenated Product 2c, Δ = Peak corresponding to Hydrogenated Product 2d, * = Unidentified Products)

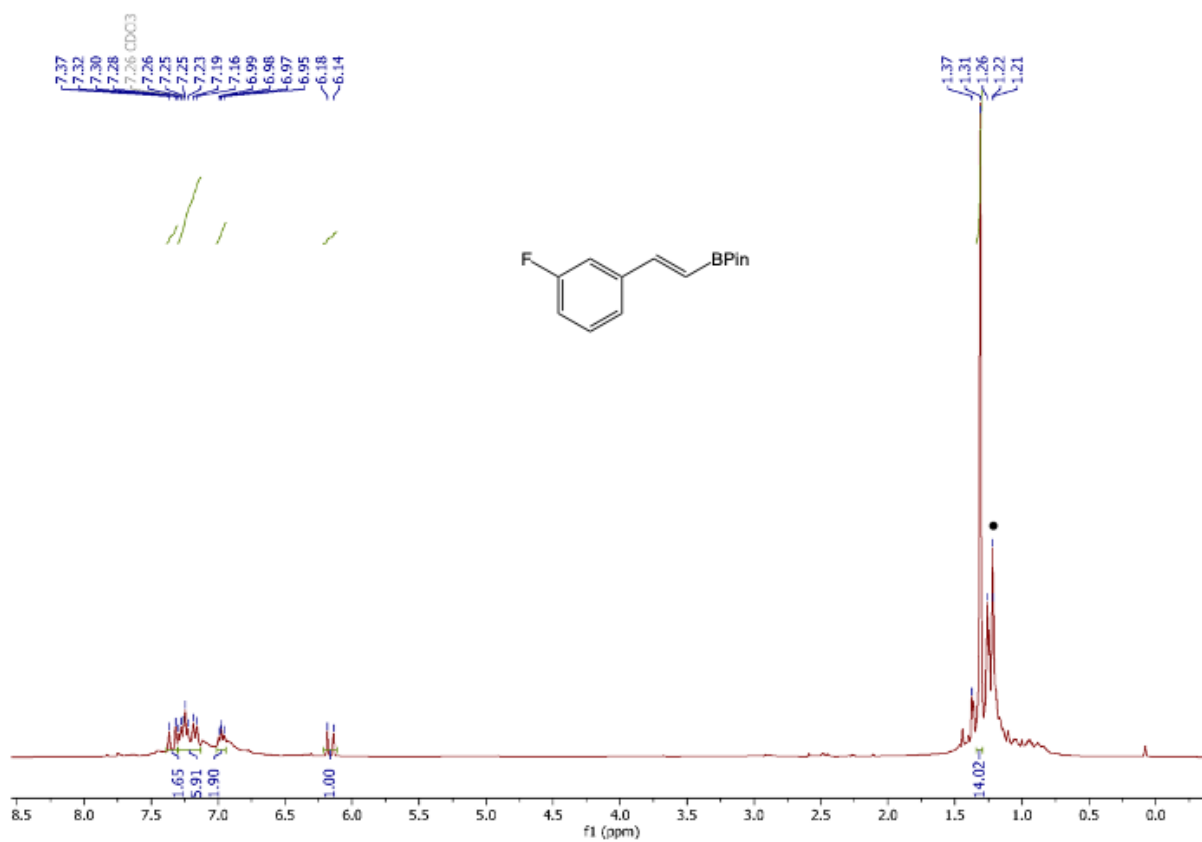


Figure S34: ¹H NMR (CDCl₃, 400MHz) of 2-[(1E)-2-(3-Fluorophenyl)ethenyl]-4,4,5,5-tetramethyl-1,3,2-dioxaborolane (• = Peak corresponding to C-H Borylated Product 3a)

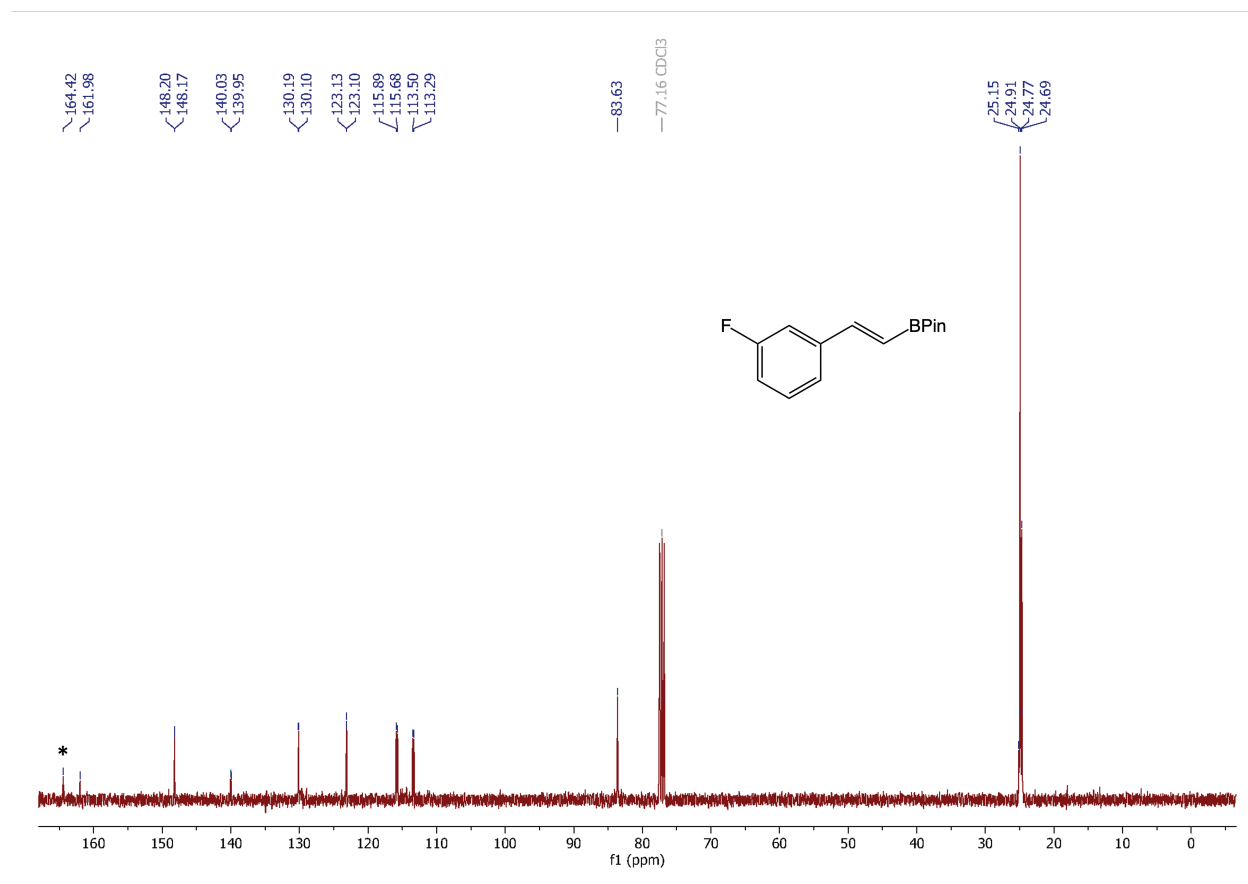


Figure S35: ¹³C NMR (CDCl₃, 100MHz) of (2-[(1*E*)-2-(3-Fluorophenyl)ethenyl]-4,4,5,5-tetramethyl-1,3,2-dioxaborolane (* = Unidentified Products)

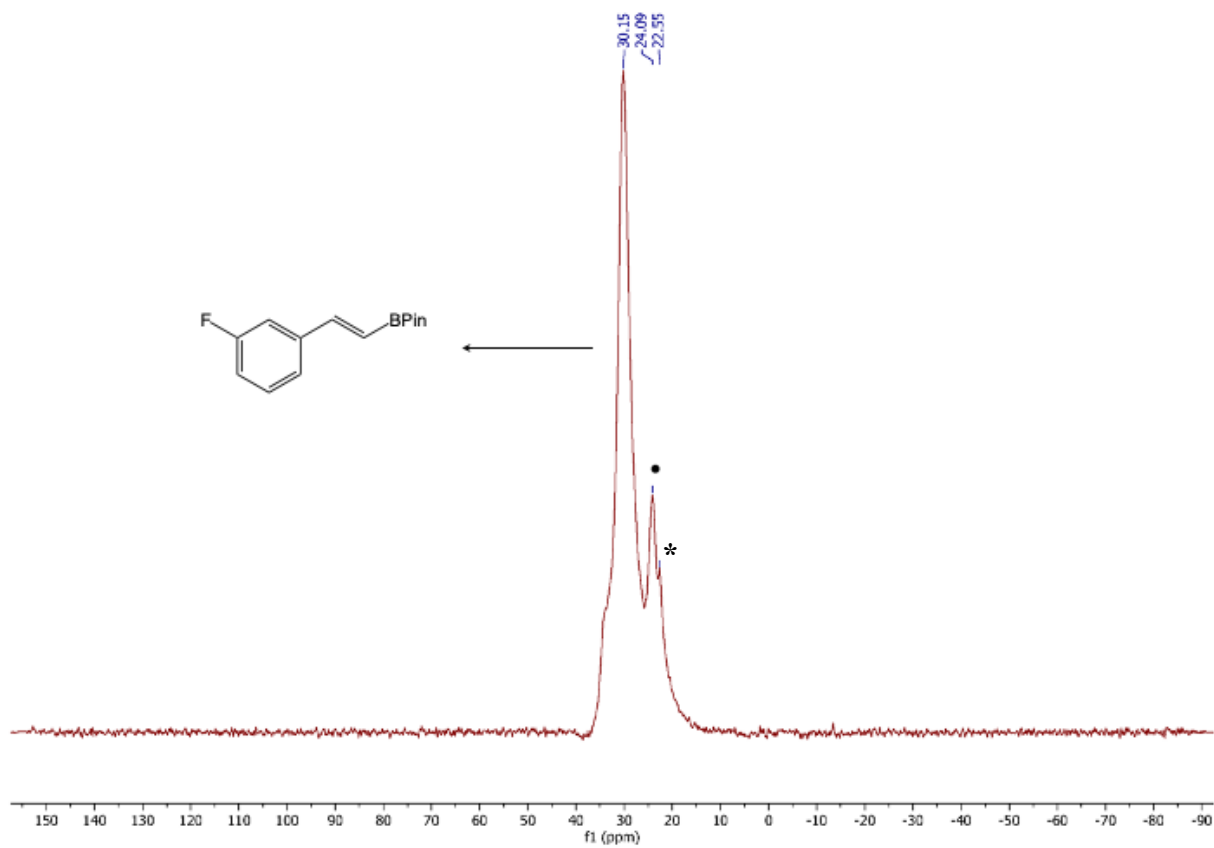


Figure S36: ^{11}B NMR (CDCl_3 , 128 MHz) of 2-[(1*E*)-2-(3-Fluorophenyl)ethenyl]-4,4,5,5-tetramethyl-1,3,2-dioxaborolane (• = Peak corresponding to C-H Borylated Product 3a, * = Impurity from HBPin)

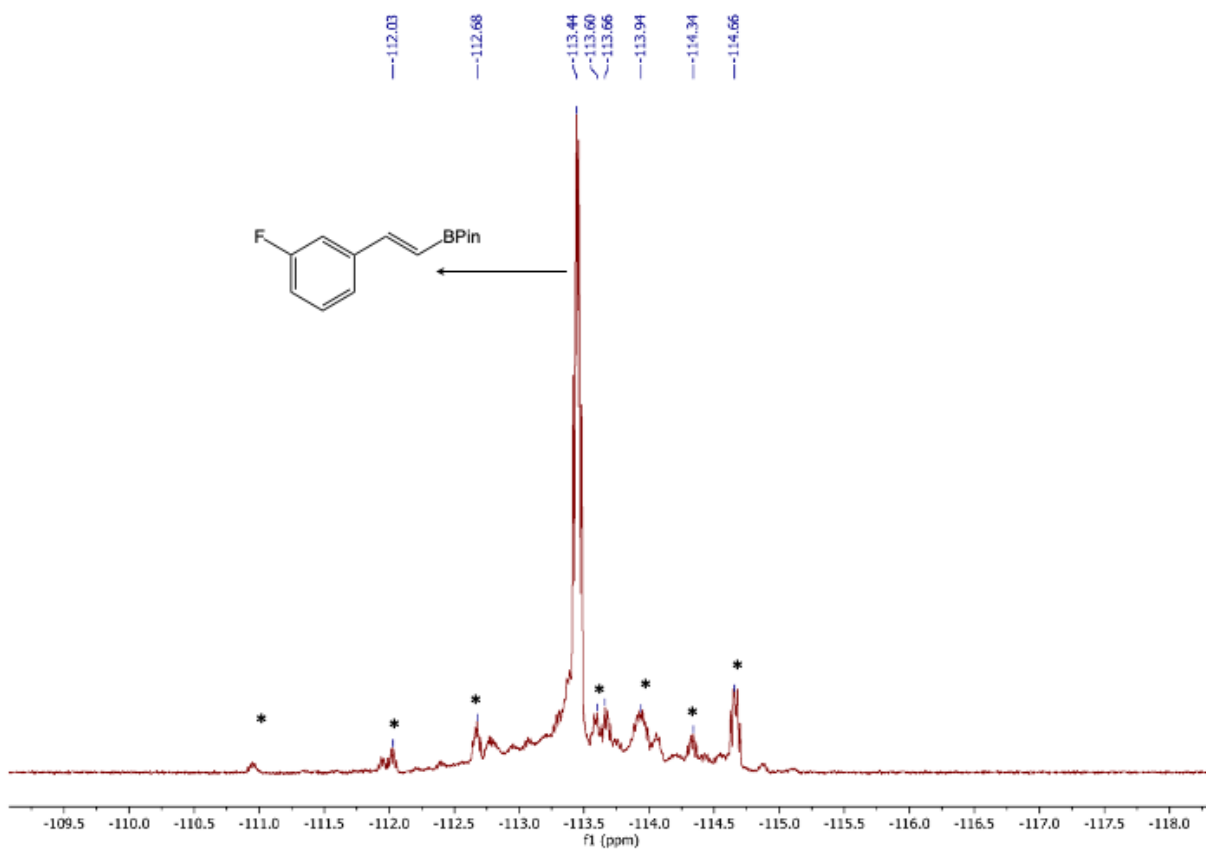


Figure S37: ^{19}F NMR (CDCl_3 , 376 MHz) of (2-[(1*E*)-2-(3-Fluorophenyl)ethenyl]-4,4,5,5-tetramethyl-1,3,2-dioxaborolane (* = Unidentified Product)

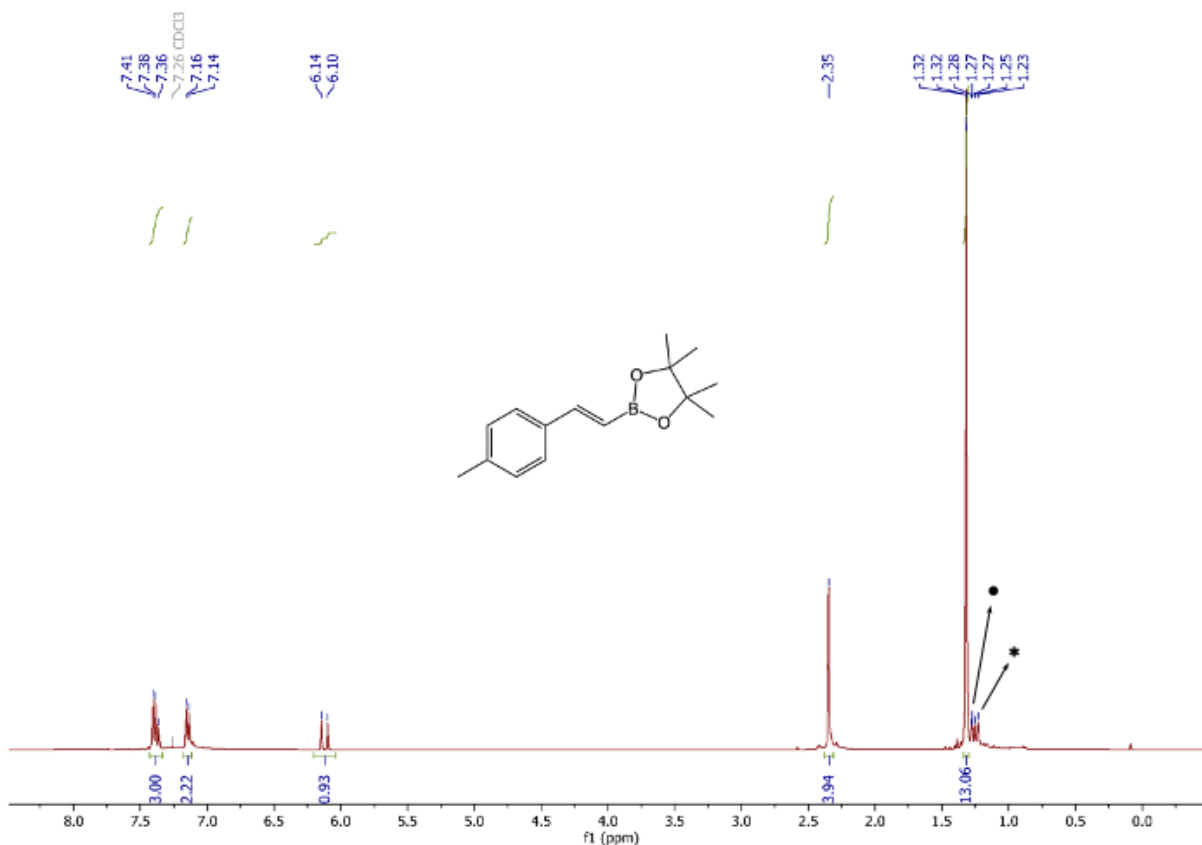


Figure S38: ¹H NMR (CDCl₃, 400MHz) of 4,4,5,5-Tetramethyl-2-[(1E)-2-(4-methylphenyl)ethenyl]-1,3,2-dioxaborolane (• = Peak corresponding to C-H Borylated Product 4a, * = Unidentified Products)

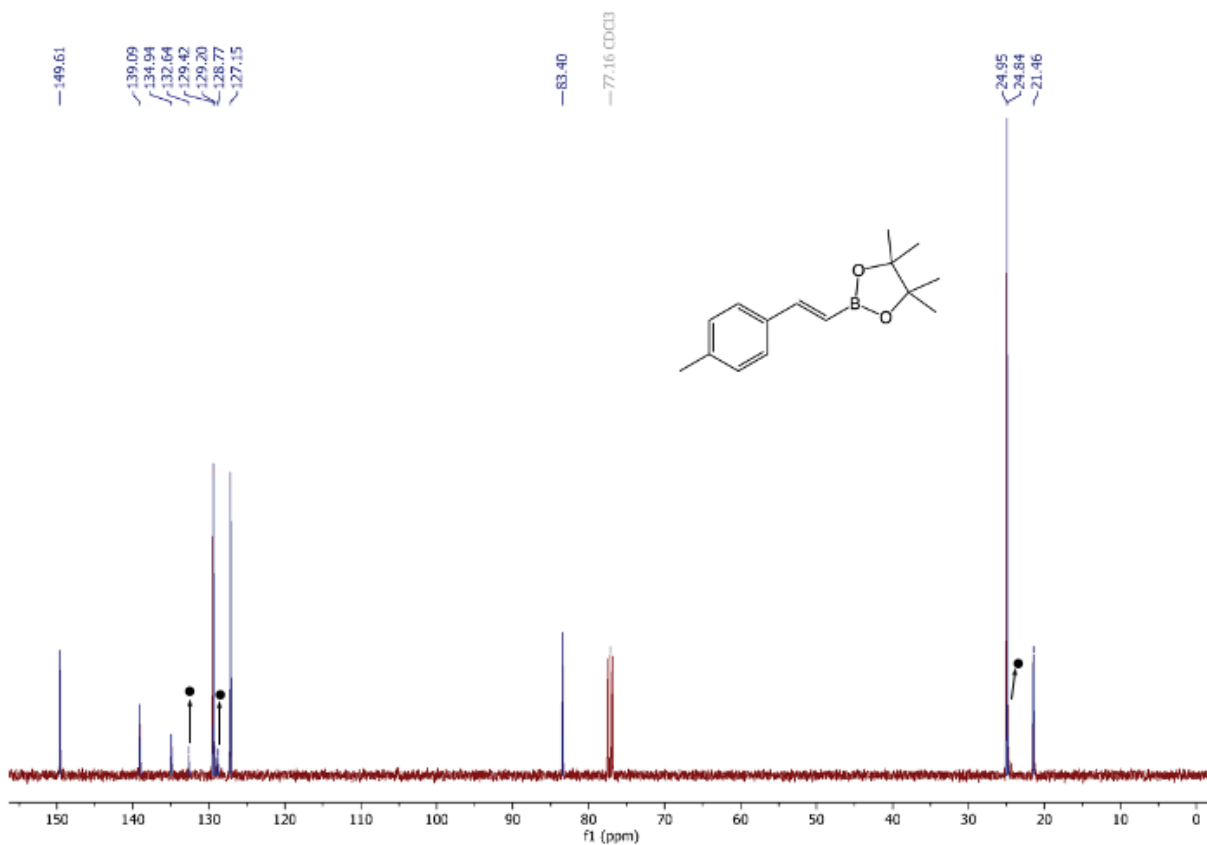


Figure S39: ¹³C NMR (CDCl₃, 100MHz) of 4,4,5,5-Tetramethyl-2-[(1*E*)-2-(4-methylphenyl)ethenyl]-1,3,2-dioxaborolane (• = Peak corresponding to C-H Borylated Product 4a)

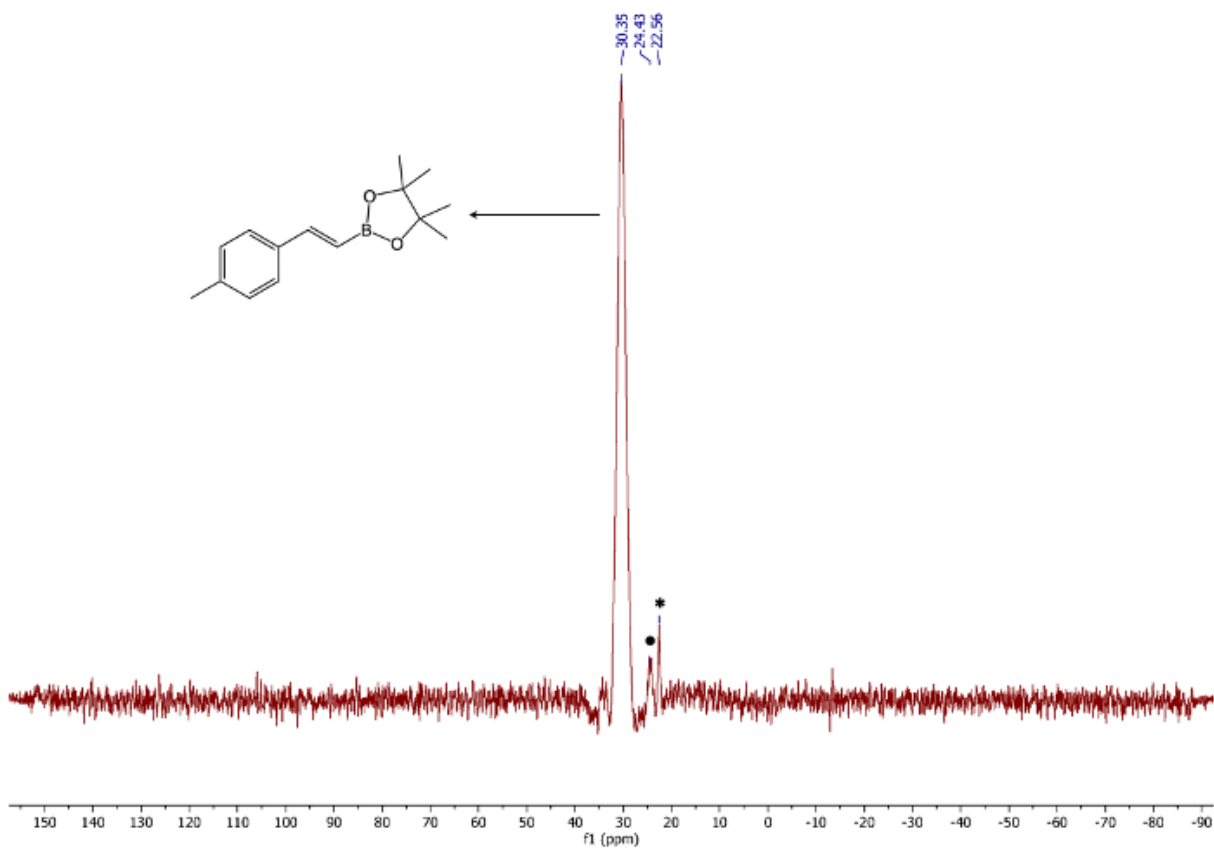


Figure 40: ^{11}B NMR (CDCl_3 , 128 MHz) of 4,4,5,5-Tetramethyl-2-[(1*E*)-2-(4-methylphenyl)ethenyl]-1,3,2-dioxaborolane (• = Peak corresponding to C-H Borylated Product 4a, * = Impurity from HBPIn)

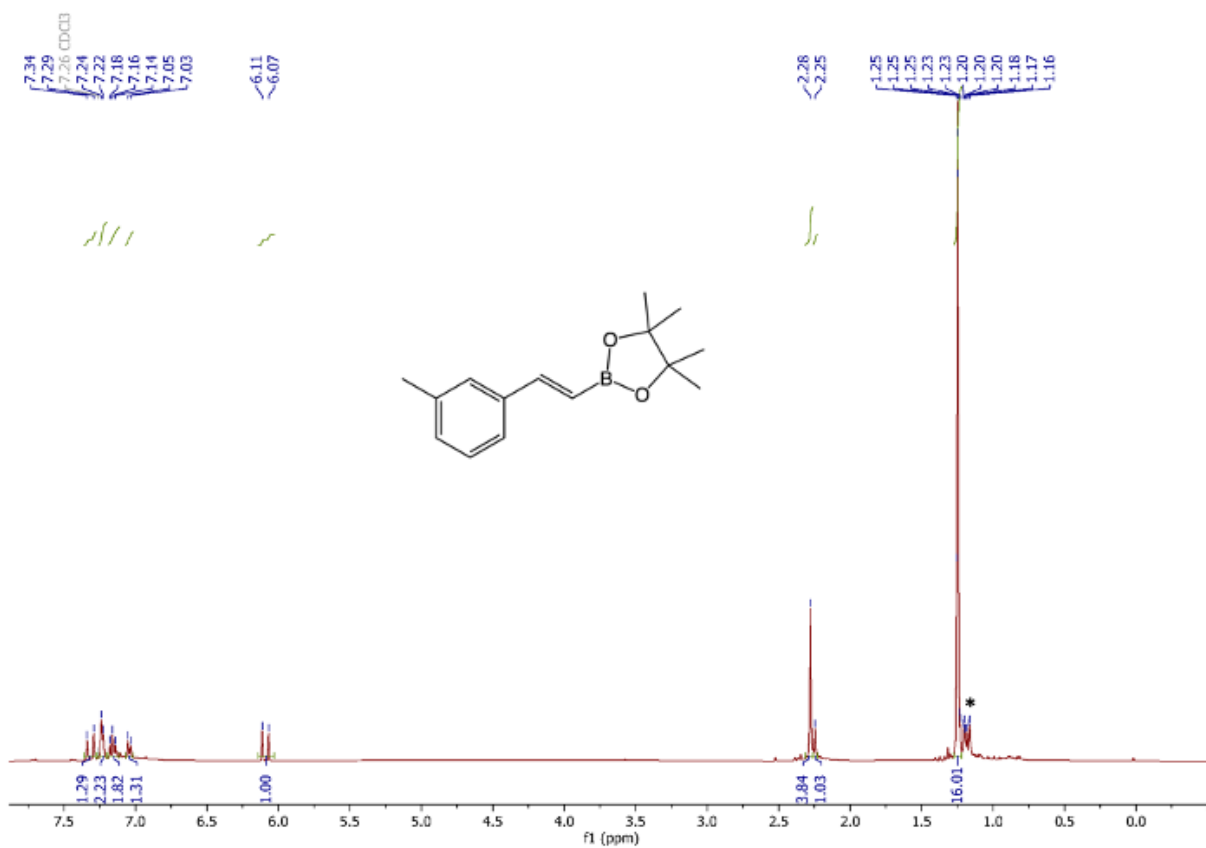


Figure S41: ^1H NMR (CDCl_3 , 400MHz) of 4,4,5,5-Tetramethyl-2-[(1*E*)-2-(3-methylphenyl)ethenyl]-1,3,2-dioxaborolane (* = Unidentified Products)

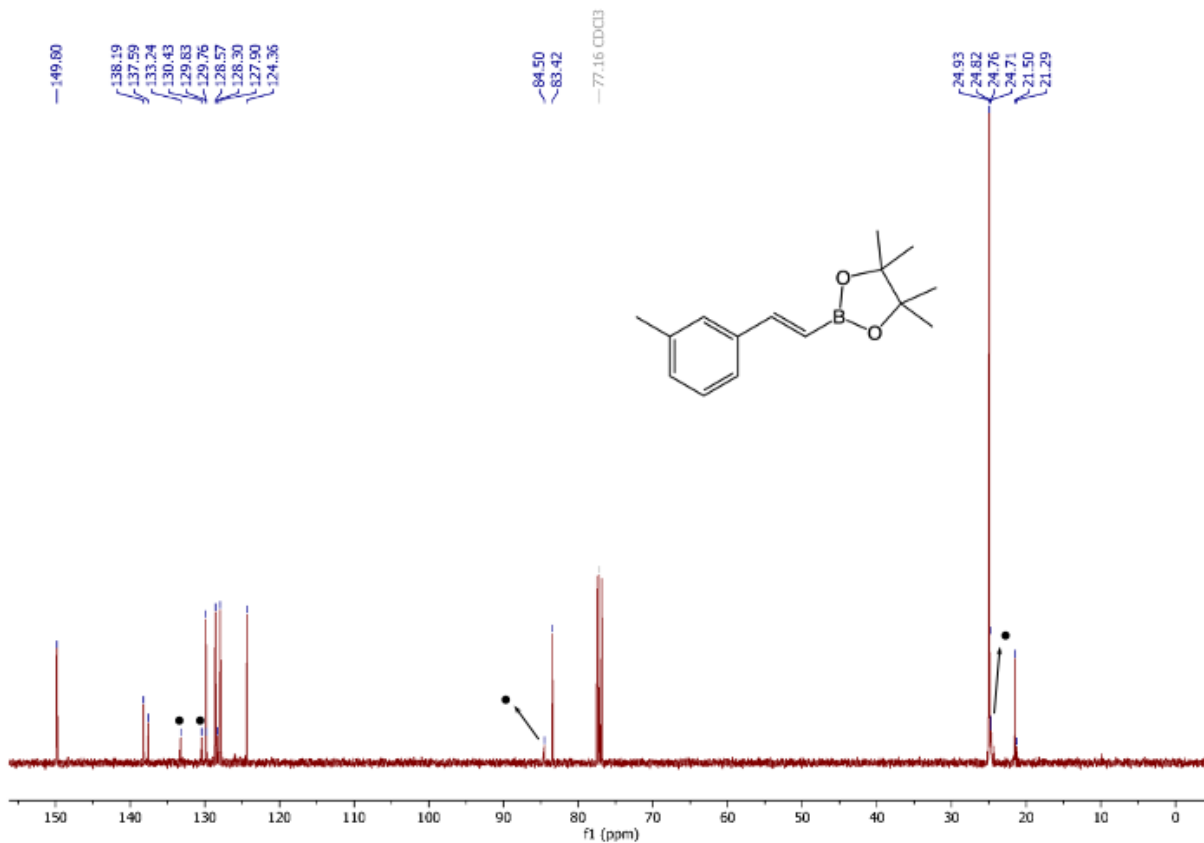


Figure S42: ¹³C NMR (CDCl₃, 100MHz) of 4,4,5,5-Tetramethyl-2-[(1E)-2-(3-methylphenyl)ethenyl]-1,3,2-dioxaborolane (• = Peak corresponding to C-H Borylated Product 5a)

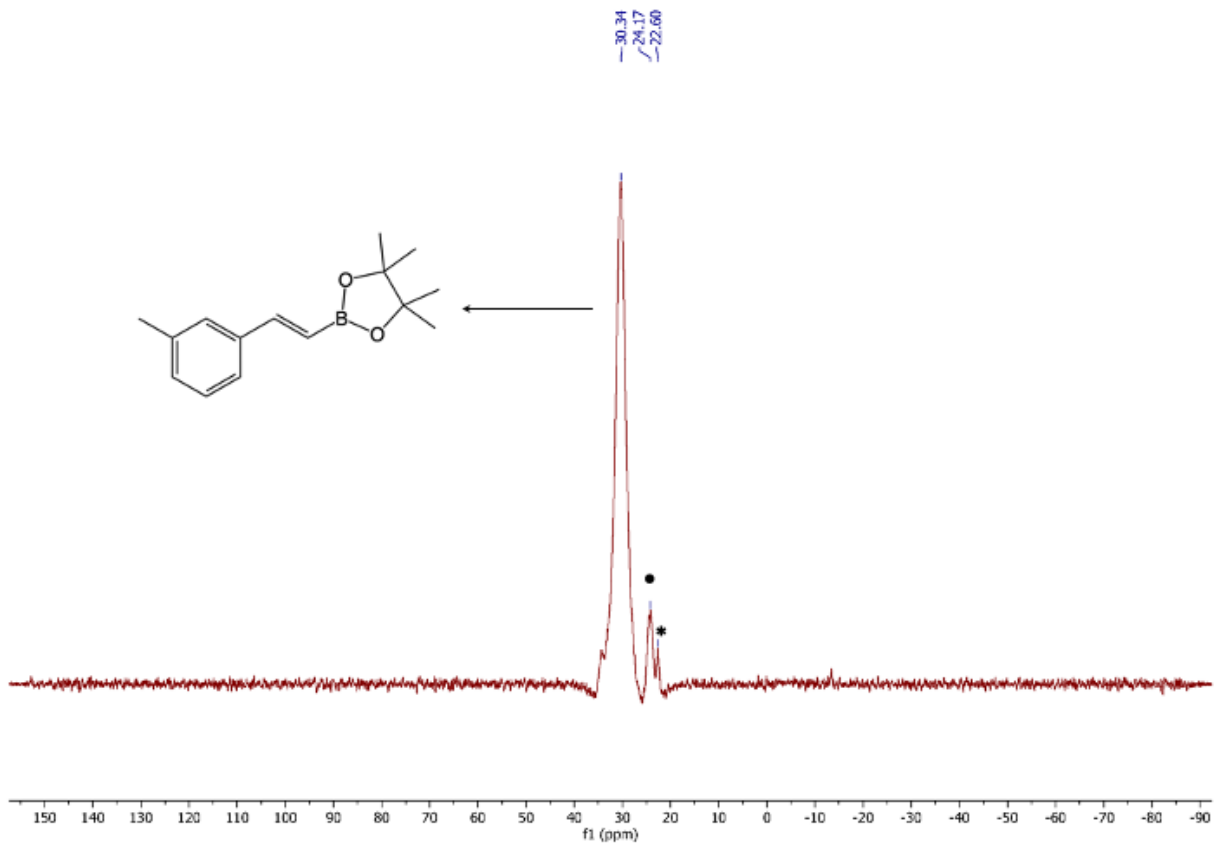


Figure S43: ^{11}B NMR (CDCl_3 , 128 MHz) of 4,4,5,5-Tetramethyl-2-[(1*E*)-2-(3-methylphenyl)ethenyl]-1,3,2-dioxaborolane (• = Peak corresponding to C-H Borylated Product 5a, * = Impurity from HBPIn)

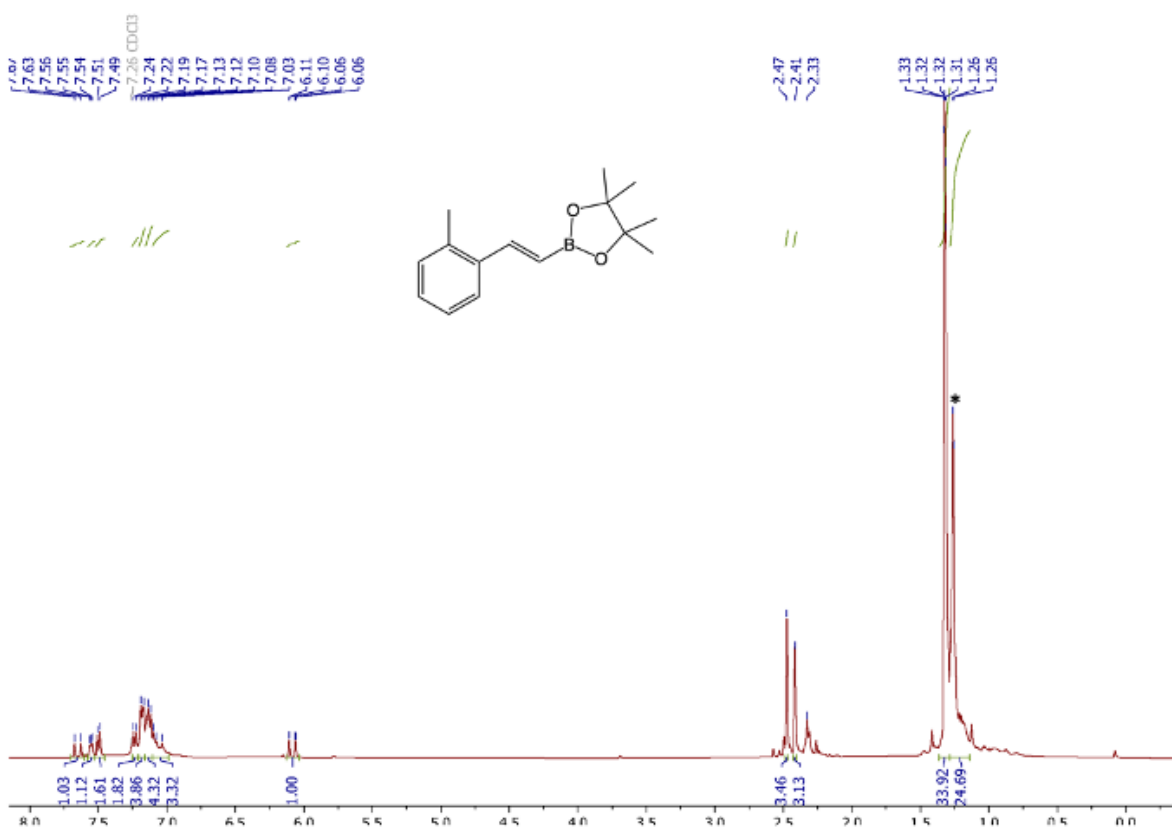


Figure S44: ¹H NMR (CDCl₃, 400MHz) of 4,4,5,5-Tetramethyl-2-[(1E)-2-(2-methylphenyl)ethenyl]-1,3,2-dioxaborolane (* = Unidentified Products)

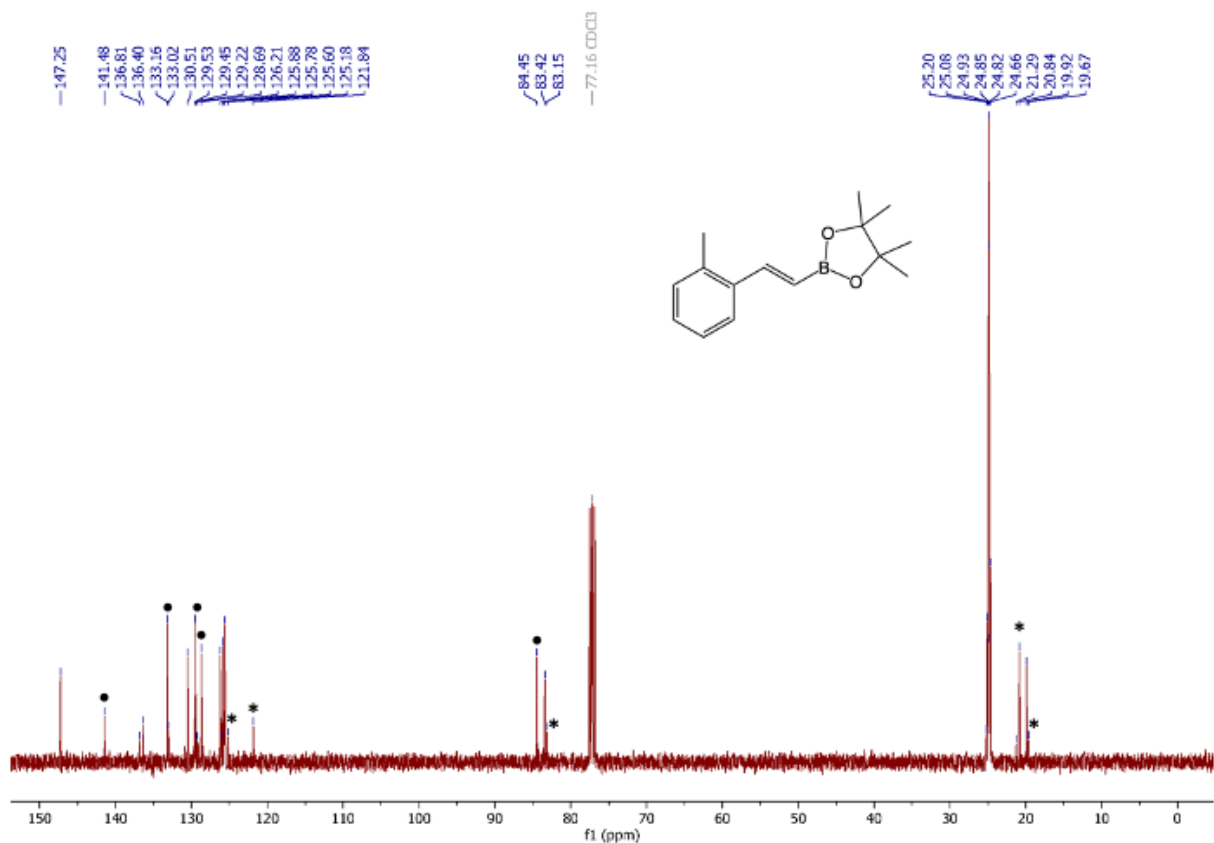


Figure S45: ^{13}C NMR (CDCl_3 , 100MHz) of 4,4,5,5-Tetramethyl-2-[(1*E*)-2-(2-methylphenyl)ethenyl]-1,3,2-dioxaborolane (• = Peak corresponding to C-H Borylated Product 6a, * = Unidentified Products)

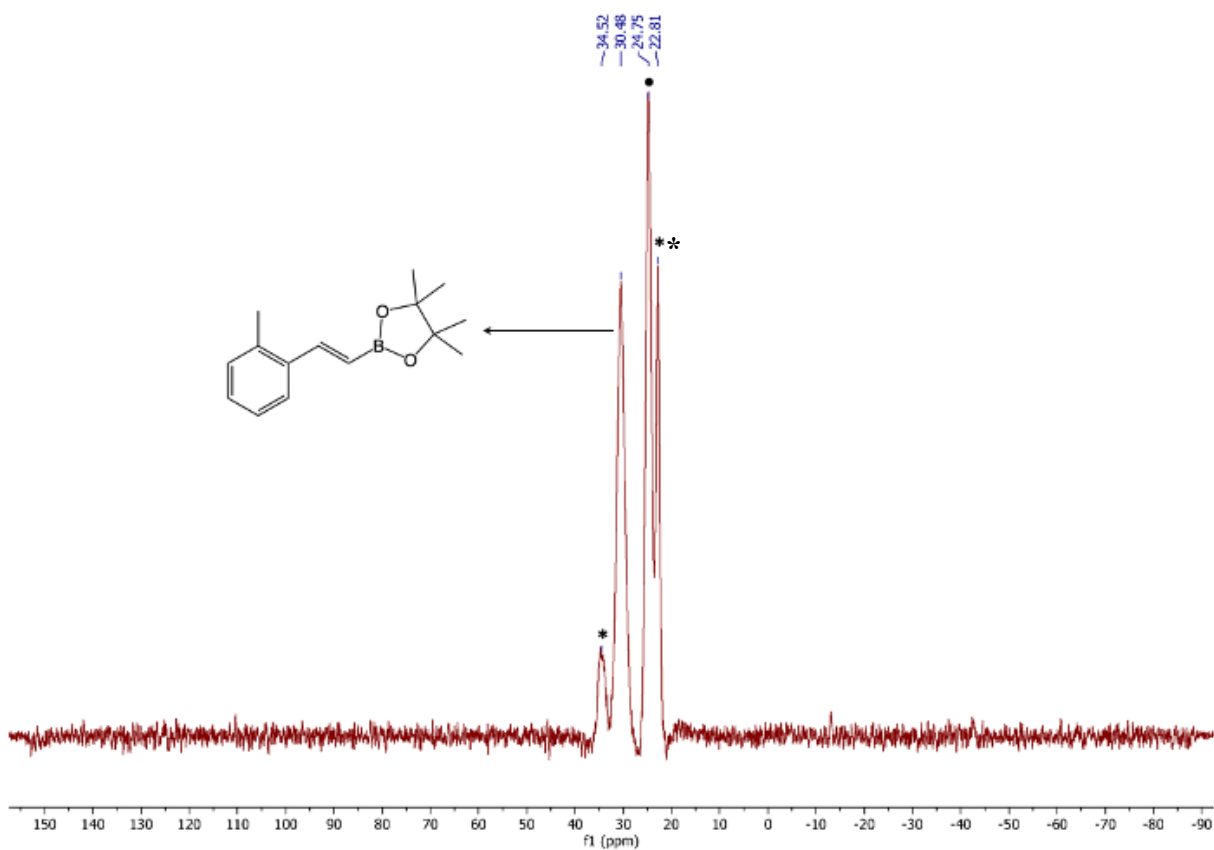


Figure S46: ^{11}B NMR (CDCl_3 , 128 MHz) of 4,4,5,5-Tetramethyl-2-[(1*E*)-2-(2-methylphenyl)ethenyl]-1,3,2-dioxaborolane (• = Peak corresponding to C-H Borylated Product 6a, * = Unidentified Products, ** = Impurity from HBpin)

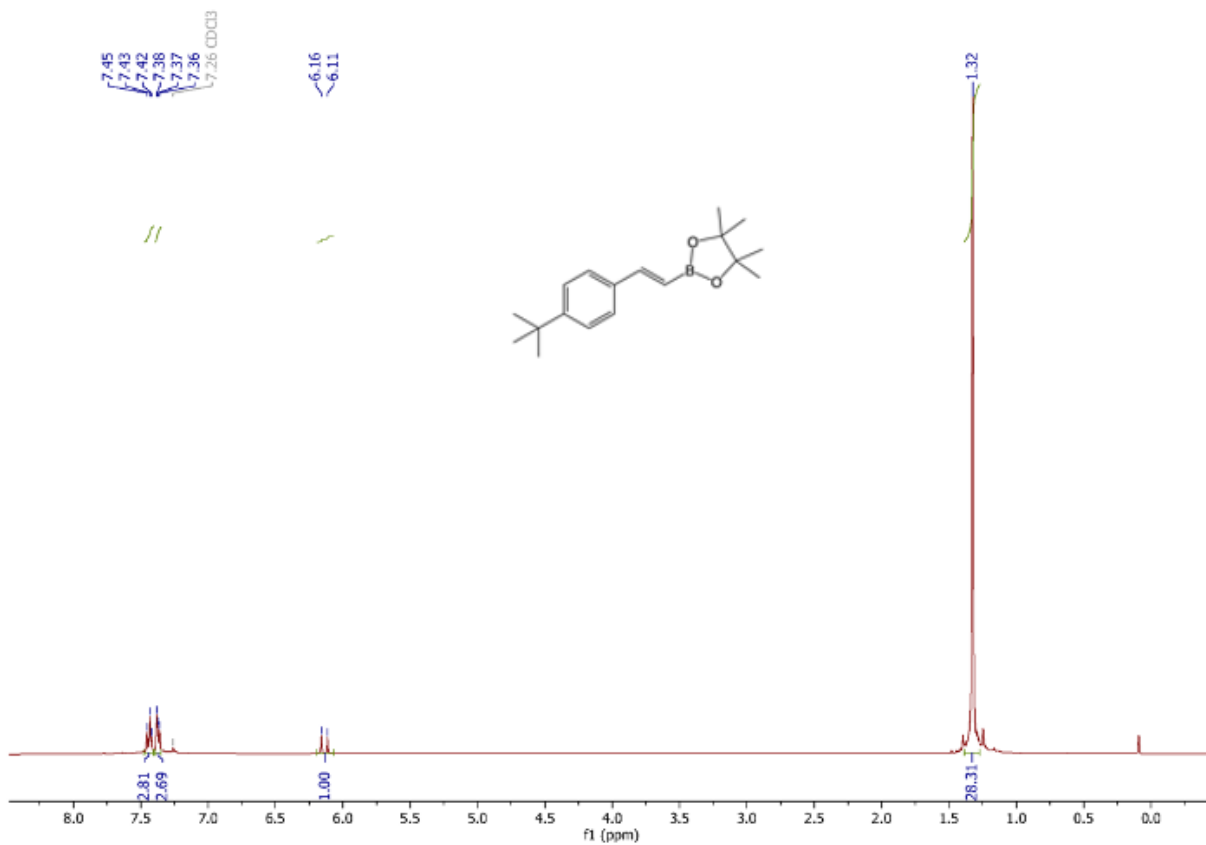


Figure S47: ^1H NMR (CDCl_3 , 400MHz) of 2-[(1*E*)-2-[4-(1,1-Dimethylethyl)phenyl]ethenyl]-4,4,5,5-tetramethyl-1,3,2-dioxaborolane

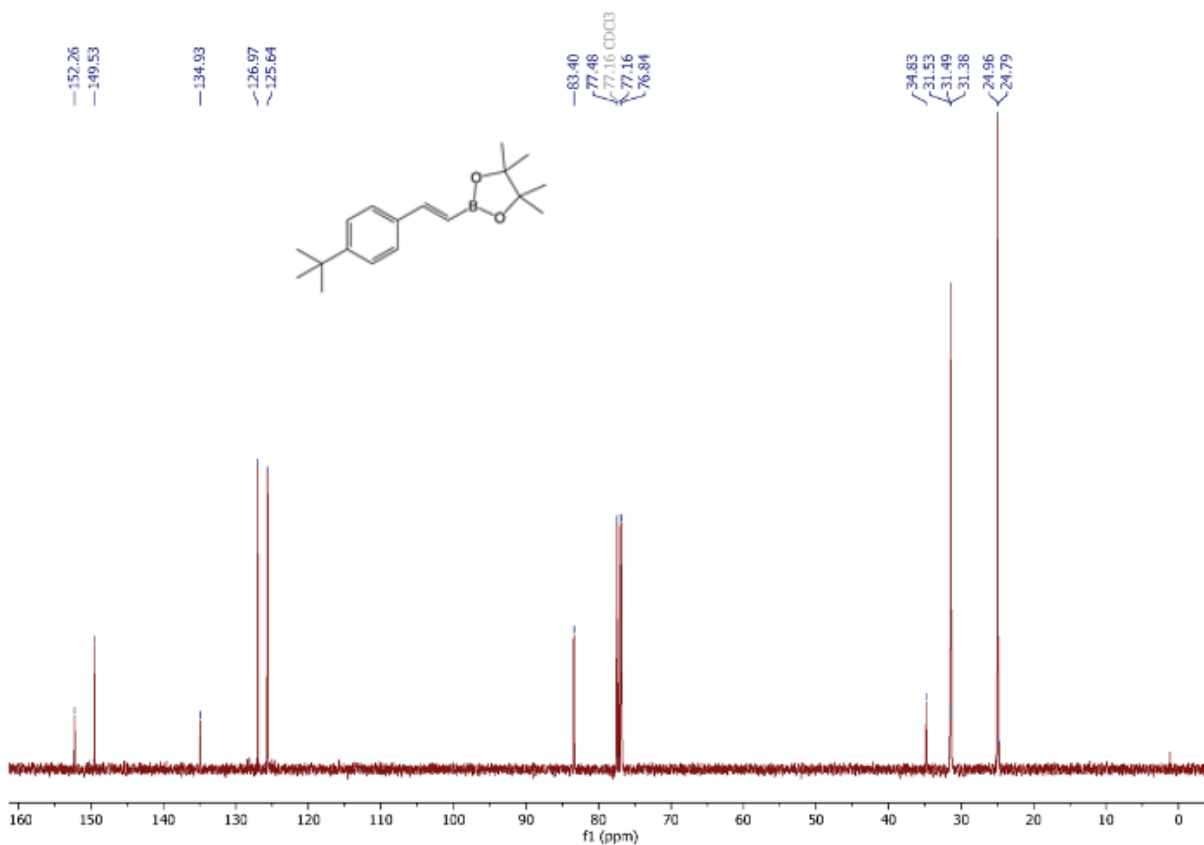


Figure S48: ^{13}C NMR (CDCl_3 , 100MHz) of 2-[(1E)-2-[4-(1,1-Dimethylethyl)phenyl]ethenyl]-4,4,5,5-tetramethyl-1,3,2-dioxaborolane

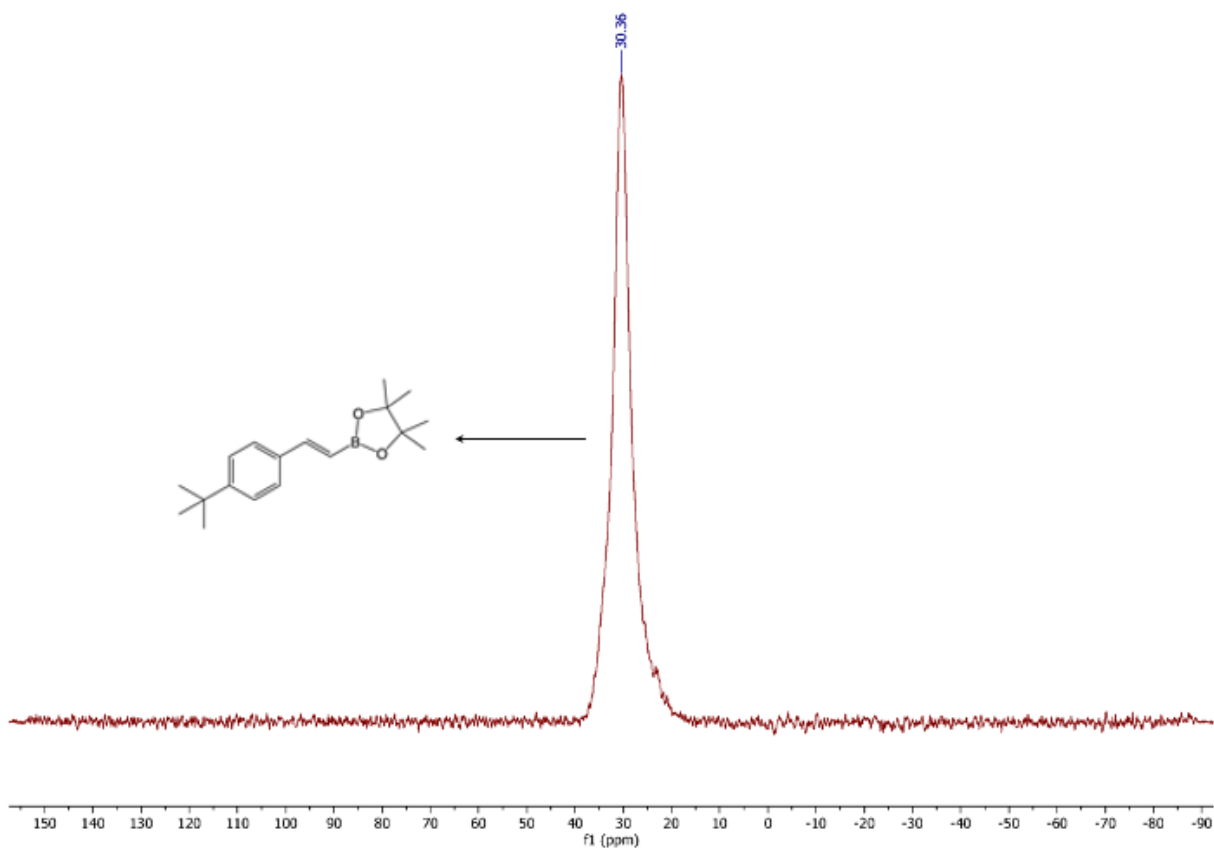


Figure S49: ^{11}B NMR (CDCl_3 , 128 MHz) of 2-[(1*E*)-2-[4-(1,1-Dimethylethyl)phenyl]ethenyl]-4,4,5,5-tetramethyl-1,3,2-dioxaborolane

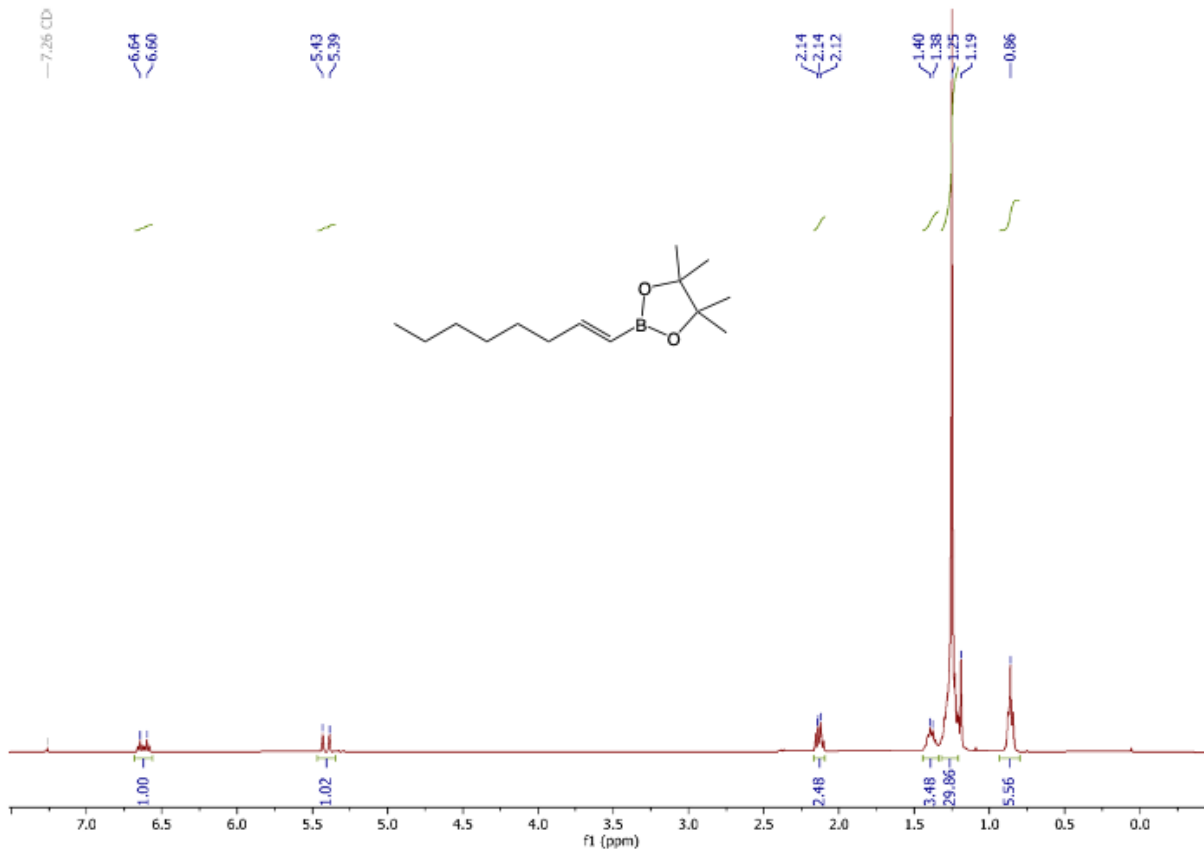


Figure S50: ¹H NMR (CDCl₃, 400MHz) of 4,4,5,5-Tetramethyl-2-(1E)-1-octen-1-yl-1,3,2-dioxaborolane

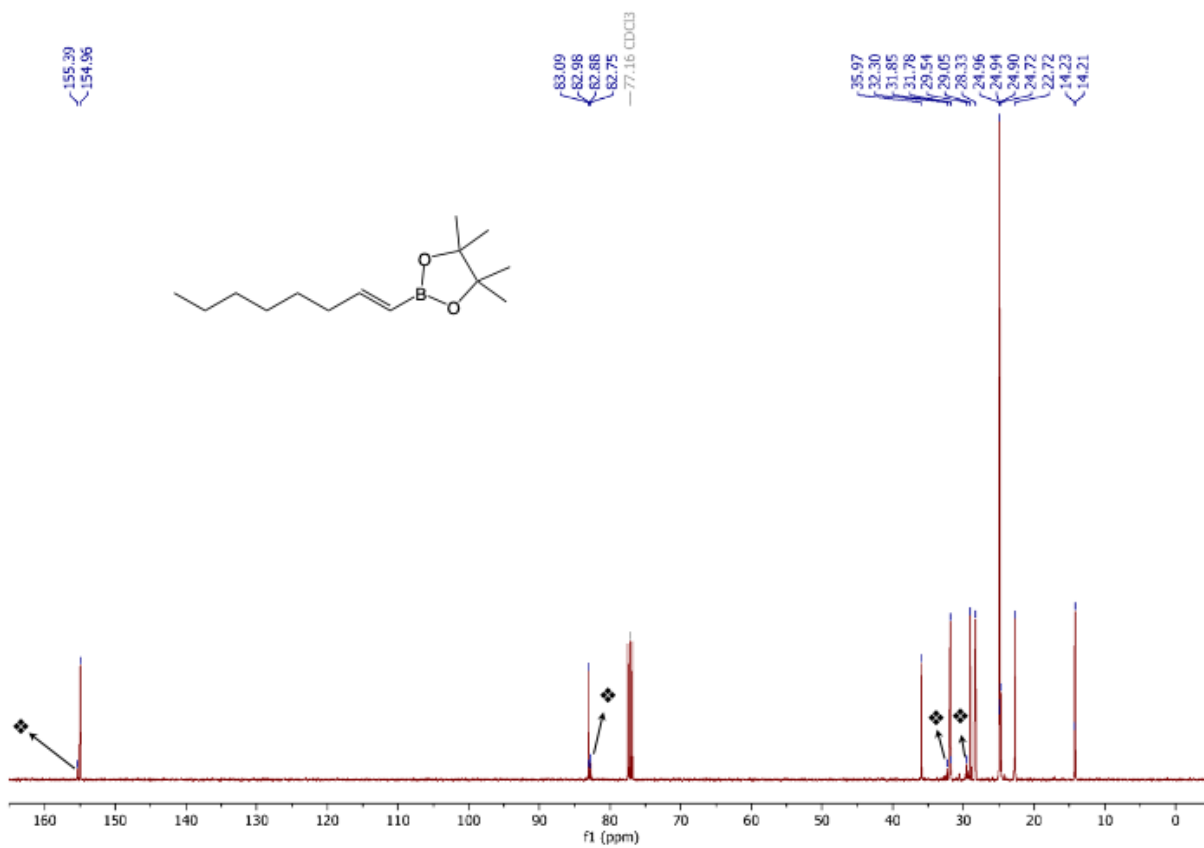


Figure S51: ^{13}C NMR (CDCl₃, 100MHz) of 4,4,5,5-Tetramethyl-2-(1*E*)-1-octen-1-yl-1,3,2-dioxaborolane (❖ = Peaks corresponding to cis isomer)

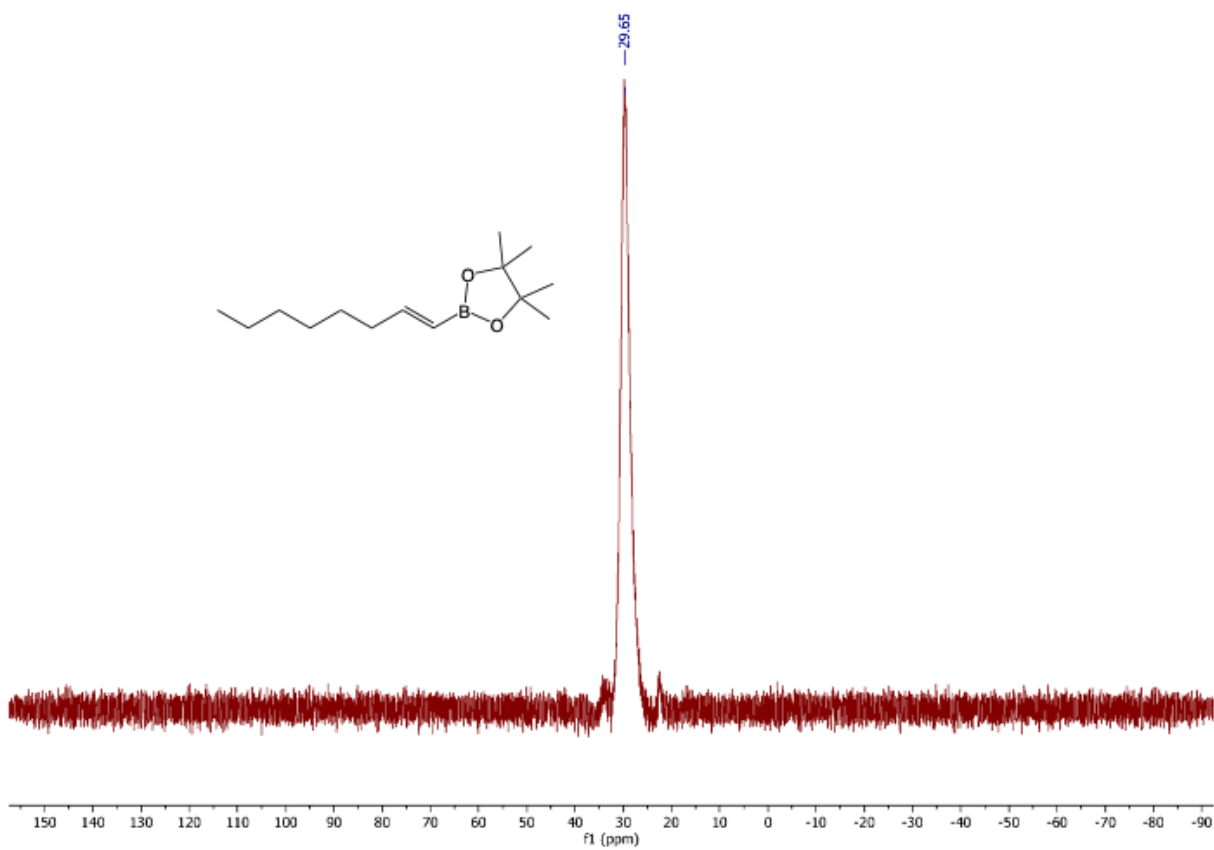


Figure S52: ^{11}B NMR (CDCl_3 , 128 MHz) of 4,4,5,5-Tetramethyl-2-(1*E*)-1-octen-1-yl-1,3,2-dioxaborolane

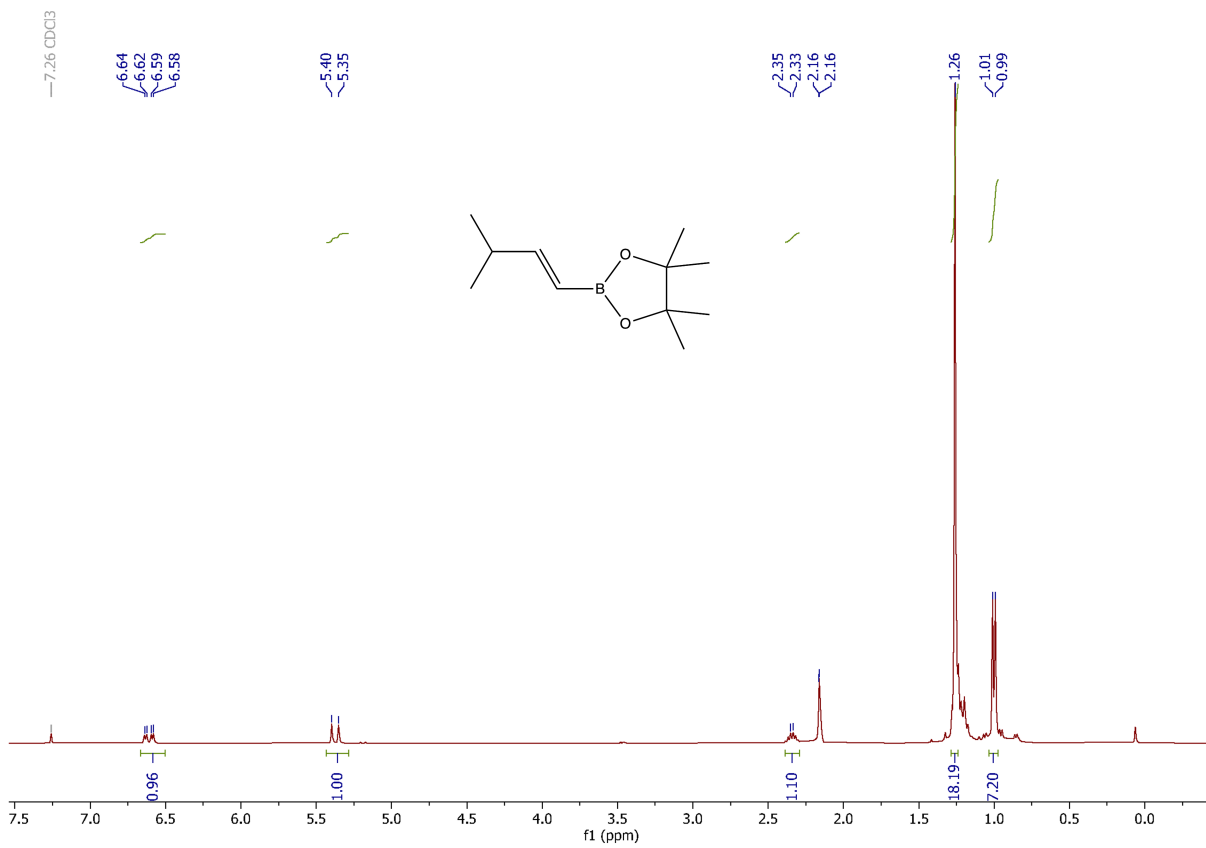


Figure S53: ^1H NMR (CDCl_3 , 400MHz) of (4,4,5,5-Tetramethyl-2-[(1*E*)-3-methyl-1-buten-1-yl]-1,3,2-dioxaborolane) (• = peak corresponding to acetone)

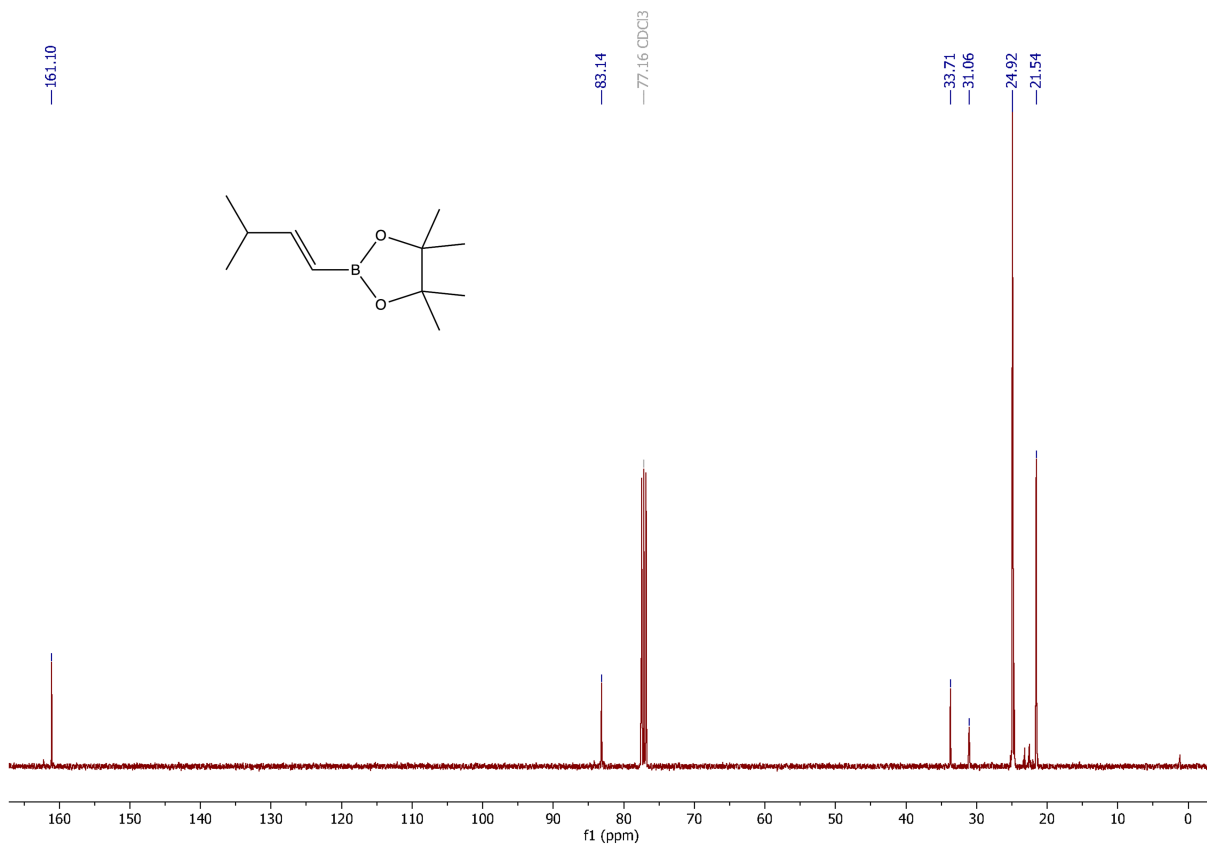


Figure S54: ¹³C NMR (CDCl₃, 100MHz) of 4,4,5,5-Tetramethyl-2-[(1E)-3-methyl-1-buten-1-yl]-1,3,2-dioxaborolane

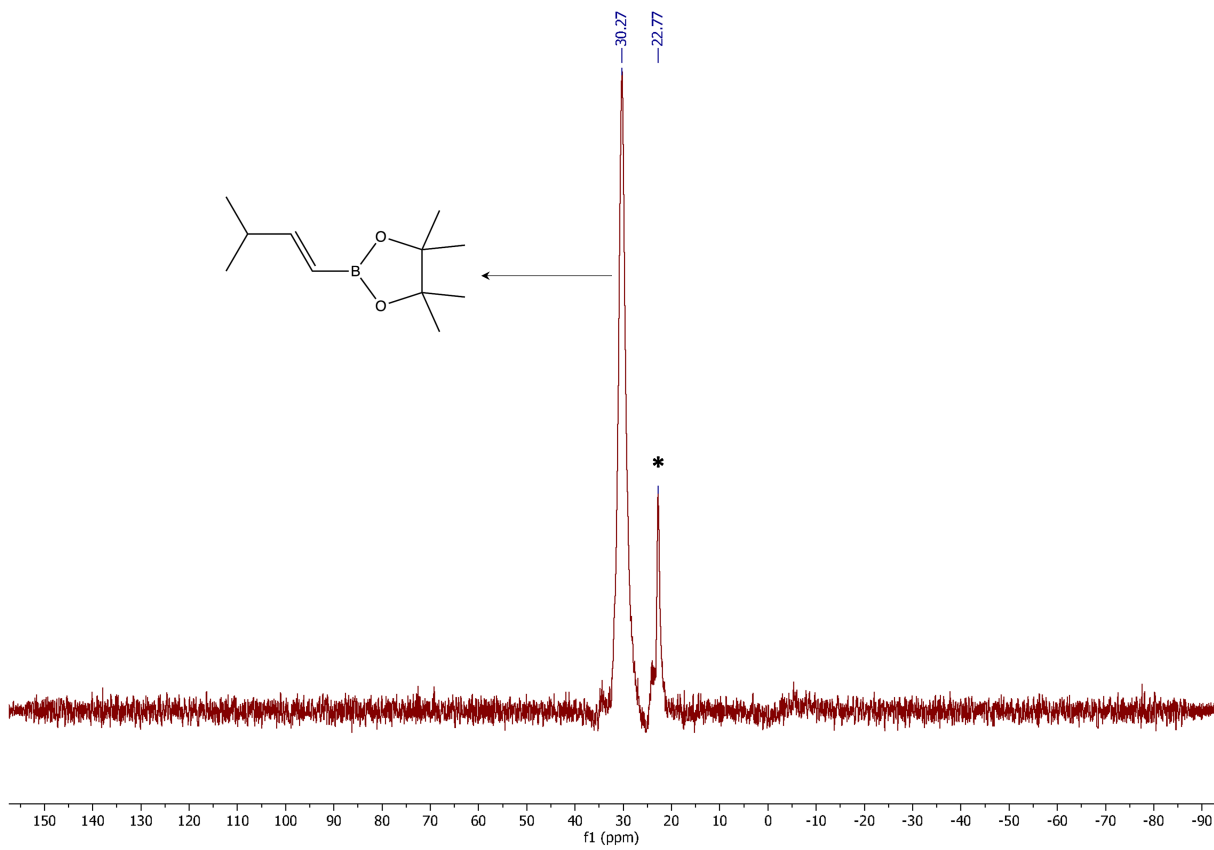


Figure S55: ^{11}B NMR (CDCl_3 , 128 MHz) of 4,4,5,5-Tetramethyl-2-[(1*E*)-3-methyl-1-buten-1-yl]-1,3,2-dioxaborolane (* = impurity from HBPIn)

10. References

1. A.B. Pangborn, M. A. Giardello, R. H. Grubbs, R. K. Rosen, F. J. Timmers, Safe and Convenient Procedure for Solvent Purification. *Organometallics* **1996**, *15*, 1518–1520.
2. D. Gallego, S. Inoue, B. Blom, M. Driess, Highly electron-rich pincer-type iron complexes bearing innocent bis(metallylene)pyridine ligands: syntheses, structures, and catalytic activity. *Organometallics* **2014**, *33*, 6885-6897 and references therein.
3. A. Brzozowska, L. M. Azofra, V. Zubar, I. Atodiresei, L. Cavallo, M. Rueping, O. El-Sepelgy, Highly Chemo- and Stereoselective Transfer Semi-hydrogenation of Alkynes Catalyzed by a Stable, Well-Defined Manganese(II) Complex, *ACS Catal.*, **2018**, *8*, 4103-4109.
4. A. Brzozowska, V. Zubar, R. -C Ganardi, M. Rueping, Chemoselective Hydroboration of Propargylic Alcohols and Amines Using a Manganese(II) Catalyt. *Org. Lett.*, **2020**, *22*, 3765-3769.
5. M. Kawatsura, J. Hartwig, Transition Metal-Catalyzed Addition of Amines to Acrylic Acid Derivatives. A High-Throughput Method for Evaluating Hydroamination of Primary and Secondary Alkylamines. *Organometallics* **2001**, *20*, 1960-1964
6. N. Iwadate, M. Suginome, Synthesis of Masked Haloareneboronic Acids via Iridium-Catalyzed Aromatic C–H Borylation with 1,8-Naphthalenediaminatoborane (danBH). *J. Organomet. Chem.*, **2009**, *694*, 1713–1717.
7. H. Wen, L. Zhang, S. Zhu, G. Liu, Z. Huang, Stereoselective Synthesis of Trisubstituted Alkenes via Cobalt-Catalyzed Double Dehydrogenative Borylations of 1-Alkenes. *ACS Catal.* **2017**, *7*, 10, 6419–6425
8. P. Zhang, J. M. Suárez, T. Driant, E. Derat, Y. Zhang, M. Ménand, S. Roland, M. Sollogoub, Cyclodextrin Cavity-Induced Mechanistic Switch in Copper-Catalyzed Hydroboration. *Angew. Chem. Int. Ed.* **2017**, *56*, 10821
9. X. Zeng, C. Gong, H. Guo, H. Xu, J. Zhang, J. Xie Efficient heterogeneous hydroboration of alkynes: enhancing the catalytic activity by Cu(0) incorporated CuFe₂O₄ nanoparticles *New J. Chem.*, **2018**, *42*, 17346-17350
10. H. Shimizu, T. Igarashi, T. Miura, M. Murakami, M, Rhodium-Catalyzed Reaction of 1-Alkenylboronates with Aldehydes Leading to Allylation Products. *Angew. Chem. Int. Ed.*, **2011**, *50*, 11465-11469.